The University Of Sheffield.

A New Framework for Right-First-Time Production of Granules and Tablets: A Systems Engineering Approach to Modelling and Optimization

By:

Wafa' H. AlAlaween

Supervisors:

Prof. Mahdi Mahfouf

Prof. Agba D. Salman

A thesis submitted in partial fulfilment of the requirements for the degree of Doctor of Philosophy

Department of Automatic Control and Systems Engineering

The University of Sheffield

UK

November 2017

Contents

List of Figures

List of Tables

Nomenclature

AI	Artificial intelligence
ANN	Artificial neural networks
ANOVA	Analysis of variance
API	Active pharmaceutical ingredient
BIC	Bayesian information criterion
$CaCO_3$	Calcium Carbonate
CFD	Computational fluid dynamics
DS	Dempster-Shafer
EM	Expectation Maximization algorithm
FDA	Food and Drug Administration
FLS	Fuzzy logic system
GMM	Gaussian mixture model
HSG	High shear granulation
IT2FLS	Interval type-2 fuzzy logic system
KM	Karnik-Mendel algorithm
KTGF	Kinetic theory behind the granular flow
L/S	Liquid to solid
MISO	Multi-input single-output

MOP	Multi-objective optimization problem
MOPSO	Multi-objective particle swarm optimization
PBM	Population balance model
PEG	Polyethylene Glycol
PSO	Particle swarm optimization
QbD	Quality by Design
QbT	Quality by Testing
R^2	Coefficient of determination
RBF	Radial basis function
RMSE	Root mean square error
SCG	Scaled conjugate gradient
SOP	Single optimization problem
T1FLS	Type-1 fuzzy logic system
T2FLS	Type-2 fuzzy logic system

Publications

Journal Papers

1. AlAlaween, W.H., Khorsheed, B., Mahfouf, M., Gabbott, I., Reynolds, G.K., Salman, A.D, 2018. Transparent Predictive Modelling of the Twin Screw Granulation Process using a Compensated Interval Type-2 Fuzzy System. European Journal of Pharmaceutics and Biopharmaceutics. 124, 138-146.
2. AlAlaween, W.H., Mahfouf, M., Salman, A.D., 2017. Integrating physics with data analytics for the hybrid modelling of the granulation process. AIChE. 63, 4761-4773.
3. AlAlaween, W.H., Mahfouf, M., Salman, A.D., 2016. Predictive modelling of the granulation process using a systems-engineering approach. Powder Technology. 302, 265-274.
4. AlAlaween, W.H., Mahfouf, M., Salman, A.D. When swarm meets fuzzy logic: *right-first-time* production of pharmaceuticals using batch optimization. Applied Soft Computing. Under review.

Conferences

1. AlAlaween, W.H., Mahfouf, M., Salman, A.D., 2017. Development of a predictive framework for a high shear granulation process. AIChE Annual meeting. Minneapolis, USA.
2. AlAlaween, W.H., Mahfouf, M., Salman, A.D., 2016. Data-Driven Deterministic and Stochastic modelling of the Wet Granulation Process. Joint IFPRI Robert Pfeffer symposium & UK Particle Technology Forum. Guilford, UK.
3. AlAlaween, W.H., Mahfouf, M., Salman, A.D., 2015. *Right-first-time* production of granules- a system modelling and optimization approach. The 7th International Granulation Workshop. Sheffield, UK.
4. AlAlaween, W.H., Mahfouf, M., Salman, A.D., 2015. Towards modelling of the granulation process. ACSE Symposium. Sheffield, UK.

Acknowledgment

Praise is due to Allah, the most beneficent and the most merciful, for his uncountable blessings.

As the end of my three-year PhD journey is approaching, I would like to take this opportunity to express my sincere gratitude to all of those who have always stood by my side all the time. Without their support, I would not have been able to accomplish this work.

My family has been my rock during my PhD. From the bottom of my heart, I would like to thank my beloved parents. I can barely find the words to express all the wisdom, care, love and support you have given me. I am very much indebted to my brothers and sisters who have constantly supported me in every possible way.

I would also like to express my sincere appreciation to my supervisors Professor Mahdi Mahfouf and Professor Agba Salman. You have been a tremendous support during this journey, your honest feedback and advice were extremely valuable and have significantly improved the quality of my work. My PhD has been an amazing learning experience that enriched both my knowledge and skills, and you have exceptionally contributed to this experience.

I would also like to thank all staff members of the Department of Automatic Control and Systems Engineering in the University of Sheffield for their continuous support during my PhD.

My time at Sheffield has been made enjoyable due to the many friends and colleagues who became a part of my life. I am grateful for the time I spent with you and for the best memories I have had. I wish you all the best of luck.

Finally, I would like to express my sincere gratitude to the University of Jordan for the financial support.

Abstract

In this research, the concept of *right-first-time* production of the granules and tablets is achieved via a systems-engineering based approach. The research has been undertaken via two different but synergising phases. In the first phase, various modelling frameworks based on data, process knowledge and laws of physics are proposed to represent the most critical operations (*i.e*. granulation and tabletting) of the tablet production line. In the second phase, these modelling paradigms are exploited in a *reverse-engineering* framework in order to identify the optimal operating conditions to produce a tablet with predefined properties. Therefore, a new approach that embeds constrained multi-objective optimization algorithms is presented to facilitate the implementation of the *reverse-engineering* framework by which the concept of *right-first-time* production is achieved. All the proposed modelling and optimization paradigms are successfully validated via real laboratory-scale experiments, where the granules and tablets are successfully produced right from the first time, and also the waste and recycling ratios are significantly minimized.

Chapter 1

Introduction

1.1 The Pharmaceutical Industry: Challenges and Difficulties

Recently, the pharmaceutical industry, as most other industries, has experienced significant changes in the economic policies and the regulatory environments, where global competition has led to a decrease in the competition-free lifespan of products and a significant decrease in profit margin (Shah, 2004; Suresh and Basu, 2008). Therefore, companies and agencies have adopted the Quality by Design (QbD) paradigm instead of the dominant approach, the so-called Quality by Testing (QbT) approach. The latter, which is based on the empirical design of the manufacturing processes, depends on testing and rejecting the batches that do not meet the imposed specifications (Food and Drug Administration (FDA), 2006; Yu, 2008). By contrast, the QbD approach involves developing a deep process understanding of the effects of the raw materials, the process design and the operating conditions on the product quality. Such an understanding can be then utilized to implement and develop effective quality control strategies (Basu *et al*., 2008; FDA, 2006; McKenzie *et al*., 2006; Reinhardt, 2001; Yu, 2008). Although many companies and agencies have implemented the QbD concept in order to control the process and the variables

affecting it, such an implementation was based on experimental studies only (Barrasso *et al*., 2015). Consequently, the manufacturing unit operations of the pharmaceutical production line remain relatively ill-defined and inefficient when compared to other industries that include different chemical processes (McKenzie *et al*., 2006; Rogers *et al*., 2013). This can be attributed to the challenges and difficulties associated with the process design. In general, such challenges include, but are not limited to, the drug development process (*e.g*. clinical trials) and time, the different physical and chemical properties of each active pharmaceutical ingredient (API) and the effects of these properties on the final product and on the manufacturing processes (McKenzie *et al*., 2006; Reinhardt, 2001). Moreover, one of the greatest challenges is dealing with a fine powder in order to improve its flowability, homogeneity and compactibility. Therefore, granulation, as a size enlargement process, is more often than not utilized to ensure that these properties are obtained and maintained (Abberger *et al*., 2002; Benali *et al*., 2009; Cavinato *et al*., 2010; Khayati *et al*., 2010; Ma *et al*., 2010; Parikh, 2010; Wu *et al*., 2008). In addition to the aforementioned challenges, including the granulation process in the tablet production line has added more challenges to the pharmaceutical industry. For instance, the complex nature of such a process, which, as a single operation, can determine the fate of the final product, makes it difficult to anticipate the granulation behaviours, the granules' properties and, consequently, the tablets' properties, and makes it also difficult to control the production line. Furthermore, the scaling-up of the granulation process from a laboratory scale to a production one is another challenge that has been faced by the pharmaceutical industry (Reinhardt, 2001; Watano *et al*., 2005). These can be the main reasons behind the high recycling ratios, the inefficient operations, and working below the planned capacity in the pharmaceutical industry (Barrasso *et al*., 2015; McKenzie *et al*., 2006; Rogers *et*

al., 2013; Walker, 2007). For the current development paradigm, 27-30% of the total sales of $735 billion in the pharmaceutical industry in 2008 was consumed by the manufacturing operations, such a percentage is considered to be a large proportion of the revenue for many pharmaceutical companies (Basu *et al*., 2008; Global pharmaceutical market forecast, 2008). Therefore, there is a strong need to systematically face these challenges in order to optimise the production line from two viewpoints: product quality and process control.

Process systems engineering paradigms can play a significant role in facing the aforementioned challenges and difficulties. Predictive modelling paradigms, for example, can be utilized instead of actual experiments throughout the process development (Gao *et al*., 2012; Jarvinen *et al*., 2013; Ramachandran *et al*., 2011; Singh *et al*., 2013, 2012; Troup and Georgakis, 2013). They can also be used to enhance the process understanding, explore the design space and define the critical process parameters (Akkisetty *et al*., 2010; Boukouvala *et al*., 2012; 2010; Gernaey *et al*., 2012; Gernaey and Gani, 2010; Schaber *et al*., 2011). Moreover, modelling approaches can pave the way for a systematic process control, and optimization of the final product critical quality attributes.

1.2 Aims and Objectives of the Research

The ultimate aim of this research work is to develop models, which can be utilized to facilitate the production of granules and tablets right from the first time. Achieving such an aim can help companies in the pharmaceutical industry and other industries to:

- Optimize the product critical quality attributes, and also meet any stringent regulations,

- Minimize the amount of the expensive API used in the process development,
- Minimize the new drug development time and, consequently, maximize the competition-free lifespan,
- Minimize the waste and the recycling ratios,
- Maximize the profit,
- Retain leverage in the domain area.

Many objectives need to be ascertained in this research work to ensure that the ultimate aim is systematically achieved. These objectives are as follows:

- Developing modelling frameworks that can:
    - ✓ Predict the properties of the granules and tablets successfully,
    - ✓ Take into account the stochastic phenomena,
    - ✓ Deal with limited, defective and sparse data,
    - ✓ Provide a good understanding of the processes under study, particularly the granulation one.
- Developing a *reverse-engineering* framework that can:
    - ✓ Identify the optimal operating conditions for the granulation and tabletting processes and the optimal granules' properties in order to produce tablets with predefined properties,
    - ✓ Minimize the waste and recycling ratios,
    - ✓ Consider equipment limitations,
    - ✓ Take into account the predictive performance of the modelling frameworks.

1.3 Thesis Structure

As we shall see in later chapters, the ultimate aim of this research work has been ascertained through different stages. The thesis is organized in such a way that each stage is discussed and clarified in a chapter, as illustrated in Figure 1.1. Thus, the overall thesis structure can be described as follows:

Chapter 2 introduces a synopsis of the tablet production line and the granulation and tabletting processes. The related research work in pharmaceutics and granulation is briefly summarised.

The experimental work that was conducted at the laboratory scale is described in Chapter 3, where the factors that have the significant effects are identified and investigated. The collected data are utilized to develop various modelling frameworks. Since the already existing data-driven models (*e.g.* a neural network) were not capable of representing the processes under investigation, this being due to the sparse and limited amount of data, a new modelling framework, which is therefore called an integrated network, is proposed in Chapter 3. Such a model predicts the outputs by modelling and training the data in two consecutive phases. Such a structure is considered in this research work as it is able to extract relevant information from a conservative number of data points, and to capture the complex input/output relationships in the original data because of the number of functions and weights involved. The efficiency of such a model is then improved by characterizing the resulted error using the Gaussian mixture model (GMM) in order to take account of any potential bias in the predicted outputs. Since the successful model is the one that not only can predict the outputs successfully but also can provide the required understanding of a process, particularly if it is ill-defined, fuzzy logic systems (FLSs)

are utilized in this research work to provide a simple ('but not simpler')[1] understanding of the processes.

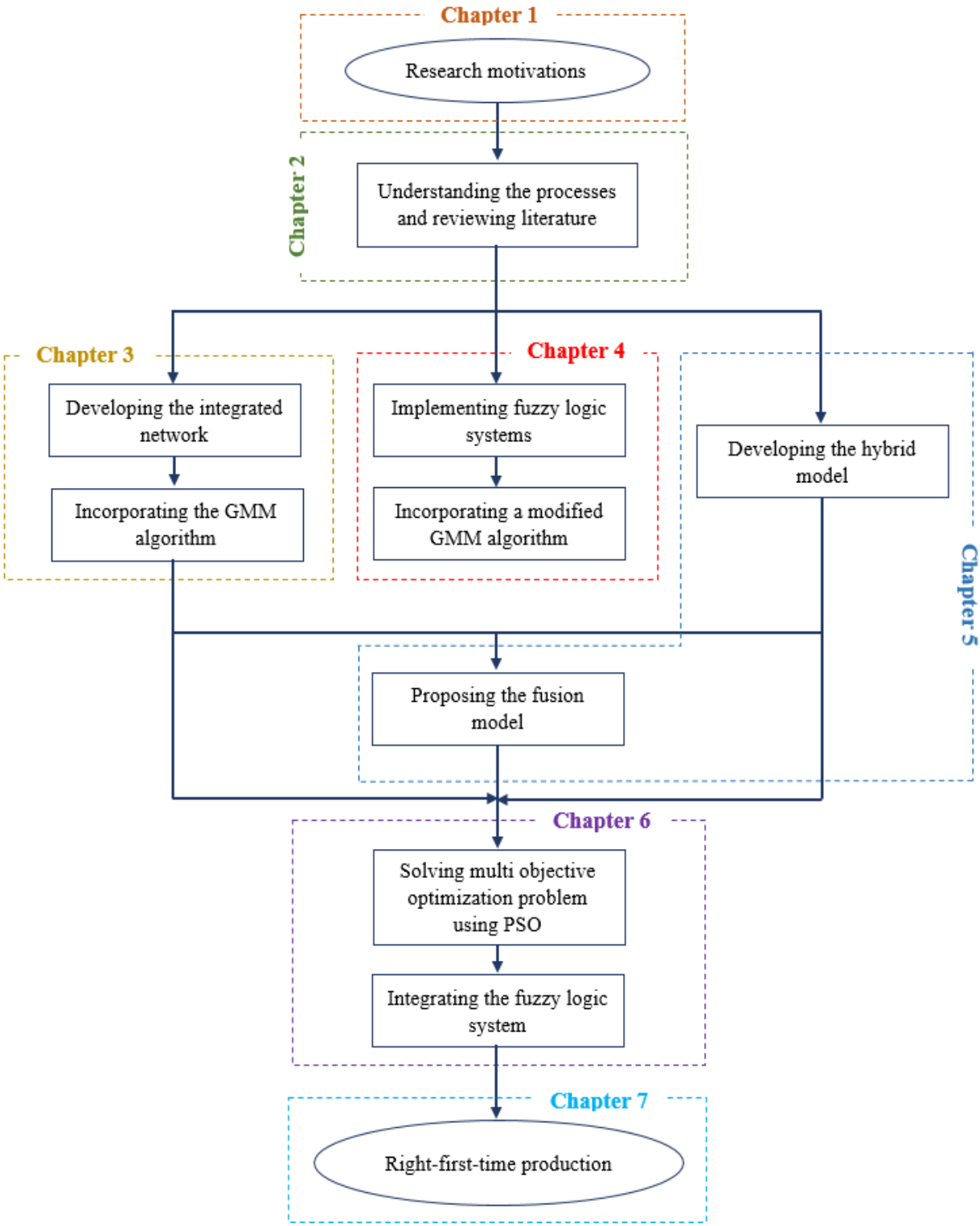

Figure 1.1. Flow diagram of the thesis structure.

[1] Albert Einstein

In Chapter 4, a new systematic modelling framework incorporating FLSs and a modified GMM algorithm is proposed. First, FLSs are elicited in order to predict the outputs of the granulation and tabletting processes, and also to extract informative rules from the collected data, such rules can help user to understand and, consequently, to control these processes. It is worth mentioning at this stage that such a choice is motivated by the fact that fuzzy logic can deal with uncertainties more naturally and, consequently, it can be used to model complex processes using simple and easy to understand rules. Second, a modified GMM algorithm is integrated in the fuzzy systems in order to characterize the error residuals emanating from these systems. Such a model is implemented in such a way that the extracted rules are refined to compensate for any potential bias, which may result from unmodelled behaviours. Although, in this research work, such a framework provided user with a simple understanding of the processes under investigation, the predictive performance has unexpectedly decreased. Therefore, there is a strong need to develop a model that can accurately predict the outputs and can also provide the required understanding.

A hybrid model that consists of three components, namely, a computational fluid dynamics (CFD) model, a population balance model (PBM) and a radial basis function (RBF) network, is proposed in Chapter 5. Such a model is developed not only to predict the outputs of the granulation process but also to understand the evolution and the flow of the granules inside the mixer. Since the granulation process can determine the fate of the final product, accurate predictions of the outputs are usually required. Therefore, a new fusion model that integrates a fuzzy logic theory and the Dempster-Shafer (DS) theory is also presented in this chapter. The motivation for such a new model stems from the fact that integrating predictions from different paradigms can lead to a more robust and accurate topology.

In Chapter 6, a new approach that integrates a particle swarm optimization (PSO) algorithm with a FLS is proposed. Such an approach is utilized to facilitate the development of a *reverse-engineering* framework, by which the concept of *right-first-time* production of the granules and the tablets is achieved. Furthermore, such a framework minimizes waste and recycling ratios.

Finally, Chapter 7 draws salient conclusions with respect to the whole research work with some pointing vectors to future research in this challenging but exciting area of engineering.

1.4 Thesis Contributions to the Current State of Knowledge

This thesis presents original and innovative modelling and optimization frameworks that significantly contribute to the current state of knowledge in granulation and its related industry as well as in systems engineering. The original contributions of this research can be summarized as follows:

- The idea of an integrated network is proposed. Such a network is original in that:
    - ✓ It can extract meaningful information from a sparse and limited amount of data by successfully representing the complex input/output relationships,
    - ✓ It consists of models with different structures that can play a complementary role in modelling the possible patterns of a process,
    - ✓ It circumvents one of the major obstacles for developing data based models; defining the best structure.
- A compensated FLS is developed. Such a model that integrates the FLSs and the GMM is original in that:

- ✓ It provides a simple linguistic understanding of the relationships between the process inputs and outputs,
- ✓ It characterizes the error residuals in a way that can compensate for the assumption that the errors follow a normal distribution, and, more importantly, can refine and retain the rules that are extracted by the FLSs.

- The idea of developing a hybrid framework is presented. The hybrid model, which integrates physical based models and data-driven ones, is original in that:
  - ✓ It combines the strengths of the topologies involved,
  - ✓ It provides a good understanding of the processes under investigation at different levels,
  - ✓ It compensates for some of the assumptions that are normally made to simplify the computational efforts.
- A new fusion model is proposed. Such a model is original in that:
  - ✓ It provides more accurate predictions, and also it improves the reliability of the modelling frameworks,
  - ✓ It resolves any conflict(s) that may exist between the different paradigms,
  - ✓ It shows how different paradigms perform in a space area.
- A *reverse-engineering* framework based on a constrained multi-objective optimization algorithm is presented. Such a framework is original in that:
  - ✓ It inverts complex models in such a way that takes into consideration the performance of these models in the feasible space,

- ✓ It systematically identifies a single optimal solution for a multi-objective optimization problem (MOP).

- *Right-first-time* production of the granules and tablets is ascertained at the laboratory scale. Also, recommendations are made to ascertain such a concept in the related industry.

Chapter 2

Granulation and Tabletting Processes: Background

2.1 The Tabletting Process

In the pharmaceutical industry, tablets are the most popular prescribed drug forms, this being due to the ease of swallowing, solubility, handling and storing such a form of pharmaceuticals (Ennis, 2006). Typically, tablets can be produced by direct compression of a powder, which comprises of a mixture of APIs and excipients, which can usually include diluents, binders, lubricants and many other ingredients (Berthiaux *et al*., 2008; Bouwman *et al*., 2005; Parikh, 2010). Despite the simplicity of such a process, it can only be used when the powder mixture has good properties in terms of flowability, compressibility, and homogeneity, which is not the case for most of the pharmaceutical ingredients. To elucidate, cohesive materials usually stick onto the die, and also some materials may segregate even after blending process (Wu *et al*., 2008; 2005). Therefore, granulation processes, which are size enlargement processes for fine particles, are, more often than not, used to obtain and maintain these properties. A typical tablet production line that involves a granulation process is presented in Figure

2.1. Various processes (*e.g.* coating) can be included in the production line depending on the tablets to be produced. However, the granulation and tabletting processes are considered to be the key stages.

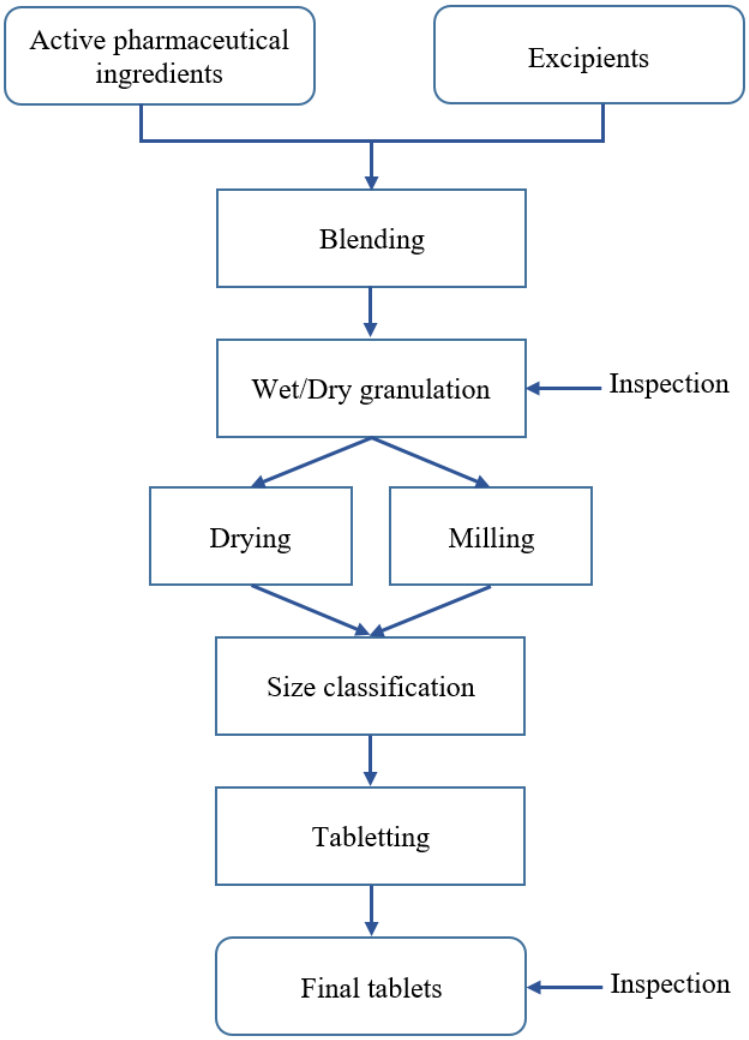

Figure 2.1. A typical tablet production line that involves a granulation process.

Although good powder properties are usually obtained and maintained, including such a process makes it difficult to anticipate the properties of the tablets and to control the whole production line leading, as a result, to high recycling ratios and inefficient operations (Walker, 2007). Thence, diverse research topics have been

covered in pharmaceutics under the umbrella of granulation. The granule properties that may affect the properties of the tablets produced have been extensively investigated (Alderborn, 1988; Ma *et al*., 2010; Parikh, 2010; Walker *et al*., 2005). For instance, Ma and co-workers (2010) investigated the effects of the binder viscosity, its content (*i.e*. liquid to solid (L/S) ratio) and the granules size on the strength and the disintegration time of the tablets, where it was found that the size of the granules had no effect on the strength of the tablets, but the strength increased by increasing the binder content. However, it has been demonstrated later that the granule size affects the strength of the tablets, but the granule size may not affect the properties of the tablet when the compression force is sufficient to break the granules (Sarkar *et al*., 2011). Furthermore, other factors (*e.g*. the compression force and the force rate) that may affect the final properties of the tablets have also been examined in the related literature (Veen *et al*., 2000). By examining the effect of these parameters, it has been shown that the tablet strength decreases when the force rate increases, and the strength of the tablets depends on the properties of the powder used (Marshall *et al*., 1993; Veen *et al*., 2000).

In addition, some of the research papers and books have focused on the formulation by changing the excipient materials and studying their effects on the properties of both the granules and the tablets (Ma *et al*., 2010; Mangwandi *et al*., 2015; Parikh, 2010; Patel *et al*., 2012). The structure transformation of the APIs that may take place during the granulation process has also been investigated (Grunenberg *et al*., 1995; Guo *et al*., 2011; Morris *et al*., 2011). Moreover, the effects of using various granulation and drying techniques on the tablet quality have been extensively studied (Berggren and Alderborn, 2001; Hegedus and Pintye-Hodi, 2007; Huang *et al*., 2010; Murray *et al*., 2007; Patel *et al*., 2011). For example, some researchers have

investigated the effect of various drying methods, which usually follow wet granulation processes, on the strength and the dissolution time of the tablets (Murray *et al*., 2007; Pintye-Hodi, 2007).

Despite the huge body of research in pharmaceutics, it is relatively thin compared to research in granulation, since the latter is considered to be the cornerstone that affects the downstream processes not only in this sector but also in other ones such as detergent, food, chemical and agricultural (Guo *et al*., 2011; Ma *et al*., 2010; Mangwandi *et al*., 2015; Morris *et al*., 2011; Murray *et al*., 2007; Parikh, 2010; Pintye-Hodi, 2007).

2.2 The Granulation Process

Research in granulation started more than 5 decades ago, while some of the pioneering research started much earlier (Capes and Danckwerts, 1965; Newitt and Conway-Jones, 1958). Thenceforth, granulation has attracted a lot of interest, where a great number of books and research papers has been devoted to studying different types of materials for different industries using different equipment (Abberger *et al*., 2002; Benali *et al*., 2009; Cavinato *et al*., 2010; Khayati *et al*., 2010; Knight *et al*., 1988; Li *et al*., 2013; Van den Dries and Vromans; 2004). However, granulation remains an art more than a science where the granulation behaviour and the properties of the granules cannot be anticipated in advance, or even explained. A wide range of topics related to the granulation processes has been covered, these topics include, but not limited to, understanding the effects of the granulation parameters, understanding the physical and chemical science behind the granulation mechanisms, determining the granulation end-point, and modelling of the granulation processes (Alderborn, 1988; Braumann *et al*., 2007; Chaudhury *et al*., 2014; Grunenberg *et al*., 1995; Huang

et al., 2010; Iveson, 2002; Katikaneni *et al*., 1995; Liu *et al*., 2013; Morris *et al*.; 2001; Poon *et al*., 2008; Yu *et al*., 2017; Yu *et al*., 2015). In this research work, these topics are briefly summarized.

Generally, granulation processes can be classified into two major categories; dry and wet granulation. During dry granulation, such as roller compaction, high pressure is applied to the powder mixture to enhance the interparticle bonds without the use of a binder. These granulation processes are suitable for the powder that is highly sensitive to heat and moisture (Ennis, 2006). Whereas in wet granulation, the particles are usually enlarged by adding a sufficient amount of binder to the powder mixture, in addition to the agitation that results from an impeller in a shear mixer, an applied air in a fluidized bed, or twin screws in a twin-screw granulator. Granulation processes can be operated, and so classified, as batch (*e.g*. high shear) or continuous (*e.g*. roller compaction) processes (Chaudhury *et al*., 2014; Ennis, 2006; Yu *et al*., 2015).

Among all the granulation processes, wet granulation processes have received more attention, especially, shear granulation. In general, shear granulation processes can be classified into two types: a low or a high shear one, such a classification is based on the speed of the impeller and the applied force (Knight *et al*., 2001). The latter is the most popular type particularly in the pharmaceutical industry (Ennis, 2006; Guo *et al*., 2011; Litster and Ennis; 2004). The reasons behind this relate to the hard, the dense, and the spherical granules that can be produced using such a process, and to the short production time due to the fast growth and densification processes (Benali *et al*., 2009; Osborne *et al*., 2011; Saito *et al*., 2011; Vonk *et al*., 1997). Since the high shear

granulation (HSG) process is extensively used in the pharmaceutical industry, it will be discussed in more details in this chapter, and also in subsequent chapters.

2.2.1 High Shear Granulation: Granulator Geometry

High shear granulation (HSG), as a wet batch granulation process, is a complex process by which the fine particles are usually enlarged by the addition of a binder under the influence of a rotating impeller. Although the high shear granulators have, in general, different geometries and designs, which significantly affect the final properties of the granules produced (Briens and Logan, 2011; Litster and Ennis, 2004; Saito *et al*., 2011), most of them comprise of a mixing vessel with a top or a bottom driven impeller applying high compression and shear forces to the particles or the granules (Badawy *et al*., 2000; Fu *et al*., 2004; Le *et al*., 2009; Mangwandi *et al*., 2012).

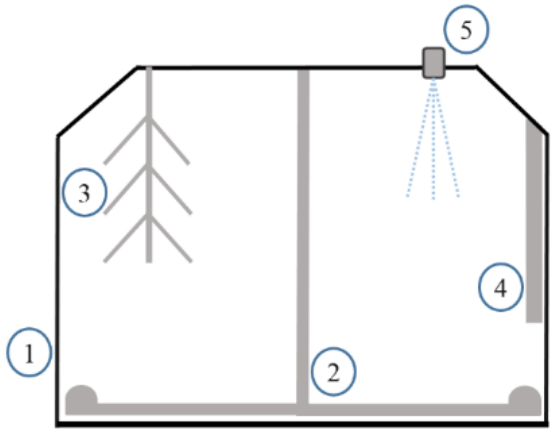

Figure 2.2. Schematic diagram of the main parts of the high shear granulators: (1) granulator vessel, (2) impeller, (3) chopper, (4) scrapper, and (5) nozzle for binder addition.

Most of the granulators are equipped with a chopper in order to break up large agglomerates, and hence enhance a homogeneous distribution of the binder and the APIs (Briens and Logan, 2011; Chitu *et al*., 2011; Kiekens *et al*., 1999). However, the change of the flow pattern that results from the presence of the chopper or the granulation process itself may lead to caking[2] (Albadarin *et al*., 2017; Saleh *et al*., 2015) during the process, especially, at high impeller speed (Albadarin *et al*., 2017; Briens and Logan, 2011; Rahmanian *et al*., 2009; Saito *et al*., 2011; Saleh *et al*., 2015). Thus, a scrapper is usually provided to prevent the granules from sticking in the wall of the vessel and, consequently, leading to caking reduction (Danjo *et al*., 1997; Watano *et al*., 2005). A schematic diagram of the high shear granulator is shown in Figure 2.2.

2.2.2 The Granulation Mechanisms

The different mechanisms occurring and interacting inside the granulator play a significant role in shaping the final properties of the granules (Biggs *et al*., 2003; Iveson *et al*., 2001; Litster and Ennis, 2004; Salman *et al*., 2003; Van den Dries *et al*., 2003). The three main mechanisms are as follows:

- Wetting and nucleation,
- Growth and consolidation,
- Breakage and attrition.

[2] Powder caking is a common phenomenon in granulation and/or agglomeration. Caking is the phenomenon of transforming the powder into a coherent unflowable mass. Although such a phenomenon is undesired one, it is widespread phenomenon in the related industries. Also, such a phenomenon may take place not only during the granulation processes but also during transportation and storage of a powder.

Once these mechanisms are fully understood in terms of when and how they take place and interact inside the granulation vessel, the prediction of the properties of the granules and the process control can become easy tasks. In the high shear granulators, the granulation process starts when the binder is added to the powder particles, where the first interaction between the particles and the binder occurs to form the nucleus, as shown in Figure 2.3.

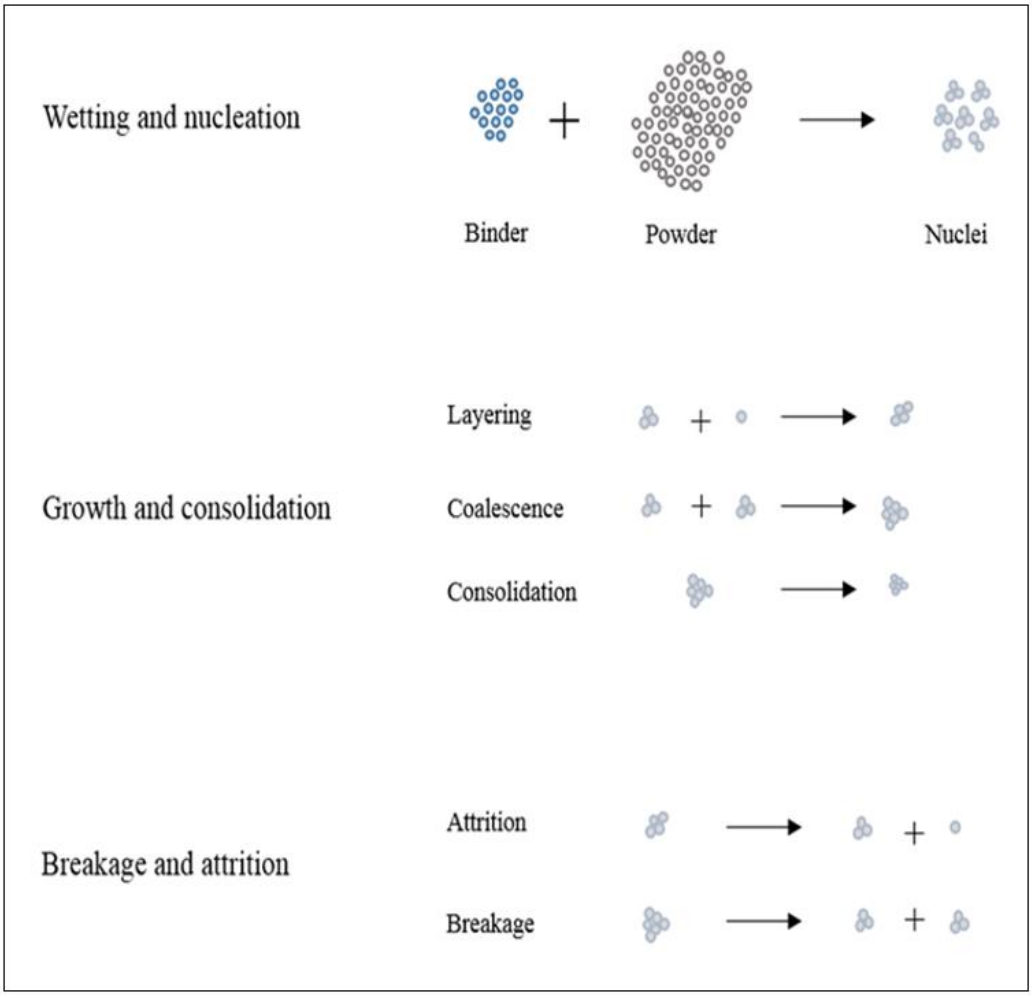

Figure 2.3. Schematic diagram of the granulation mechanisms (adapted from Litster and Ennis, 2004).

Different types of nucleation regimes may occur (Hapgood *et al*., 2003; Litster and Ennis, 2004; Osborne *et al*., 2011), and these will be discussed in more details later in this chapter. Because of the subsequent collisions among the nuclei themselves and between the nuclei and the particles, these nuclei usually grow by different mechanisms: layering, where a small particle or granule sticks with a large granule to form a larger one, and coalescence, where two similar in size granules agglomerate to form a single larger one (Dhanarajan and Bandyopadhyay, 2007; Iveson and Litster, 1998; Litster and Ennis, 2004; Van den Dries *et al*., 2003; Wauters *et al*., 2002). As a result of the compression force, which is due to the collisions among the granules themselves and between them and the vessel wall, consolidation occurs where the porosity usually decreases by squeezing out air (Iveson and Litster, 1998; Wauters *et al*., 2002). Breakage and attrition mechanisms, which also take place because of the collisions, are the reverse processes of the coalescence and layering, respectively. To elucidate further, in attrition, small particles break out of a larger granule, whereas in breakage, the granule breaks into two or more quite similar in size granules (Dhanarajan and Bandyopadhyay, 2007; Litster and Ennis, 2004; Liu *et al*., 2009; Reynolds *et al*., 2005; Van den Dries *et al*., 2003; Wauters *et al*., 2002).

These three main mechanisms are not as simple as they may seem at first glance, because it is simply unknown when a collision between two granules happens, which of these mechanisms will take place (Braumann *et al*., 2007; Darelius *et al*., 2006; Liu *et al*., 2000; Poon *et al*., 2008; Ramachandran and Barton, 2010; Verkoeijen *et al*., 2002). Moreover, the complex nature of the interaction among these three mechanisms makes the prediction, or even the explanation, of the granulation behaviours and hence the properties difficult tasks, especially, when it is very difficult

to monitor such a process on-line (Iveson *et al*., 2001; Litster and Ennis, 2004; Litster and Ennis, 1998).

2.2.3 The Granulation Parameters

The properties of the granules are highly sensitive to a set of input parameters. A reasonably good understanding of the process has been achieved by understanding the effects of these parameters on the properties of the granules as well as on the granulation mechanisms, where changing one of these parameters can make one of the granulation mechanisms dominates the other ones leading to different granule properties (Benali *et al*., 2009; Chitu *et al*., 2011; Mangwandi *et al*., 2011; Rahmanian *et al*., 2009; Tu *et al*., 2009;). In general, the input parameters can be classified into three types, namely; process, formulation and equipment parameters, as listed in Table 2.1 (Faure *et al*., 2001; Guo *et al*., 2011; Rahmanian *et al*., 2009). Among all the input parameters, the impeller speed, the binder properties and its content, the particle size, the granulation time, and the granulator design are considered to be the most crucial variables in the HSG process (Badawy *et al*., 2000; Huang *et al*., 2010; Mangwandi *et al*., 2015).

Table 2.1. The three types of the granulation input parameters.

Process Parameters	Formulation Parameters	Equipment Parameters
• Impeller speed • Chopper speed • Temperature • Granulation time • Mixing time • Bowl load	• Amount of liquid • Type of binder • Density • Particle size distribution • Solubility • Flow properties • Humidity • Viscosity	• Design of the bowl • Design of the impeller • Design of the chopper • The number of impeller blade • Bevel angle • Method of binder addition

Although some of the relationships between the input parameters and the properties of the granules seem to be incompatible, for instance the relationship between the impeller speed and the granule size, where some researchers proved that it is direct (Schaefer *et al*., 1990), whereas other researchers proved that it is an inverse relationship (Knight *et al*., 1998; Schaefer *et al*., 1986), significant advances in the understanding of the granulation process have been achieved. However, the need for further understanding of the evolution of the granules during the granulation process is required, as well as having a quantitative representation of such an understanding (Bjorn *et al*., 2005; Bouwman *et al*., 2006; Darelius *et al*., 2006; Faure *et al*., 2001; Guo *et al*., 2011; Ramachandran and Barton, 2010; Saito *et al*., 2011; Van den Dries and Vromans, 2004).

2.2.4 The Modelling Paradigms

A significant amount of research has hitherto focused on the modelling of the granulation processes, in order to provide the required understanding of the granulation mechanisms, to predict the properties of the granules, and to take a step towards the development of control strategies for such a process (Bjorn *et al*., 2005; Hapgood *et al*., 2009; Liu *et al*., 2013; Mort, 2005; Ramachandran *et al*., 2009). Because of the lack of associated physical equations that can be used to describe the granulation processes, the models that have been proposed in the related literature are either empirical or semi mechanistic models such as PBMs and regime maps (Hapgood *et al*., 2003; Iveson *et al*., 2001; Liu *et al*., 2000; Ramachandran and Barton; 2010; Ramaker *et al*., 1998).

A regime map is one of the useful techniques that has been used to describe the granules, and also to provide the required understanding of the process at the micro

level. For instance, a growth regime map was presented (Iveson and Litster, 1998). Figure 2.4 shows such a map, where the granulation behaviours are represented as a function of the deformation number, which represents the ratio of the impact kinetic energy to the absorbed energy, and the maximum pore saturation.

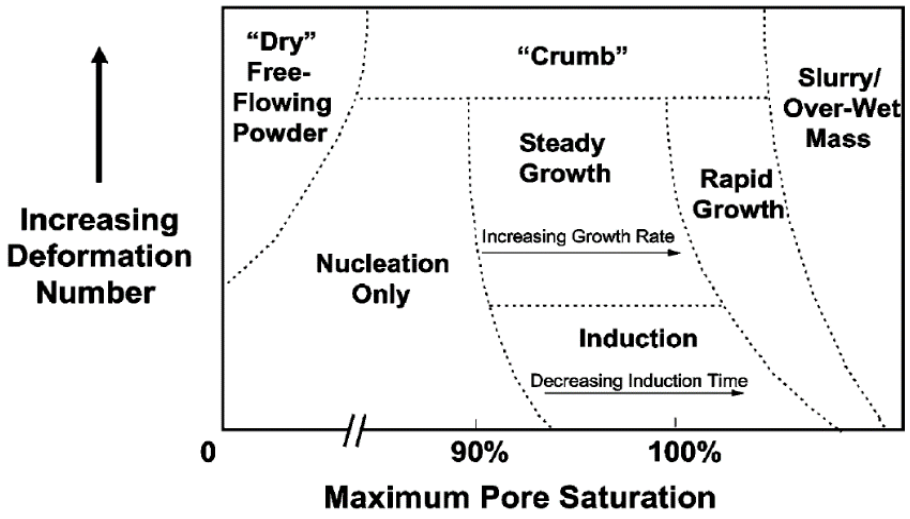

Figure 2.4. The growth regime map (Iveson and Litster, 1998).

It has been observed that different growth behaviours can take place inside the granulator: (i) steady growth, as the name indicates, the granules grow steadily with time, where the weak granules coalesce by collisions; (ii) induction growth where slow growth is usually followed by rapid growth (Iveson and Litster, 1998; Vonk *et al*., 1997); (iii) nucleation behaviour where the growth of the nuclei is very limited because the amount of the binder is insufficient, (iv) crumb behaviour takes place when the contents are too weak to produce granules that are strong enough to resist the applied compression force, and (v) over-wetting where slurry is formed because the amount of the binder is more than the required amount (Hoornaert *et al*., 1998; Iveson *et al*., 2001; Ramaker *et al*., 1998). Regardless of the growth behaviour that may take place inside

the mixer, the maximum size of the granules that can be obtained is limited, this being due to the equilibrium between the growth and the breakage rates (Ramaker *et al*., 1998; Reynolds *et al*., 2005). The quantitative boundaries of the regime map were defined based on experimental results (Iveson *et al*., 2001), where it has been reported in the open literature that these boundaries depend mainly on the properties of materials, the applied force and temperature (Tu *et al*., 2009).

Since all the growth behaviours depend on the wetting and nucleation mechanisms, a nucleation regime map was previously proposed (Hapgood *et al*., 2003). Such a map is a function of the dimensionless spray flux, which is a function of the droplet size, the flow rate, and the powder bed in the spray zone, and the dimensionless droplet penetration time, which is the ratio of the penetration time to the circulation time, which is the time the powder takes to leave and return again to the spray zone (Hapgood *et al*., 2003). At low spry flux and fast penetration time, one droplet forms a nucleus and, as a result, the size distributions of both of them are correlated, this represents the ideal nucleation conditions, the so-called the drop controlled regime. If any of these criteria cannot be met, then the droplets accumulate in the powder surface where they are usually broken by the mechanical mixing and agitation forces, the so-called the mechanical dispersion regime. In the mechanical dispersion regime, the size distributions of the nuclei and the droplets are not correlated. Intermediate regime occurs when both of the previously stated regimes play a role in the nuclei formation (Iveson *et al*., 2001).

In general, the regime maps help to identify the dominant mechanism using simple parameters, hence, these maps can be used as scaling-up approaches (Hapgood *et al*., 2003). However, one cannot quantitatively predict the properties of the granules.

To elucidate, it is difficult to anticipate the change in the granules' properties when a change in one of the input parameters takes place (Iveson *et al*., 2001). Moreover, these maps consider the change in granule size only and ignore the other properties of the granules such as shape, porosity and strength (Iveson and Litster, 1998; Tu *et al*., 2009).

In the related literature, there are many other approaches that have been utilized to model and represent the granulation process. The modelling paradigms that have been developed and applied are either data-driven (*e.g*. neural networks) or physical based models (*e.g*. PBMs) (Bjorn *et al*., 2005; Braumann *et al*., 2007; Mansa *et al*., 2008; Miyamoto *et al*., 1997; Ramachandran and Barton, 2010; Sanders *et al*., 2003; Watano *et al*., 1997; Yu *et al*., 2015). These approaches will be discussed in more details in later chapters.

2.3 Summary

Granulation, as an enlargement process, has been extensively utilized in different industries including, but not limited to, chemical, mineral, agriculture, food, and pharmaceutical industries, in order to improve the properties of a powder and facilitate the downstream processes. This may be the main reason behind the huge body of research that has hitherto been devoted to the understanding and the modelling and simulation of such a process. However, granulation remains an art more than a science where neither the granulation behaviour nor the associated properties can be predicted well in advance, leading, as a result, to inefficient operations and high recycling ratios (waste). Among all the granulation processes, HSG has been extensively used because of its short processing time due to the fast growth and densification processes.

In this chapter, several studies that have been presented in the related literature were briefly summarized. Some of these studies have been devoted to the understanding of the granulation process and its three main mechanisms, and the effect of the different input parameters on the final properties of the granules produced. Other studies have been directed at the modelling and simulation of such a process. Various modelling approaches have been proposed in the open literature, these approaches are either data-driven or physical based paradigms. More details about these paradigms will be presented in later chapters.

Various data and physical based models for the granulation and tabletting processes will be developed, as we shall see in the subsequent chapters. In the next chapter, a new modelling framework called an integrated network will be developed to represent both the granulation and the tabletting processes.

Chapter 3

Predictive Modelling of the Granulation and Tabletting Processes Using a Systems-Engineering Approach[3]

3.1 Introduction

As mentioned in the previous chapter, many research studies have focused on the understanding of the granulation and the tabletting processes (Benali *et al*., 2009; Bouwman *et al*., 2006; Chitu *et al*., 2011; Mangwandi *et al*., 2011). In the related literature, one can notice that the focus was and will always be on the granulation process, this being due to the fact that such a process is considered to be the most difficult phase of the whole production line. Once the granulation process can be successfully modelled and predicted, the development of a modelling framework for the tabletting process will become an easy task. Therefore, the main focus in this chapter, and in the subsequent chapters, is on the granulation process.

[3] The content of this chapter is published in "AlAlaween, W.H., Mahfouf, M., Salman, A.D., 2016. Predictive modelling of the granulation process using a systems-engineering approach. Powder Technology. 302, 265-274".

In general, a deeper understanding of the granulation processes either via data, expert knowledge and/or laws of physics should pave the way for an effective and robust modelling framework to predict the associated behaviours. Several studies have been devoted to the modelling of the granulation processes, but because of the lack of associated physical equations that should describe these processes, such models are normally either empirical or semi mechanistic models (Bjorn *et al*., 2005). As already stated in Chapter 2, a regime map has been used to describe the granulation mechanisms, namely; wetting and nucleation, growth and consolidation, and breakage and attrition (Hapgood *et al*., 2003; Iveson and Litster, 1998). Although it was not fully able to represent the associated mechanisms and the properties quantitatively, a comprehensive understanding of the granulation processes at the micro-level was, however, reached (Tu *et al*., 2009). In addition, PBMs, by which the rate of change in the number, mass, or volume of the granules during the process is investigated, have been used to predict the properties of the granules and the granulation behaviour (Immanuel and Doyle III, 2005; Liu *et al*., 2013; Poon *et al*., 2008; Sanders *et al*., 2003). Various granules' properties and granulation mechanisms have hitherto been investigated. One of the difficulties in carrying-out the population balance based modelling lies in the consideration of all interactions among the granulation mechanisms which are fundamental requirements necessary for shaping the properties of the granules (Iveson, 2002). To characterize such interactions, an integration between a multi-dimensional PBM and a stochastic method (*e.g.* Monte Carlo) has been proposed (Braumann *et al*., 2007). In addition, the number of the properties that can be monitored using such a technique is limited, with up to three properties only being examined in most published research papers and books. In fact, finding a

solution can even prove to be a difficult exercise when more granules' properties be included (Iveson, 2002).

With the recent advances in computing power, data based modelling approaches have been utilized to model the granulation processes, where the main aim is to find a mapping between a set of inputs and outputs instead of deriving the real physical equations (Bishop, 1995). Linear regression models have been employed to predict the properties of granules and to find the optimal set of input parameters (Miyamoto *et al*., 1997; Westerhuis *et al*., 1997). Such modelling paradigms are, in fact, incapable of accounting for the sophisticated nonlinear relationships or even the complex interactions among the input parameters that control the granulation processes (Bishop, 1995). Artificial neural networks (ANN) and fuzzy systems have been investigated previously to predict the properties of granules and to scale-up the granulation processes (Mansa *et al*., 2008; Murtoniemi *et al*., 1994; Watano *et al*., 1997; Yu *et al*., 2015). However, because these so-called soft-computing techniques represent powerful interpolators, there exist no guarantees that they will perform well beyond the training range (Bishop, 1995). Although these techniques have been extensively employed in various other equally challenging areas (*e.g.* industrial, academic, and medical) where their effectiveness and efficiency have been demonstrated (Chen *et al*., 2015; Datta *et al*., 2015; Kim *et al*., 2008), they have not been well exploited to deal with the challenges and uncertainties in the granulation processes. The reason for this relates to the availability of meaningful data/information needed to derive effective predictive models for granulation. Consequently, these techniques and other data-driven approaches can represent a promising development in dealing with the problems surrounding the granulation processes if meaningful information can be extracted from the available data.

In this chapter, a modelling framework which includes the idea of an integrated network is proposed in order to extract meaningful information from a conservative number of granulation data, which were collected from a series of laboratory experiments, where the main motivation behind such a framework is to achieve a satisfactory model performance exploiting such a limited amount of real (systematic) data. In order to improve the model performance, the network-based error predictions are characterized using a GMM to account for any behaviour deemed of a stochastic nature.

3.2 The Experimental Work

In order to develop the modelling frameworks to describe and simulate the HSG and the tabletting processes, a set of laboratory-scale experiments were conducted. The experimental work is illustrated in Figure 3.1.

3.2.1 The Granulation Process

Calcium Carbonate ($CaCO_3$, D_{50}=0.085mm) was granulated using a high shear Eirich mixer (1 Litre vertical axis granulator with a top-driven impeller, Maschinenfabrik Gustav Eirich GmbH & Co KG, Hardheim, Germany). Polyethylene Glycol (PEG 1000) with a melting point of approximately 40ºC was used as a binder. Before the start of the granulation experiment, the binder was melted, and the powder was pre-heated to approximately 35ºC to make sure that the binder would not solidify before the granulation process. The binder was poured-in on the powder bed while both the vessel and the impeller were rotating in the same direction (clockwise). For all experiments, the binder addition lasted for approximately three minutes.

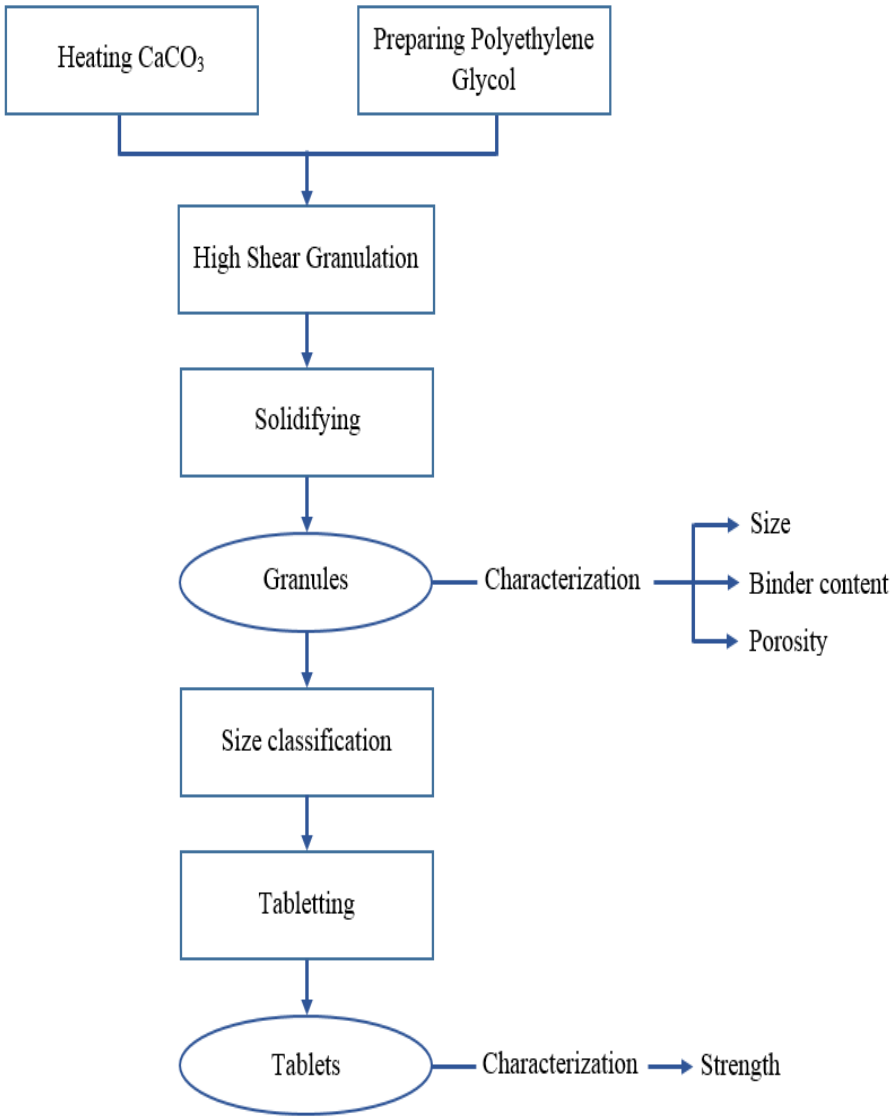

Figure 3.1. Flow diagram of the experimental work.

The Eirich granulator is equipped with a scrapper and impellers with different shapes. It is worth mentioning at this stage that only two impellers were used in this research, as shown in Figure 3.2; the two impellers not being in the centre of the 16cm diameter vessel.

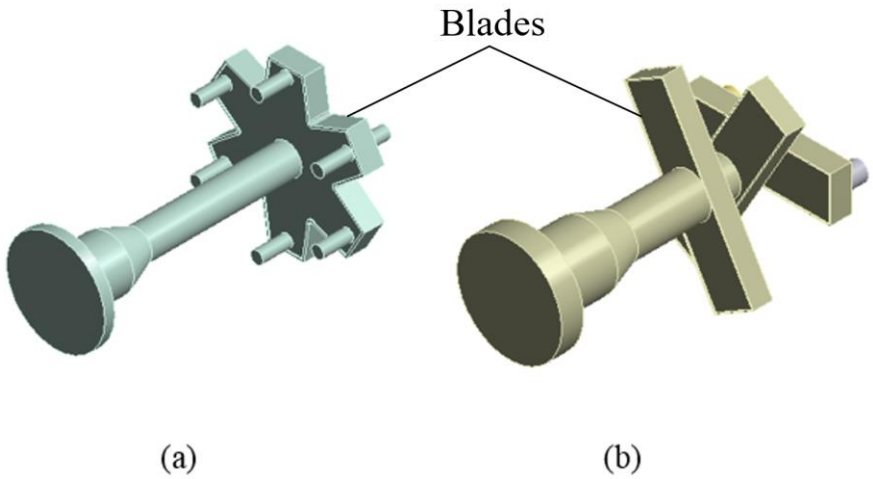

Figure 3.2. CAD drawing of the impeller types (a) impeller type I, bin impeller, and (b) impeller type II, star impeller (Reproduced with Permission from Maschinenfabrik Gustav Eirich GmbH & Co KG., Hardheim, Germany, January 2017).

In this research work, the impeller shape is considered as an input variable in addition to three other variables, namely; impeller speed, granulation time and liquid to solid (L/S) ratio, as listed in Table 3.1. The speed of the vessel was kept constant at 170 rpm. The levels of each variable were defined by conducting a set of trial experiments. Although, there are many parameters that may affect the granulation process, the aforementioned ones are the most crucial parameters for the HSG process using specific materials (Briens and Logan, 2011; Chitu *et al*., 2011; Fu *et al*., 2004; Guo *et al*., 2011; Litster and Ennis, 2004; Rahmanian *et al*., 2009).

Statistical correlation analysis was performed between the investigated input parameters and the properties of the granules, where the size was represented using the three diameters: D_{10}, D_{50} and D_{90}. Reasonable correlation coefficients among most of them are shown in Table 3.2, even though some parameters have different correlation values between the two types of the impeller, for example the relationship between the

granulation time and porosity using impeller type I is stronger than the same relationship when impeller type II was used. By using the analysis of variance (ANOVA), it was found that the impeller type, as an input variable, has an effect on the properties of the granules, where the P-value is less than 0.05.

Table 3.1. The inputs and outputs of the granulation process.

Inputs	Inputs' levels	Outputs
Impeller speed	1000, 2000… 6000 (rpm)	Size (µm)
Granulation time	6, 10, and 15 (min)	Binder content (%)
L/S ratio (w/w)	13, 14, and 15 (%)	Porosity (%)
Impeller shape	Two different shapes	

The granulation experiments were carried-out based on a full factorial design of experiments resulting in 108 experiments. Once the granulation experiment was completed, the granules were left at room-temperature to allow the binder to solidify. The size of the granules was then measured using the Retsch Camsizer (Retsch Technology GmbH, Haan, Germany). The porosity and the binder content of the granules were measured for different size classes in the size range (180-2000µm) using a Pycnometer (Fu *et al*., 2004) and the method discussed in (Knight *et al*., 1998), respectively. It is worth mentioning at this stage that each measurement was repeated three times. Figure 3.3 shows the data (*i.e*. experiment) distributions using two variables at a time. It is noticeable that the collected data are sparse and limited. This is considered as one of the difficulties in modelling the granulation process, especially for some industrial applications, including the pharmaceutical industry, where the acquiring of such data alone can be an expensive enterprise.

Table 3.2. The correlation coefficients[*].

Outputs	Impeller type I					Impeller type II				
	Size			Binder content[**]	Porosity[**]	Size			Binder content[**]	Porosity[**]
Inputs	D_{10}	D_{50}	D_{90}			D_{10}	D_{50}	D_{90}		
L/S ratio	0.53	0.36	0.14	0.23	-0.21	0.49	0.46	0.37	0.61	0.02
Granulation time	0.21	0.19	0.09	-0.19	0.32	-0.30	-0.27	0.02	-0.2	-0.12
Impeller speed	0.04	-0.27	-0.35	0.15	-0.04	-0.07	-0.36	-0.64	0.21	-0.1

[*] Pearson correlation coefficient measures the strength and the direction of a linear relationship between two variables.
[**] The binder content and porosity values for the size class (500-710µm) are presented.

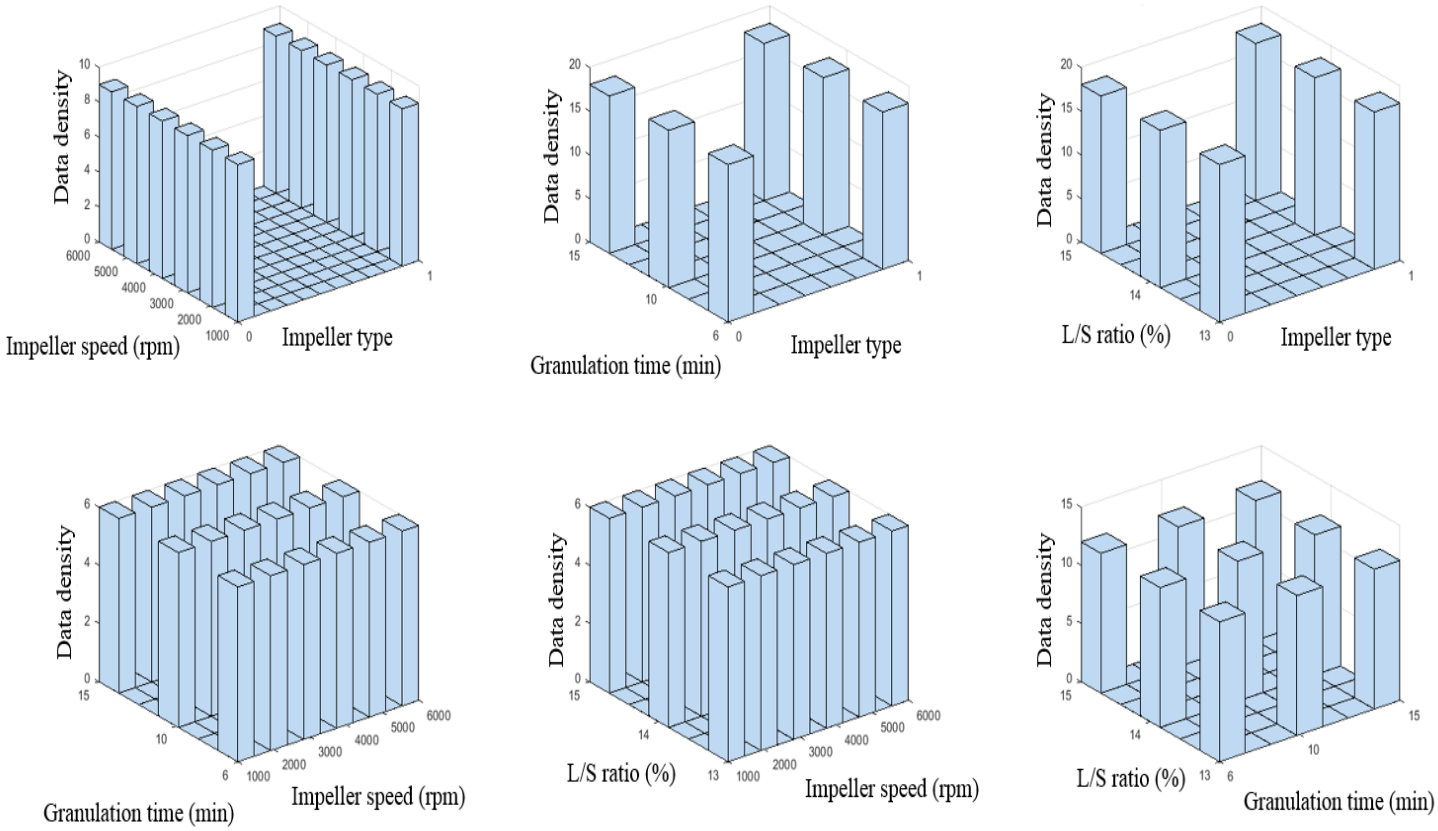

Figure 3.3. The density distributions of the experimental data.

3.2.2 The Tabletting Process

Once the granules produced were classified, the granules in the size ranges (500-710μm) and (710-1000μm) were compressed using a 10mm diameter set of die and punch to produce tablets. All the operating conditions (*e.g*. compression force and speed) of Instron (3369 dual column, Buckinghamshire, UK) were kept constant. Thus, only the effects of the properties of the granules were investigated. Finally, the strength of the tablets produced was measured using Zwick/Roell Z0.5 (Zwick/Roell, Germany). It is worth emphasising at this stage that five tablets were produced from each size class for each experiment, and the average value was used in this research.

3.3 The Integrated Network

3.3.1 The Integrated Network: Model Development

In the last 2 decades or so, the theme of computational intelligence has been extensively reflected in several disciplines such as medicine and metallurgy (Nunes *et al*., 2005; Vertyagina and Mahfouf, 2014; Zhang *et al*., 2015), where the observed data are utilized to establish data-driven models that can replace or complement physical based models where they simply do not exist or they may be too complex to elicit. Therefore, the core of such type of modelling rests with process data (Yang *et al*., 2011). In the case of the granulation process, the difficulty stems from the lack of representative information. In addition, the complex input/output relationships may not be captured by the available amount of sparse data. As stated previously, an integrated network as a data-driven model is proposed in this chapter. Developing such a structure does not only consist of mapping the inputs to the outputs, but also discovering knowledge that may not be easy to extract by the already available approaches.

The idea of the so-called 'network' relies on having a number of models with different structures, thus, (i) complex input/output relationships could be captured because of the number of functions and weights included (Opitz and Maclin, 1999), (ii) models with different structures could play a complementary role in modelling the possible patterns of the process, and (iii) training the data through two stages could help to extract the associated knowledge required for accurate property predictions (Gaffour *et al*., 2010).

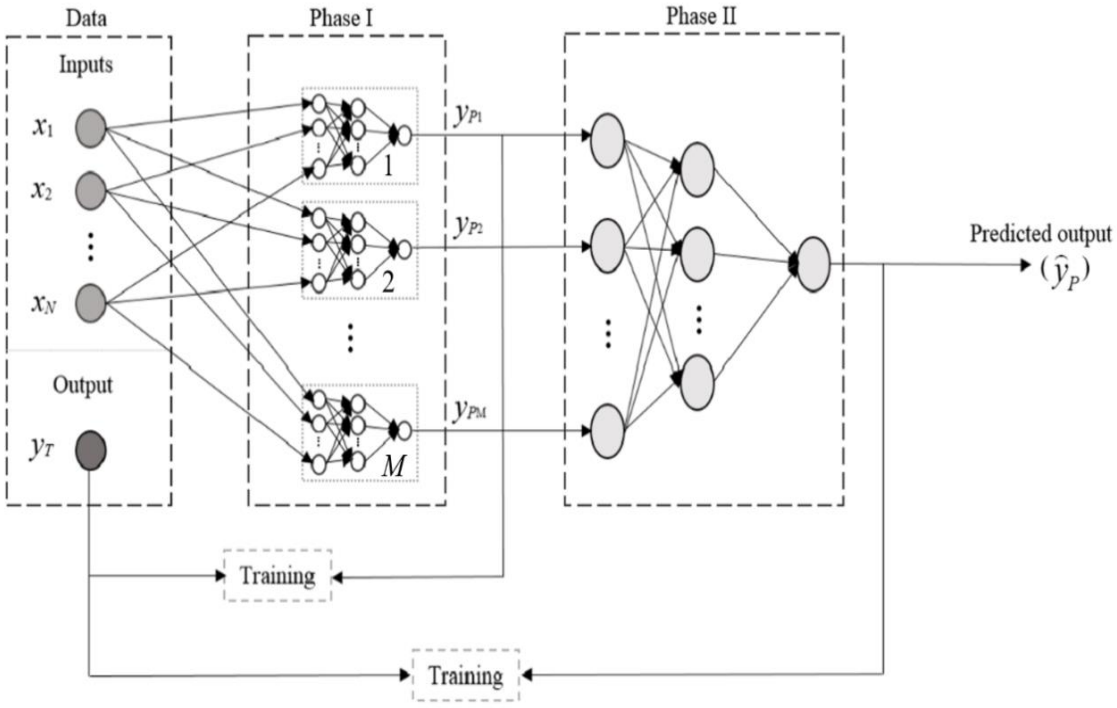

Figure 3.4. The architecture of the integrated network.

Figure 3.4 depicts the integrated network architecture for multi-input single-output (MISO). The network relies on predicting the final output using two modelling phases. In phase I, the *N* inputs (x_n) and the target output (y_T) are used to train *M* models with different structures. These models can be neural networks or neuro-fuzzy models. The predicted outputs from each model (y_{P1}, y_{P2}… y_{PM}) and the target output (y_T) are

then utilized to train another model in phase II to lead to the final predicted output ($\hat{y}_P$), where this model should be capable of modelling linear and non-linear relationships to extract the hidden information and to capture the complex relationships in the original data. The efficiency of the RBF network has been proved via several application areas (Bishop, 1995; De Alejandro Montalvo *et al*., 2015; Ebtehaj *et al*., 2016; Gaffour *et al*., 2010), hence, it is employed in this research work to model the HSG and tabletting processes.

Generally, an RBF network consists of three layers, namely; an input layer, basis functions acting as a hidden layer, and an output layer. Each basis function is a function of the radial distance from a defined centre. These functions are usually used to map an input vector to its corresponding target. Thus, the predicted output is presented as follows (Bishop, 1995):

$$y_P(x) = \sum_{i=1}^{I} w_i \phi_i(x) + w_0 \tag{3.1}$$

where w_i and w_0 are the coefficient connecting the i^{th} basis function to the output neuron and the bias, respectively, and ϕ_i is the basis function. A popular selection of such a function is Gaussian, this being due to its ability to approximate any function with a reasonable accuracy using a sufficient number of Gaussian components (Bishop, 1995). The RBF network is also used in phase II. Analytically, the two phases of the integrated network are simply a combination of composition and superposition of the basis functions. To prove the capabilities of the presented structure and by using a single RBF model in the two phases, the final predicted output can then be written in the form:

$$\hat{y}_P = \sum_{k=1}^{K} w_k^{(2)} \phi_k \left(\sum_{i=1}^{I} w_i \phi_i(x) + w_0 \right) + w_0^{(2)} \tag{3.2}$$

the parameters in (3.2) are as defined previously, where the superscript number is used to distinguish the parameters of the second phase from the ones used in the first phase. Assuming that all models are optimized in terms of the number of basis functions and the connecting coefficients, the composite function presented in (3.2) is able to minimize the error that is the difference between the predicted output and the target. It has been proved that the composite function is dense in a convex data space (Cybenko, 1988; Mateljevic and Pavlovic, 1995), which means that the difference between the predicted and the target values would be smaller.

Although, the number of models in the first phase has been neglected in the discussion above, it however plays a crucial role in the proposed structure. By including the *M* models, the inner function of (3.2) could be written as a superposition of the basis function. In a similar way, the theorem that has been presented in (Cybenko, 1989; Mhaskar and Micchelli, 1992) demonstrates that the approximated function is also dense in the data space. Thus, the combination of the superposition and composition of the basis functions could considerably improve the model performance.

The scaled conjugate gradient (SCG) algorithm is utilized with the backpropagation network to determine the network parameters for both phases (Bishop, 2006; Bishop, 1995). The root mean square error (RMSE) is usually employed to select the best network structure (*i.e.* the number of basis functions) that achieves a trade-off between a good training and generalization capability (Bishop,

2006; Bishop, 1995; Gaffour *et al*., 2010; Yang *et al*., 2003). These steps are shown in Figure 3.5.

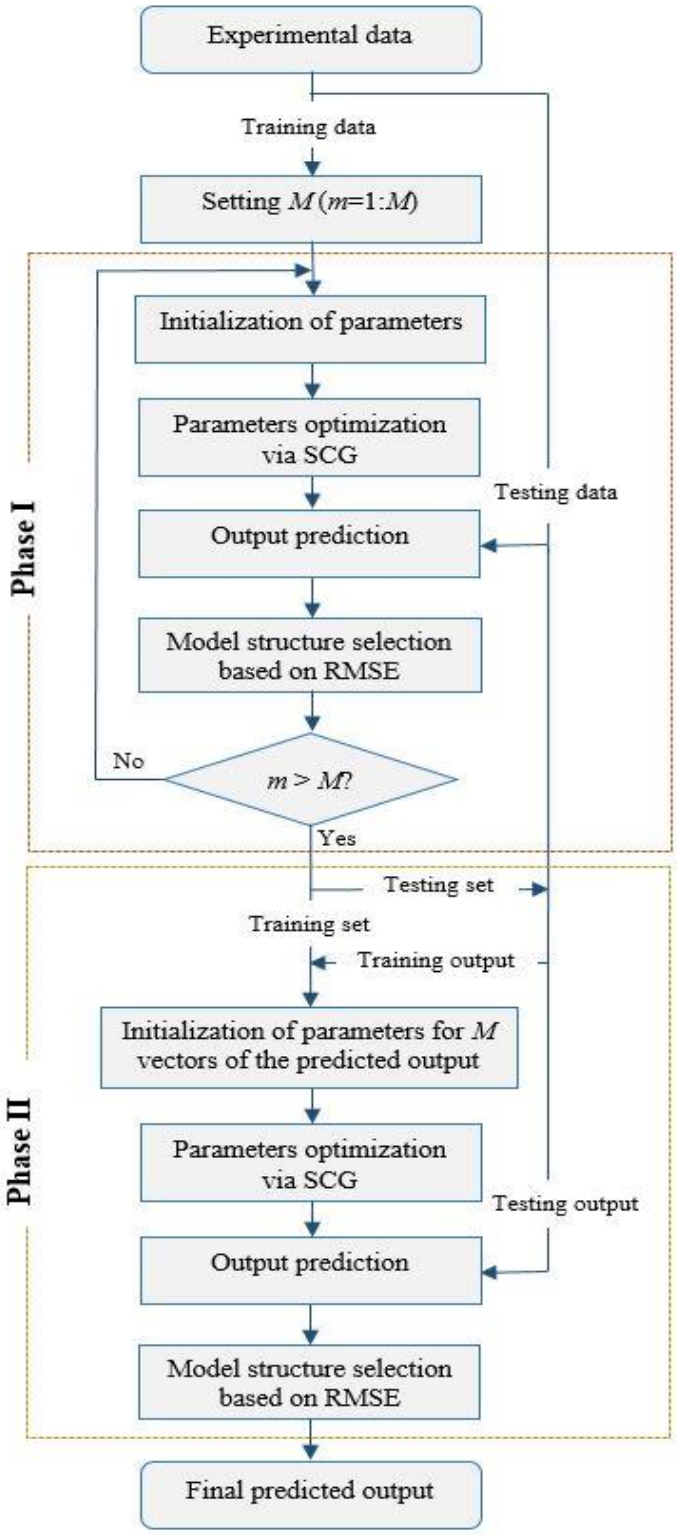

Figure 3.5. Flow chart of the integrated network.

3.3.2 The Integrated Network: Results and Discussion

A. The Granulation Process

A single RBF network was developed here to model the HSG process using a program written using Matlab software by the author of this thesis. The data were divided into two sets: training and testing. In general, the training data set allows the model to learn the relationships among the granulation inputs and the outputs, while the testing data set assesses its generalization performance. The division of the data into these sets has a significant influence on the performance of the model; by the division of the data one means not only the number of data points in each set but also their distribution in the space under study. Different division methods have hitherto been investigated, including the 10-fold cross-validation technique, but it has been found that dividing the data randomly into a training set (5/6) and a testing set (1/6) was the best methodology in order to develop a meaningful model with a reliable performance (Bishop, 2006). The number of RBFs that was selected corresponds to the minimum error evaluated via the RMSE. The SCG optimization algorithm was employed for training.

For a single size class (710-1000μm) and using 8 RBFs, the performance of the RBF network for the binder content is shown in Figure 3.6, with a RMSE (training, testing) = [0.916, 0.958]. The coefficient of determination value is R^2 (training, testing) = [0.54, 0.31]. These performance measures indicate that the RBF-based model on its own was not able to capture the complex input/output relationships and to achieve adequate generalization capability. In a similar manner, the results obtained for the other variables are summarized in Table 3.3, where the size is represented by its three diameters: D_{10}, D_{50}, and D_{90}.

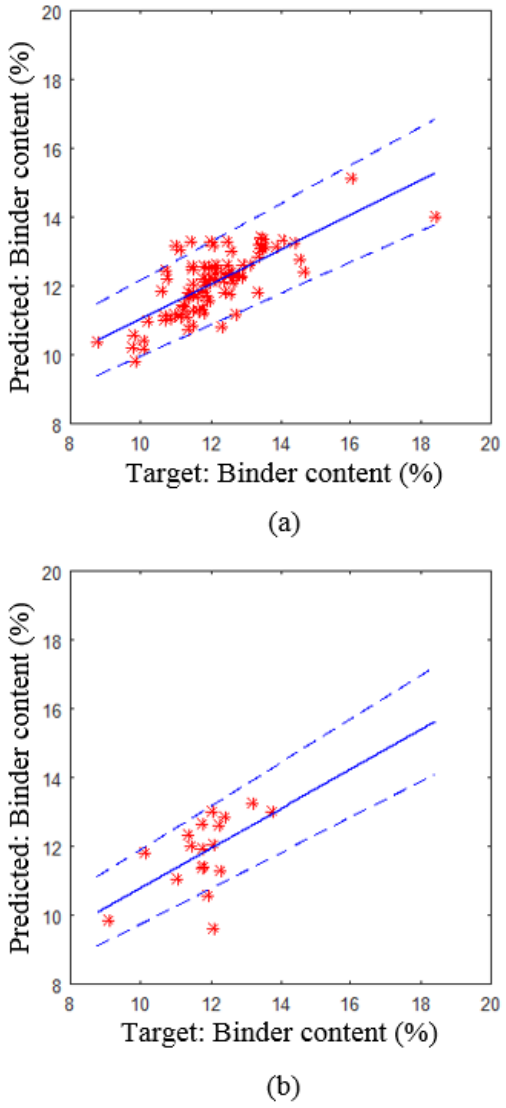

Figure 3.6. The RBF model for the binder content:
(a) training, (b) testing (with 10% bands).

To improve the prediction performance of the RBF network, an ensemble model was implemented (Opitz and Maclin, 1999), where the outputs of multiple networks are combined, commonly, by a simple averaging method (Zhao and Zhang, 2011). Ten RBF networks were initialized using a different number of basis functions each time, as listed in Table 3.3, and different values for the connecting coefficients.

Table 3.3. The performances of the models represented by RMSE and R^2.

Models	Output	Binder content (710-1000µ*m*)		Porosity (710-1000µ*m*)		Size (*mm*)					
						D_{10}		D_{50}		D_{90}	
		Train	Test	Train	Test	Train	Test	Train	Test	Train	Test
RBF	R^2	0.54	0.31	0.44	0.27	0.53	0.31	0.64	0.33	0.58	0.41
	RMSE	0.92	0.96	1.83	2.82	0.15	0.21	0.26	0.72	1.12	1.01
	No. BFs	8		4		6		9		8	
RBF with bias compensation	R^2	0.64	0.55	0.54	0.15	0.68	0.34	0.72	0.34	0.65	0.37
	RMSE	0.81	0.82	1.67	3.05	0.12	0.19	0.23	0.72	1.03	1.07
	No. GCs	9		8		5		8		9	
Ensemble	R^2	0.59	0.45	0.63	0.43	0.73	0.72	0.77	0.77	0.84	0.78
	RMSE	0.99	0.67	1.71	1.82	0.12	0.08	0.31	0.2	0.81	0.73
	No. BFs	(10, 5, 1, 4, 1, 3, 7, 9, 5 and 6)		(6, 4, 5, 15, 11, 7, 13, 4, 3 and 6)		(4, 11, 7, 4, 5, 10, 9, 13, 3 and 3)		(15, 13, 10, 15, 7, 6, 3, 4, 7 and 11)		(12, 11, 14, 6, 9, 15, 4, 2, 9 and 3)	
Ensemble with bias compensation	R^2	0.63	0.61	0.67	0.29	0.79	0.62	0.76	0.8	0.86	0.79
	RMSE	0.87	0.57	1.57	1.99	0.11	0.11	0.28	0.18	0.68	0.69
	No. GCs	9		8		9		9		5	
Integrated network	R^2	0.75	0.74	0.74	0.74	0.86	0.9	0.83	0.87	0.92	0.89
	RMSE	0.62	0.9	1.31	1.91	0.08	0.04	0.23	0.14	0.45	0.67
	No. BFs (2)	10		8		6		6		8	
Integrated network with bias compensation	R^2	0.82	0.74	0.76	0.74	0.87	0.92	0.86	0.84	0.93	0.89
	RMSE	0.52	0.86	1.26	1.86	0.08	0.04	0.21	0.18	0.41	0.66
	No. GCs	10		6		6		7		8	

1. 'No. BFs' stands for the number of basis functions.
2. 'No. GCs' stands for the number of Gaussian Components.
3. 'No. BFs (2)' represents the number of basis function in the second phase of the integrated network where the 10 models in the first phase have the same structure as the ones in the ensemble model.

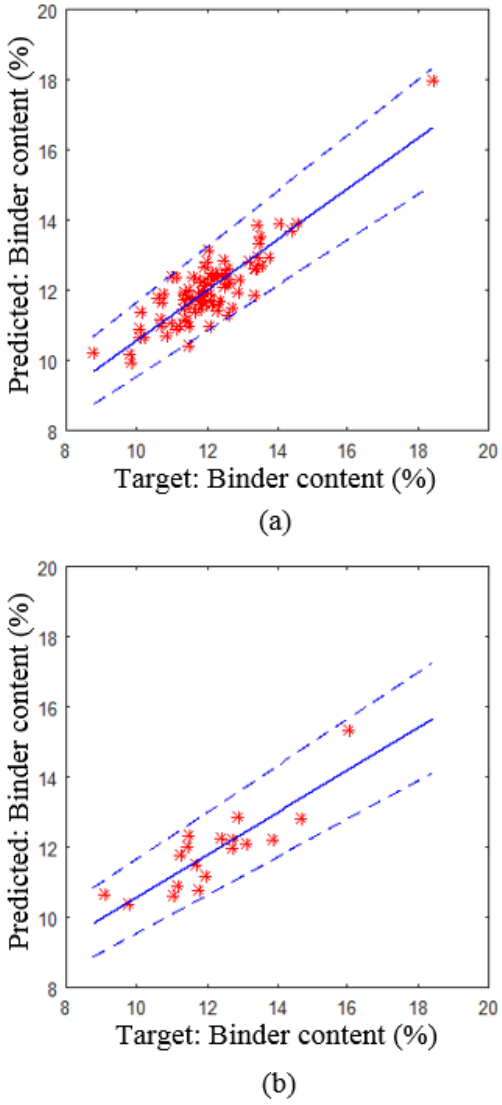

Figure 3.7. The integrated network based on 10 RBF models for the binder content: (a) training, (b) testing (with 10% bands).

The prediction performance for the ensemble model is superior to that of the single network above, with an improvement of 28% in RMSE for the testing data set. Furthermore, the new integrated network structure based on the 10 RBF models in the first phase, having the same structure as that of the ensemble model, and a single RBF model in the second phase was established. The integrated network performance for the binder content (710-1000μ*m*) is R^2 (training, testing) = [0.75, 0.74], as shown in

Figure 3.7, while examples of the predicted and the experimental distributions for all the investigated properties are presented in Figure 3.8.

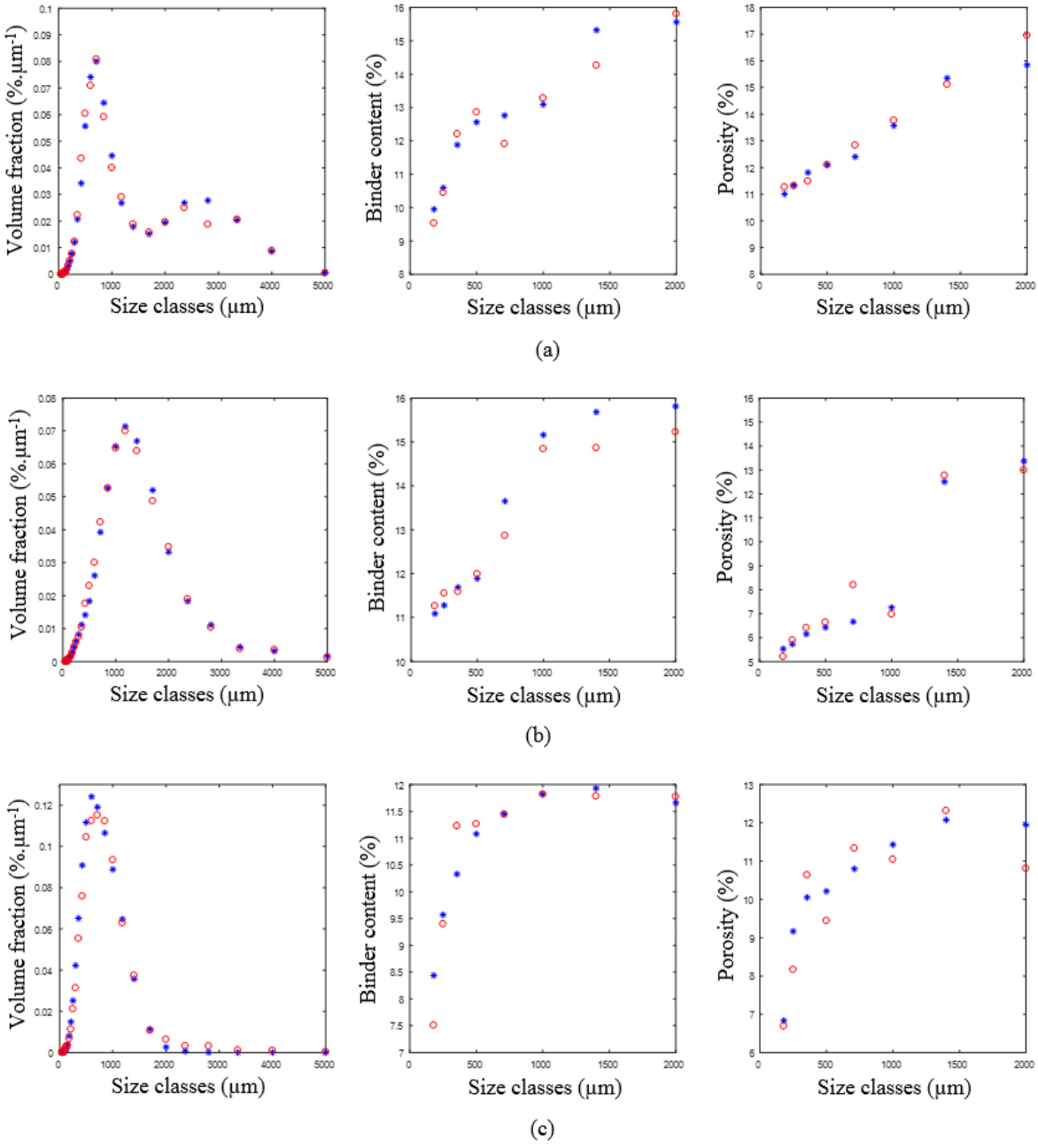

Figure 3.8. The integrated network: the predicted (o) and the experimental (*) distributions for the size, binder content and porosity (a) using impeller type II, speed=2000rpm, L/S ratio (w/w)=14% and granulation time=10min; (b) using impeller type II, speed=6000rpm, L/S ratio (w/w)=15% and granulation time=15min; (c) using impeller type I, speed=4000rpm, L/S ratio (w/w)=13% and granulation time=6min.

The obtained results prove the ability of the integrated network in dealing with the difficulties and complexity of the granulation behaviour. The R^2 value for the integrated network is approximately twice the value for the single RBF network, whereas the overall improvement over the ensemble model is approximately 34%.

B. The Tabletting Process

The integrated network was also utilized to represent the tabletting process. An integrated network based on 10 RBF models, which have different structure (*i.e.* number of basis functions), in the first phase and a single RBF model in the second phase was established. The properties of the granules and the strength of the tablets were used as the inputs and the output of the integrated network, respectively.

The model performance for the tablet strength is presented in Figure 3.9, with a R^2 (training, testing) = [0.75, 0.74]. The predictive performance for the strength was actually worse than the overall performance for the granule size, but better than the overall performances for the binder content and porosity, as listed in Table 3.3. Such a relatively low performance was actually expected because of the uncertainties in both the inputs and the output of the model that was developed for the tabletting process. To elucidate further, the heterogeneous distributions of the binder content and air (*i.e.* porosity) of the granules seemed to affect only the outputs of the model that represents the granulation process, and both the inputs and the output of the model that represents the tabletting process. It is also worth mentioning at this stage that the performance of the integrated network measured by the R^2 value was approximately four times and twice the performances of the single RBF model and the ensemble one, which was developed using 10 RBF networks, respectively. Thus, these models were not utilized to model the tabletting process.

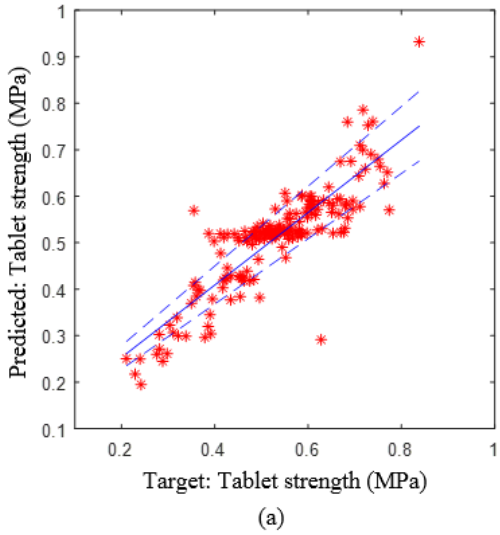

Figure 3.9. The integrated network for the tablet strength:
(a) training and (b) testing (with 10% bands).

3.4 Error Modelling Using the Gaussian Mixture Model

3.4.1 Error Modelling Using the Gaussian Mixture Model: Model Development

Occasionally, the error can play a significant role in refining the model by eliciting the information that may be hidden because of the implicit assumption that

the error is normally distributed. Different error models have already been proposed previously (Mauricio, 2008; Oliveira and Pedrycz, 2007; Yang *et al*., 2012). The model that depends on the GMM has been demonstrated to be an efficient model when it comes to the error characterization. Due to the inherent complexity of the granulation and tabletting processes with highly nonlinear behaviours and measurement uncertainties, the GMM is selected, in this research work, to provide a deeper insight into the probability density function. Moreover, such a model has the ability to approximate any probability density function with a reasonable accuracy using a sufficient number of Gaussian components, which can lead to the optimal model refinement (Bishop, 2006; Yang *et al*., 2012). For the granulation process, Figure 3.10 presents a schematic representation of the incorporation of the integrated network and the error characterization using the GMM.

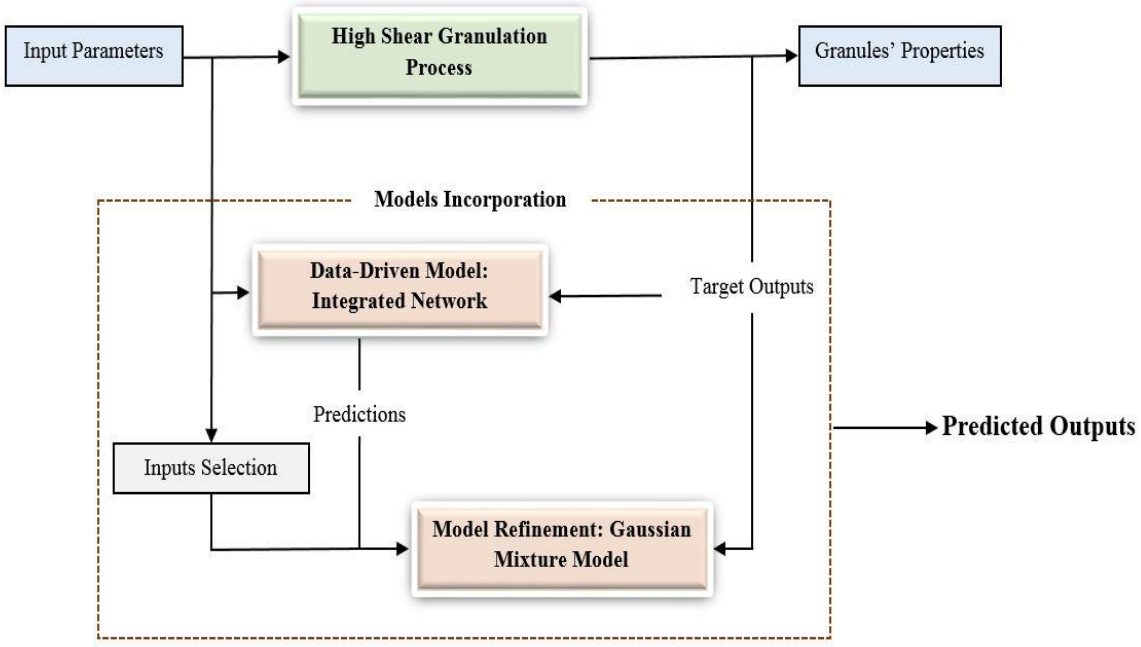

Figure 3.10. The incorporation of the integrated network and the error characterization framework.

The GMM, in general, is a stochastic model that can be represented as a linear combination of Gaussian components, where each component has its own mean and covariance. For a predefined number of Gaussian components (J), the GMM can simply be described as follows (McLachlan, 1988):

$$p\left(x^e\right)=\sum_{j=1}^{J}\pi_j \mathrm{N}\left(x^e \mid \mu_j^e,\Sigma_j^e\right) \tag{3.3}$$

where x^e is the error data which contain the selected inputs and the error vector. The number of inputs that will be included in the error characterisation should be small (Yang *et al*., 2012), since the main effect of the inputs was considered in the integrated network. The parameters μ_j^e, Σ_j^e, π_j are the mean, the covariance, and the mixing coefficient of the j^{th} Gaussian component, respectively. The superscript e is used to distinguish the parameters that are defined in the error characterisation model. To define the optimal values of these parameters, the log likelihood function should be maximized (Bishop, 2006). Therefore, the optimal parameters are given by the following set of equations:

$$\xi(z_{dj})=\frac{\pi_j \mathrm{N}\left(x_d^e \mid \mu_j^e,\Sigma_j^e\right)}{\sum_{j=1}^{J}\pi_d \mathrm{N}\left(x_d^e \mid \mu_j^e,\Sigma_j^e\right)} \quad , \qquad \forall j$$

$$\left\{\begin{array}{l} \mu_j^e=\dfrac{\sum_{d=1}^{D}\xi(z_{dj})x_d^e}{\sum_{d=1}^{D}\xi(z_{dj})} \\ \Sigma_j^e=\dfrac{\sum_{d=1}^{D}\xi(z_{dj})\left(x_d^e-\mu_j^e\right)\left(x_d^e-\mu_j^e\right)^T}{\sum_{d=1}^{D}\xi(z_{dj})} \\ \pi_j=\dfrac{\sum_{d=1}^{D}\xi(z_{dj})}{D} \end{array}\right\}, \qquad \forall j \tag{3.4}$$

where $\xi(z_{dj})$ is the probability that the d^{th} data point belongs to the j^{th} Gaussian component, and z_{dj} is a J-dimensional latent variable, which is equal to 1 when the d^{th} data point is covered by the j^{th} component where the other elements are zero. Deriving the analytical solution for these equations is a rather 'tricky' exercise but suffice to say that one of the most common methods for finding a solution for such a set of equations is the Expectation Maximization (EM) algorithm (McLachlan and Krishnan, 2008). Starting by carefully initializing the parameters using K-means clustering, $\xi(z_{dj})$ value can be estimated using the initialized parameters, the so called E-step. Accordingly in the M-step, the $\xi(z_{dj})$value is utilized to re-evaluate the parameters. The revised parameters are then utilized to update the $\xi(z_{dj})$ value. Such a procedure is reiterated until the algorithm converges, or alternatively the maximum number of iterations is reached (McLachlan and Krishnan, 2008).

However, the number of Gaussian components (J) has to be defined. The Bayesian information criterion (BIC) is adopted in this paper as a performance criterion for selecting the best number of components (Simon and Girolami, 2012). Such a choice is motivated by the fact that such a criterion can lead to a better structure (Yang *et al*., 2012). Finally, the conditional error mean, which is an indication of the bias and its value, and the conditional standard deviation are calculated using numerical methods (Yang *et al*., 2012). Generally, these methods are considered to be computationally taxing, however, it seems not to be the case in this research work, particularly with a small data set (Leader, 2004). Adding the conditional mean to the predicted output is a compensation for the bias, which can improve the prediction performance, whereas the conditional standard deviation is used to set the confidence

level (Yang *et al*., 2012). Figure 3.11 summarizes the steps of the error characterization model.

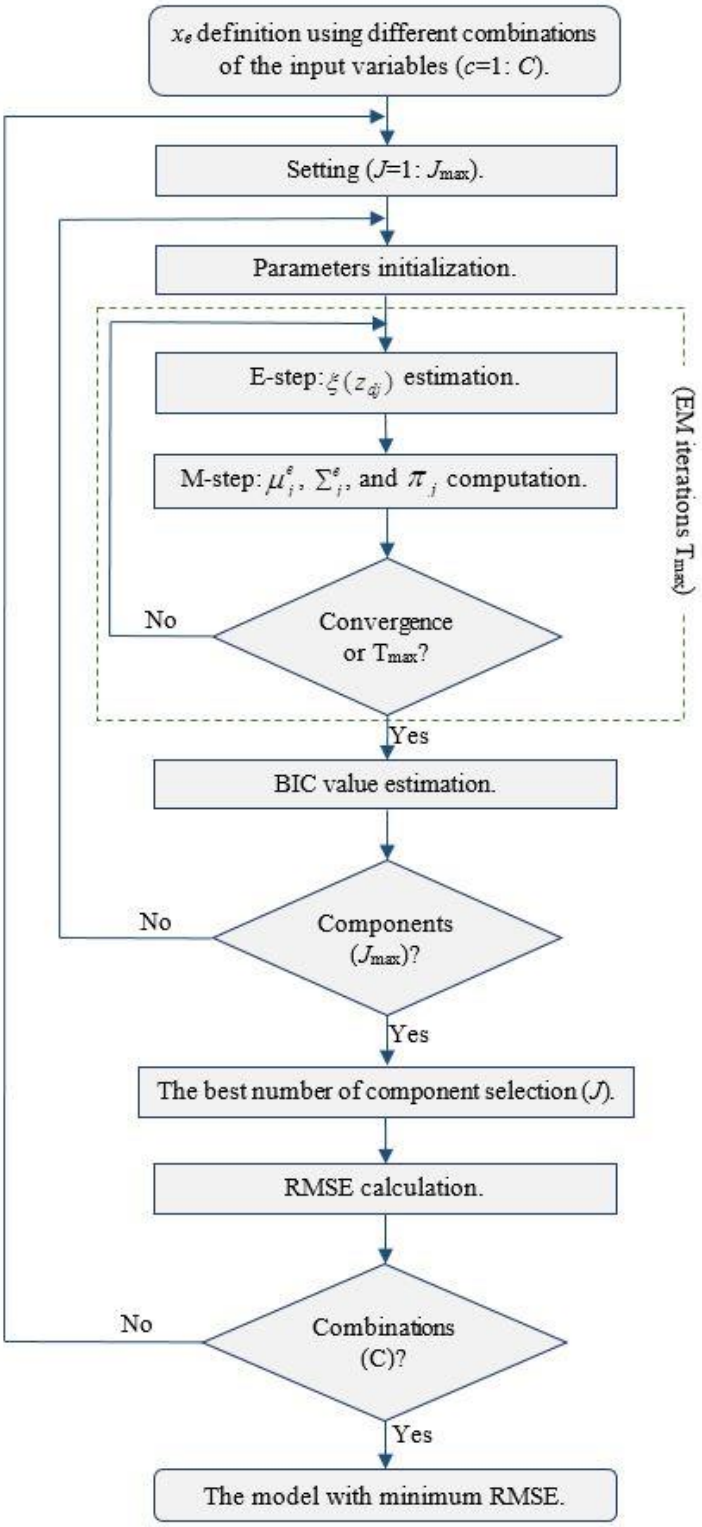

Figure 3.11. Flowchart of the error characterisation model.

3.4.2 Error Modelling Using the Gaussian Mixture Model: Results and Discussion

A. The Granulation Process

In order to improve the performance of the model by characterising the error employing the GMM, two granulation input variables out of a total of four were included. The combination that gave the maximum error compensation (*i.e.* the minimum RMSE) was finally chosen. Following the steps that were summarized in Figure 3.11 and using a program the author wrote using Matlab software, the impeller speed and the granulation time were utilized in addition to the error vector that resulted from the integrated network to develop the error model for the binder content. The selection of these parameters was expected, since the effects of these parameters appear to be incompatible as reported by previous research (Keary and Sheskey, 2004; Schaefer *et al*., 1990). This may perhaps relate to the interaction among the parameters which may result in the unpredictable behaviour of the granulation process (Knight *et al*., 1998; Schaefer *et al*., 1990; Schaefer *et al*., 1986). The training data were employed to train the GMM whereas the testing data were kept hidden. The best number of Gaussian components for the binder content was 10. Figure 3.12 shows the prediction results after bias compensation for the binder content (710-1000μ*m*) with a 95% confidence interval. Examples of the predicted and the experimental distributions for all the investigated properties are presented in Figure 3.13.

The output predictions with bias compensation presented in Figure 3.12 elucidate a satisfactory performance, where most of the predictions (96%) are laying within the 95% confidence interval. The overall improvement that was gained by employing the GMM was of approximately 14% in the RMSE which is due to the

ability of the GMM to capture the inherent undetected stochastic behaviour of the granulation process. Furthermore and similarly to the examples presented in Figure 3.13, the predictive performances for all experiments demonstrate the ability of the integrated network followed by the GMM to predict the properties successfully and to implicitly compensate for the assumptions that were made about the granulation process. The GMM was also adopted to improve the performance of the single RBF network and the ensemble model, resulting in a significant improvement for each model, as summarized in Tables 3.3 and 3.4, which summarize the overall performances for the three properties. However, it is evident that the proposed integrated network outperforms these models, even without bias compensation.

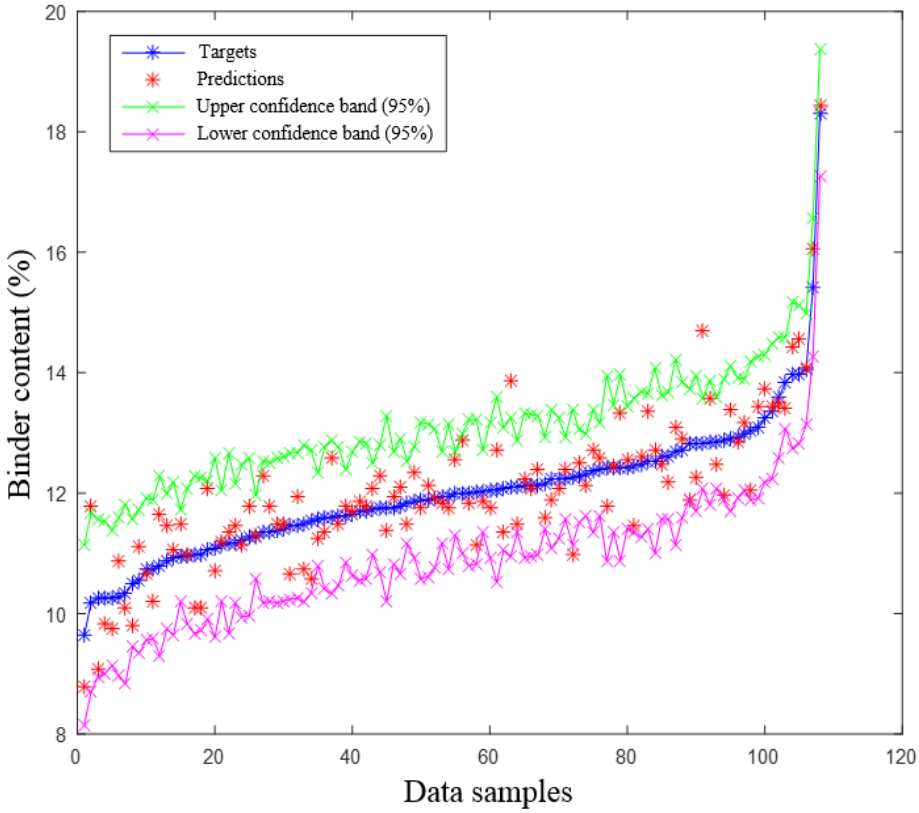

Figure 3.12. The prediction performance using the integrated network for the binder content after bias compensation (with a 95% confidence interval).

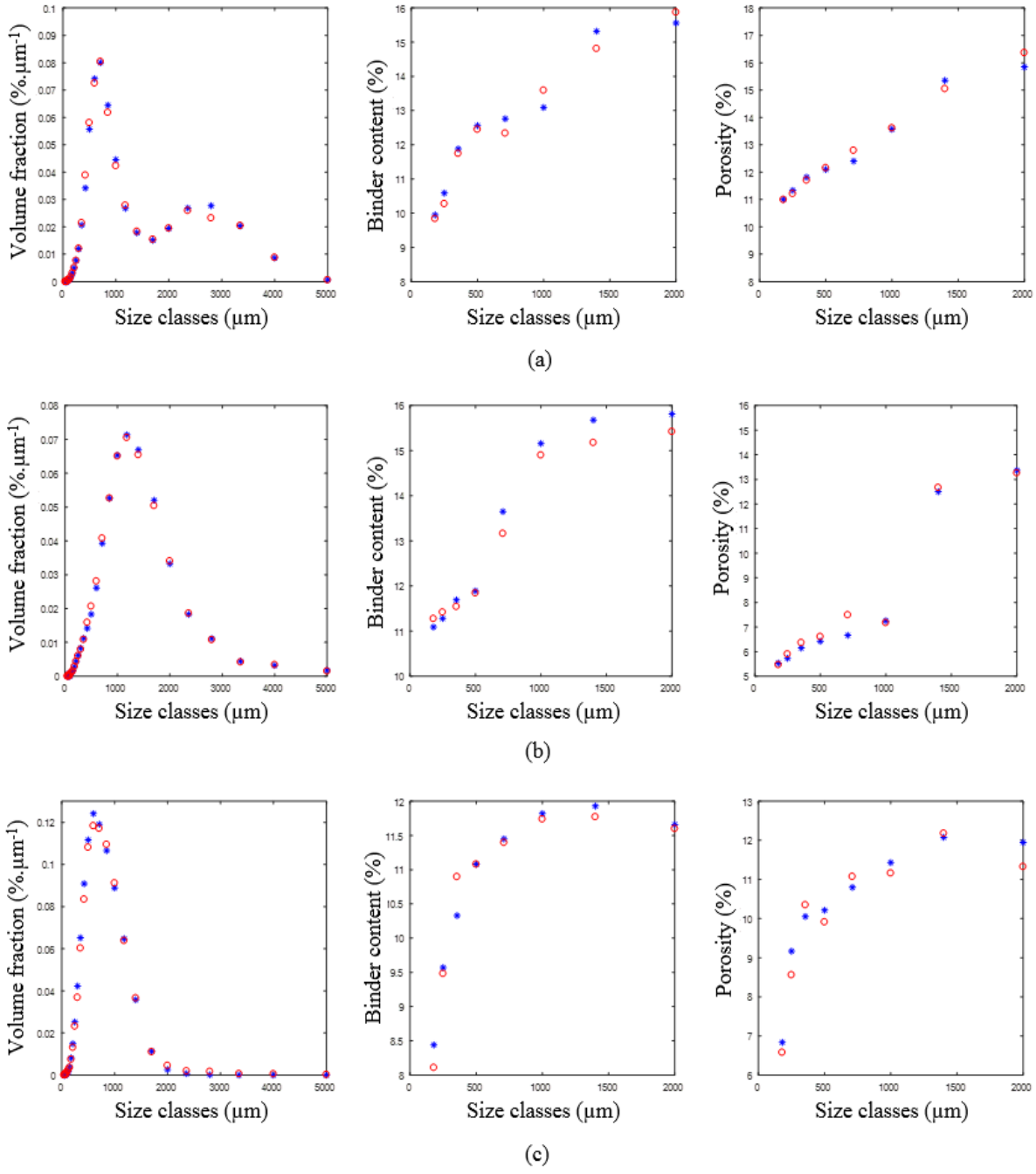

Figure 3.13. The integrated network after bias compensation using the GMM: the predicted (o) and the experimental (*) distributions for the size, binder content and porosity (a) using impeller type II, speed=2000rpm, L/S ratio (w/w)=14% and granulation time=10min; (b) using impeller type II, speed=6000rpm, L/S ratio (w/w)=15% and granulation time=15min; (c) using impeller type I, speed=4000rpm, L/S ratio (w/w)=13% and granulation time=6min.

Table 3.4. The overall performances of the models represented by R^2 and RMSE.

Model	RBF		RBF with bias compensation		Ensemble		Ensemble with bias compensation		Integrated Network		Integrated network with bias compensation	
Output	R^2	RMSE	R^2	RMSE	R^2	RMSE	R^2	RMSE	R^2	RMSE	R^2	RMSE
Size	0.5365	0.0098	0.6223	0.0083	0.7077	0.0079	0.7301	0.0073	0.7962	0.0063	0.8783	0.0055
Binder content	0.4680	1.2792	0.5358	1.2089	0.5235	1.159	0.6182	1.1086	0.7208	1.0618	0.7404	0.9352
Porosity	0.3699	1.6457	0.4781	1.4253	0.5327	1.2876	0.5586	1.2192	0.7194	1.1802	0.7402	1.0879

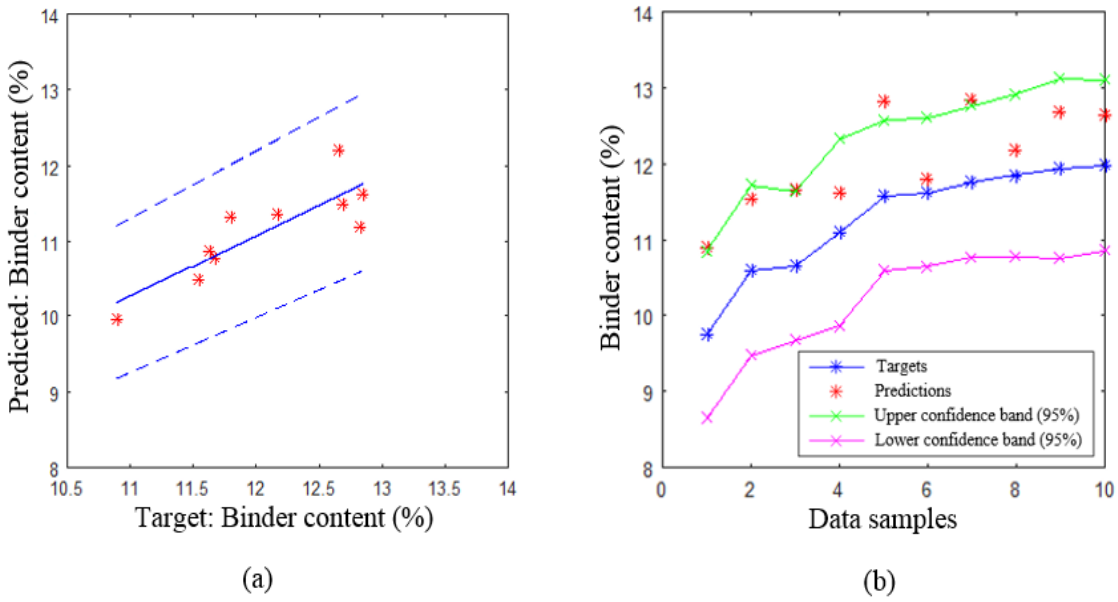

Figure 3.14. The performance for the binder content for the validation data using the integrated network: (a) predicted versus target, (b) with a 95% confidence interval.

Table 3.4 lists the results of the models for all the investigated outputs. It shows that the overall performances for the binder content and porosity are generally worse than the one for the size. The heterogeneity of the granules from the same batch but different size classes has been demonstrated in the previous research (Reynolds *et al*., 2004; Scott *et al*., 2000). It has also been shown that the same size granules have different values for these properties, such differences may be due to the uncertainties in the measurements, the heterogeneity of the same size granules or both (Osborne *et al*., 2011). Such uncertainties and heterogeneity may be the reasons behind the relatively lower prediction performances for these properties. Further investigations have to be performed to clarify this issue and to consider it in the developed model.

To prove the effectiveness and efficiency of the proposed integrated network in dealing with the challenges and difficulties surrounding the granulation process, the network was used to predict the outputs for new granulation data. Thus, 10 new experiments were conducted using different input settings, but within the examined ranges. The predicted outputs from the integrated network with error correction were compared with the measured ones. For the binder content (710-1000µm), Figure 3.14 (a) shows the performance of the integrated network for the validation data, where the R^2 (=0.76) is comparable to the one for the testing set for the same property. Most of the predictions for the validation data fit properly within a 95% confidence interval, as shown in Figure 3.14 (b). Similarly for all the outputs, the performance for the validation data is close to the one for the testing data set. Figure 3.15 shows an example of the predicted and the experimental distributions for all the investigated properties for one of the new experiments, where it is noticeable that the proposed model successfully predicted the properties of the granules.

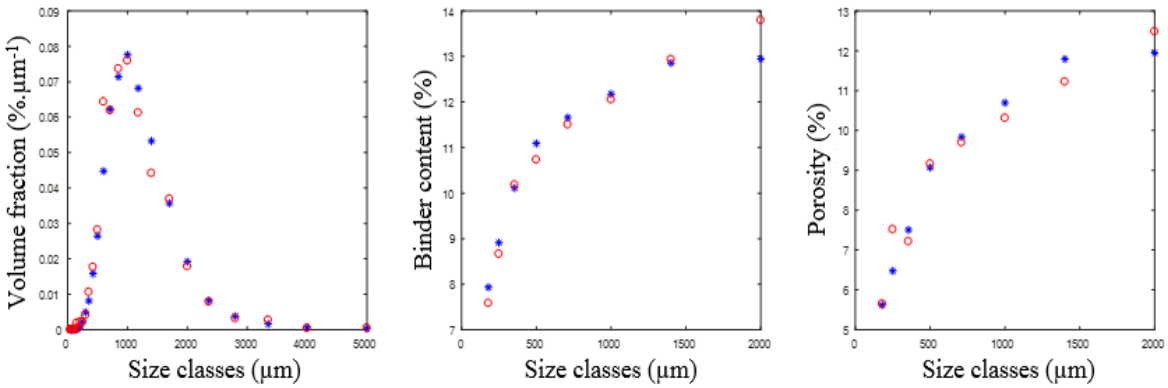

Figure 3.15. The proposed framework: the predicted and the experimental distributions for the size, binder content and porosity (using impeller type I, speed=4400rpm, L/S ratio (w/w)=13.6% and granulation time=12min).

B. The Tabletting Process

The GMM was also utilized to improve the performance of the integrated network that was established to represent the tabletting process. In addition to the error residuals, the binder content and porosity were included in the development of such a model. Because of the heterogeneous distributions of these two properties, the selection of them by the GMM algorithm was expected. The best number of Gaussian components was 9.

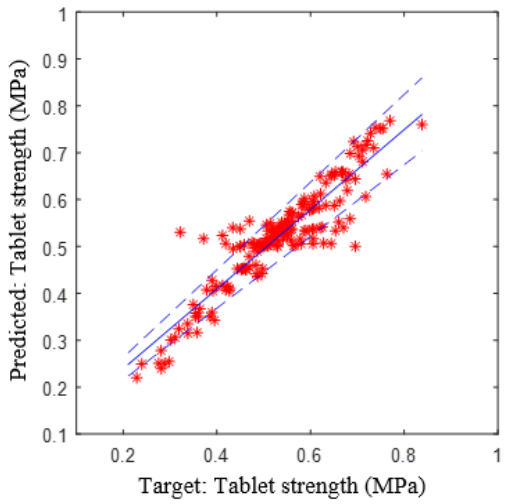

(a)

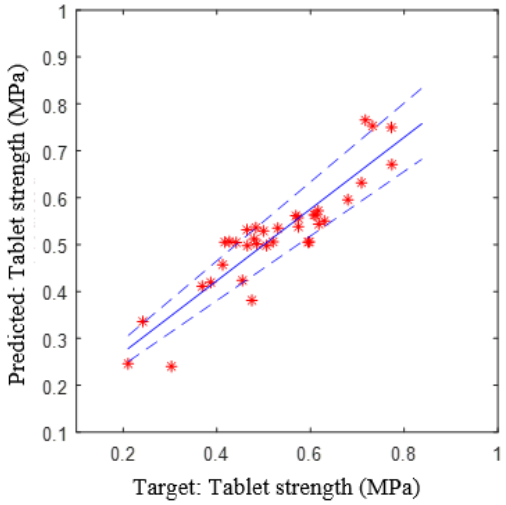

(b)

Figure 3.16. The incorporated model for the tablet strength:
(a) training and (b) testing (with 10% bands).

The model performance for the strength is R^2 (training, testing) = [0.84, 0.82], as shown in Figure 3.16. It is worth noting that most of the predictions (85%) lie within a 90% confidence interval. By employing the GMM, the overall improvement that was gained is of approximately 11% in R^2.

The proposed framework; the integrated network followed by the GMM, was also validated for the tabletting process. Tablets were produced from the 10 new granulation experiments following the same procedure that was described in Section 3.2. The integrated network followed by the GMM was utilized to predict the strength of these tablets. Then, the strength of the tablets produced was measured using Zwick/Roell Z0.5 (Zwick/Roell, Germany). By comparing the predicted strength values with the measured ones, it was found that the R^2 value is approximately 0.81, which is comparable to the one presented above. Thus, such a framework can be used to successfully predict the strength of the tablets.

3.5 Summary

Modelling the granulation process is not a trivial task because of the complex nature of such a process and the lack of physical representation of its behaviour, where the modelling approaches of the granulation process that have received the most attention have hitherto focused on analytical and numerical based techniques in the form of empirical and semi-mechanistic models. Moreover, the limited amount of data and its sparsity are considered as compounding difficulties in modelling the granulation process using data-driven models, especially for some industrial applications, including the pharmaceutical industry, where the acquiring of such data alone can be an expensive enterprise.

In this chapter, a new integrated network was developed to predict the properties of the granules produced by the HSG process and the strength of the tablets. The integrated network predicted the outputs by modelling and training the data in two consecutive phases. Such a structure was able to extract relevant information from a conservative number of data points, it was also able to capture the complex input/output relationships in the original data because of the number of basis functions and weights involved. Moreover, one of the major obstacles for developing data-driven models; defining the best structure, was overcome by using different modelling structures in the first phase of the network. The efficiency of the new network was demonstrated and validated by accurately predicting the properties of the granules, namely; size, binder content, and porosity, and the strength of the tablets. Characterizing the resulted error using the GMM was then integrated in the original model structure in order to deal with any potential bias in the predicted outputs. Such a model was able to reveal the stochastic behaviour which was utilised for further model refinement. It was shown that most of the output predictions for all the properties of the granules fit adequately within a 95% confidence interval. It was also shown that most of the predictions for the strength of the tablets lie within a 90% confidence interval.

The framework efficiency, which is believed to emanate from the integration of deterministic and stochastic modelling, was successfully demonstrated in this research work. When compared to the computationally expensive models that were mentioned previously, for example PBMs that have been developed for the granulation process, this modelling framework accurately predicted the properties of the granules within a reasonable time. However, there is a strong demand for improving the interpretability of the processes under study, particularly, the granulation one. In

addition, there is a strong need to develop a model that can deal with uncertainties in both the granulation and the tabletting processes. In the future, it would also be worth incorporating the proposed framework with other models such as a FLS, where the system is described linguistically in a transparent way that can be easily understood by users and therefore 'owned'. In addition, these models are capable of dealing with uncertainties more effectively; by uncertainty here one means not only uncertainties in the measurements but also uncertainties which result from the heterogonous distributions of the binder content and porosity during the granulation process and, consequently, the tabletting one. Moreover, the integration between the data-driven models and other physical based ones (*e.g.* PBMs and CFD) will be advantageous, particularly for the ill-defined granulation process, where the former can circumvent the limitations of such models (*e.g.* the number of outputs and the execution time). In contrast to data-driven models, physical based ones can compensate for the limited number of data points. Furthermore, incorporating these models would be very beneficial for scaling-up processes.

In the next chapter, a systematic modelling framework incorporating FLSs and a modified GMM algorithm will be presented to predict the outputs and also to provide a simple understanding of the processes under investigation.

Chapter 4

Transparent Fuzzy Logic based Predictive Modelling of the Granulation and Tabletting Processes[4]

4.1 Introduction

Generally, the modelling of a wet granulation process has received a considerable attention, where the main aim is not only to predict the properties of the granules but also to understand the process and its mechanisms. As stated previously, the modelling approaches that have been developed to represent the granulation process can be classified as either physical based or data based models. One commonly used approach is a PBM. In general, PBMs have been implemented to follow the evolution of the granules with time (Sanders *et al*., 2003; Ramkrishna, 2000). A one-dimensional PBM was typically used to study the granule size (Iveson, 2002).

[4] The content of this chapter is published in "AlAlaween, W.H., Khorsheed, B., Mahfouf, M., Gabbott, I., Reynolds, G.K., Salman, A.D, 2018. Transparent Predictive Modelling of the Twin Screw Granulation Process using a Compensated Interval Type-2 Fuzzy System. European Journal of Pharmaceutics and Biopharmaceutics. 124, 138-146", "AlAlaween, W.H., Mahfouf, M., Salman, A.D., 2017. Development of a predictive framework for a high shear granulation process. AIChE Annual meeting. Minneapolis, USA", and "AlAlaween, W.H., Mahfouf, M., Salman, A.D., 2016. Data-Driven Deterministic and Stochastic modelling of the Wet Granulation Process. Joint IFPRI Robert Pfeffer symposium & UK Particle Technology Forum. Guilford, UK".

However, the consideration of the other granule properties is really crucial, where these properties can significantly affect the critical quality attributes of the tablets produced (*e.g*. porosity) (Barrasso *et al*., 2015). Therefore, multi-dimensional PBMs have been extensively employed (Paavola *et al*., 2013; Pinto *et al*., 2007; Poon *et al*., 2008; Sanders *et al*., 2003). Although the PBMs have provided a deeper insight into the granulation process at the micro-level, all the possible interactions among the process mechanisms have not been fully considered (Iveson, 2002). Therefore, these models have been integrated with various modelling approaches such as Monte Carlo, in order to model a greater number of particle properties, and the discrete element method (Braumann, 2010; Oullion *et al*., 2009), in order to model the effect of equipment dynamics (Barrasso *et al*., 2014; Braumann *et al*., 2007; Shirazian *et al*., 2017). Recently, various compartmental models that integrate a PBM and CFD have been developed (Chaturbedi *et al*., 2017; Lee *et al*., 2015; Mansa *et al*., 2008; Murtoniemi *et al*., 1994; Watano *et al*., 1997; Yu *et al*., 2017; 2015).

Intelligent systems associated with data based models, which are simply based on intensive computations, have also been implemented to model the granulation process (Mansa *et al*., 2008). Many paradigms such as ANNs with different structures and topologies have been utilized to predict the properties of the granules produced using different granulation equipment and materials (Mansa *et al*., 2008; Murtoniemi *et al*., 1994; Watano *et al*., 1997; Yu *et al*., 2015).

Generally, these modelling paradigms have their own strengths and limitations. On the one hand, data-driven models, as powerful interpolators, can simply interpret the input/output relationships in a simple way that can easily be implemented. Moreover, they can be utilized to monitor more than three granule properties, which is

considered to be computationally taxing task for the physical based models (Iveson, 2002). On the other hand, the physical based models can be utilized on a larger scale by using the scaling-up techniques that have been proposed in the related literature (Li *et al*., 2013; Watano *et al*., 2005). However, none of the presented models can systematically deal with the uncertainties present in both the granulation inputs and outputs. Moreover, the majority of the presented models assume that the error residuals are normally distributed (Mauricio, 2008; Oliveira and Pedrycz, 2007; Yang *et al*., 2012). Such an assumption, which is not usually valid, may lead to an unmodelled behaviour, which may consequently result in performance deterioration (Yang *et al*., 2012).

The main aim of the research in this chapter is to develop a fast, transparent, more accurate and cost-effective predictive modelling framework for the HSG and the tabletting processes. For this purpose, modelling frameworks that integrate FLSs, namely; type-1 and interval type-2, and a GMM are considered.

4.2 The Type-1 Fuzzy Logic System

4.2.1 The Type-1 Fuzzy Logic System: Model Development

With recent advances in computing power, data-driven models, which include, but not limited to, ANNs, fuzzy systems and evolutionary genetic algorithms (Bishop, 2006; Mendel, 2001; Vose, 1999), have become the type of models that one seeks to represent complex processes (Karnik and Mendel, 2001; Mahfouf *et al*., 2003; Nunes *et al*., 2005; Zhang and Mahfouf, 2011), in particular, those processes where the physical model does not exist or it is simply too complex to derive. In spite of the powerful algorithms behind these, some of the data-driven approaches such as neural networks are referred to as black-box approaches (Bishop, 2006). This is because the

mechanism that maps the process inputs into its outputs does not provide users with the necessary information to understand the process under investigation. Therefore, a FLS has been extensively applied in many research areas such as those associated with medical, industrial and academic applications to develop a simple and transparent model (Nunes *et al*., 2005; Salomao *et al*., 2017; Wang and Mahfouf, 2012; Yang *et al*., 2011; Zhang and Mahfouf, 2011). Moreover, this system, as it is well-known, can typically handle uncertainties more efficiently (Mendel, 2001). Generally, the FLS is represented by fuzzy sets, which are usually described by membership functions. The most common types of the fuzzy sets are type-1 and type-2. A type-1 fuzzy logic system (T1FLS) is the one whose rules' antecedents and consequent are completely described by type-1 fuzzy sets. Figure 4.1 depicts the structure of the T1FLS.

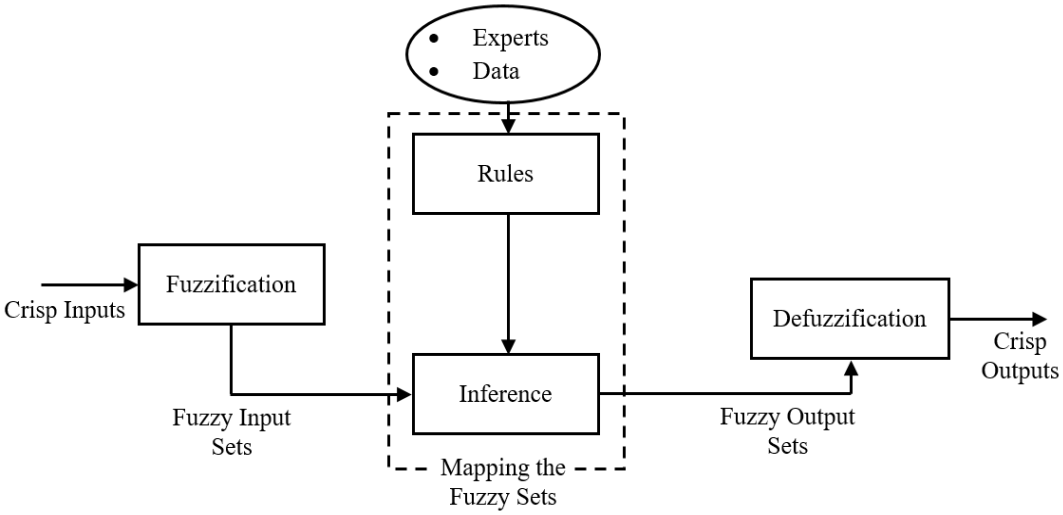

Figure 4.1. The structure of the T1FLS.

As shown in Figure 4.1, the structure of the T1FLS consists of four components, namely; fuzzification, inference, rules and defuzzification. First, a fuzzification step represents the process of mapping the crisp inputs (x_1, x_2 …x_n) to the

fuzzy input sets (A_j^i), where A_j^i is the i^{th} fuzzy set for the j^{th} variable. The fuzzy sets are usually defined by membership functions. The most commonly used membership function is the Gaussian one, this being due to the continuity and smoothness of the Gaussian function which allow users to use the FLSs as a '*universal approximator'* (Wang and Mahfouf, 2012). Such a membership function can be expressed as follows (Mendel, 2001):

$$\mu_j^i(x_j) = \exp\left[-\frac{1}{2}\left(\frac{x_j - m^i}{\sigma^i}\right)\right] \tag{4.1}$$

where m^i and σ^i are the mean and the standard deviation of the i^{th} set, respectively. In general, the inference process combines the defined rules to map the input fuzzy sets to the output fuzzy sets. These rules can be provided by experts or can be extracted from a collected data set. Both types can be presented as a collection of IF-THEN statements, as follows:

Rule^i: IF x_1 is A_1^i … and x_n is A_n^i, **THEN** y is B^i.

where B^i represents the i^{th} output fuzzy set, when a Mamdani fuzzy system is considered (Mendel, 2001). Finally, the output fuzzy set is defuzzified to get a crisp one (Mendel, 2001).

4.2.2 The Type-1 Fuzzy Logic System: Results and Discussion

A. The Granulation Process

A T1FLS was utilized to model the HSG process. The collected data were divided randomly into two data sets: training (90) and testing (18). The training data set, as the name implies, allows the model to learn the relationships between the inputs

and the output by extracting informative rules, whereas the testing data set is used to validate the model by assessing its generalization capabilities. In order to model the HSG process successfully, one should understand the nature of the process input variables (*i.e*. continuous or discrete). In this research work, all the input variables are continuous except the impeller shape variable, which is considered as a crisp variable. The number of rules that was selected corresponds to the minimum error between the predicted and the experimental output evaluated by the RMSE.

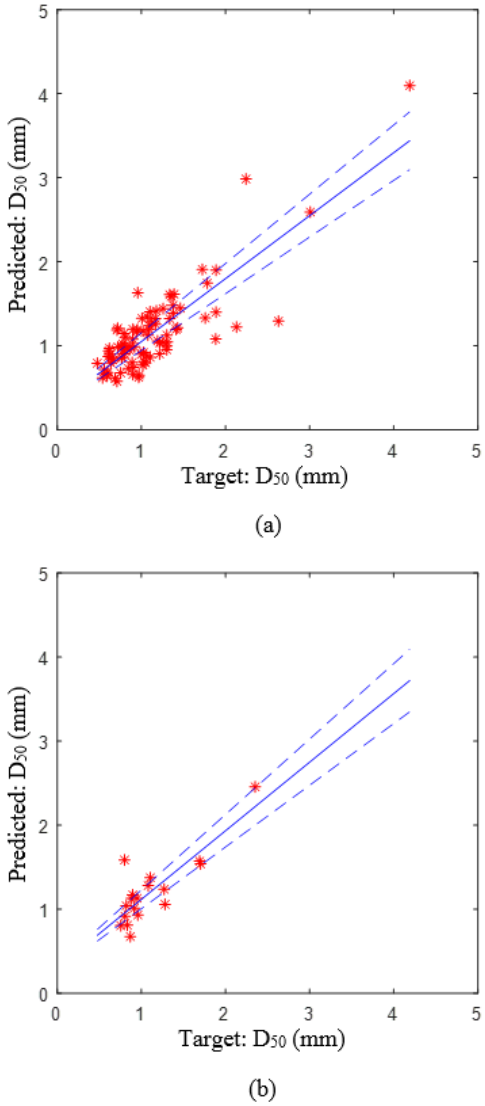

Figure 4.2. The T1FLS for D_{50}: (a) training, (b) testing (with 10% bands).

For a predefined number of rules and by using a program the author wrote using Matlab software, the model parameters were carefully initialized using the hierarchical clustering algorithm (Zhang and Mahfouf, 2011). The model parameters were then optimized by employing the steepest descent algorithm with an adaptive back-propagation network (Mendel, 2001).

Using 6 rules, Figure 4.2 shows the model performance for D_{50}. The RMSE values for the training and testing sets are 0.31mm and 0.25mm, respectively. It is noticeable that the RMSE value for the training set is worse than that for the testing set, this can be an indication of a training problem. However, it seems not to be the case in this work, where such a difference is due to the D_{50} values; most of the values in the testing set are less than 2mm, whereas, in the training set, some of the values are greater than 2mm, thus, the RMSE value for the training set was expected to be relatively greater than the one for the testing set. This can be clearly evidenced by looking at the values of R^2 (training, testing) = [0.69 0.70], where these values are comparable.

Two sample rules out of a total of six are illustrated in Figure 4.3, and their corresponding linguistic forms read as follows:

Rule 1: IF *the impeller type is Type I and impeller speed is small and granulation time is small and the L/S ratio is small,* ***THEN*** *D_{50} is small.*

Rule 2: IF *the impeller type is Type II and impeller speed is large and granulation time is large and the L/S ratio is medium,* ***THEN*** *the D_{50} is medium.*

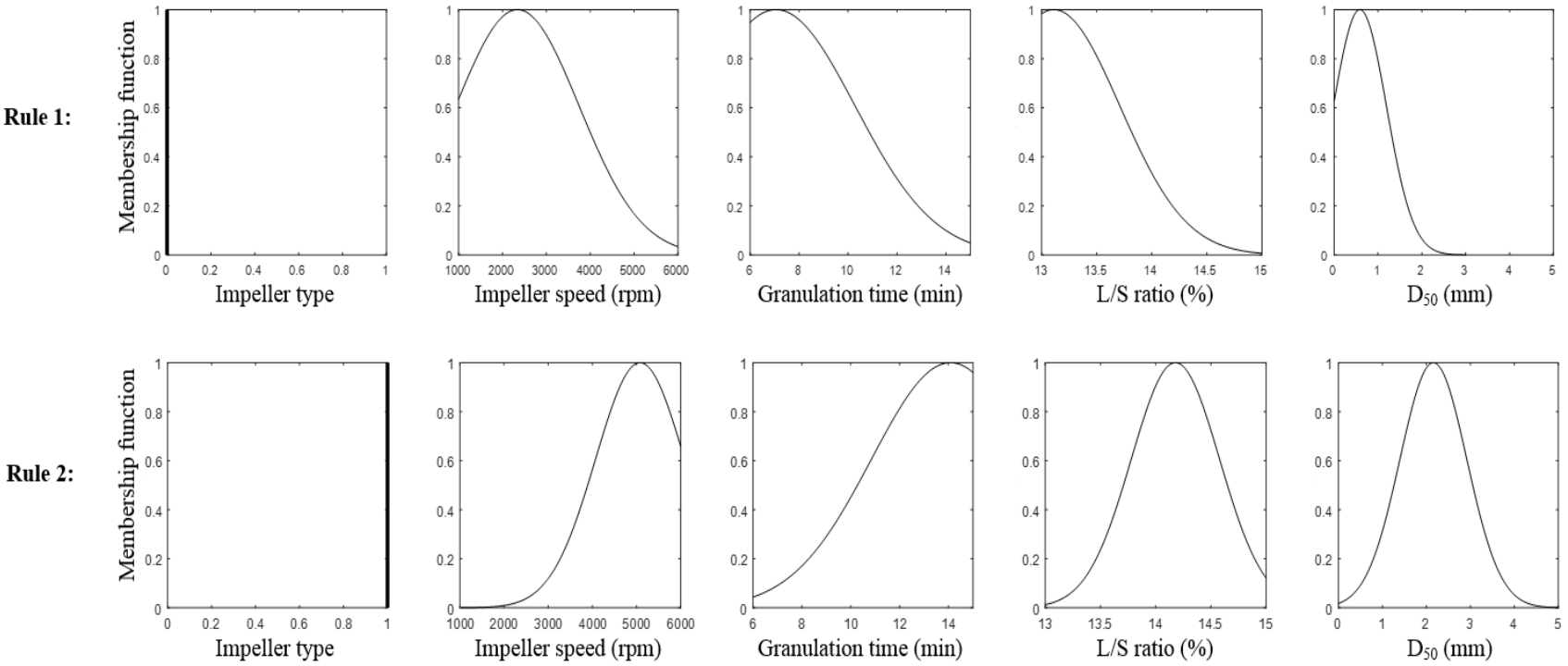

Figure 4.3. The rule base of the T1FLS for D_{50}.

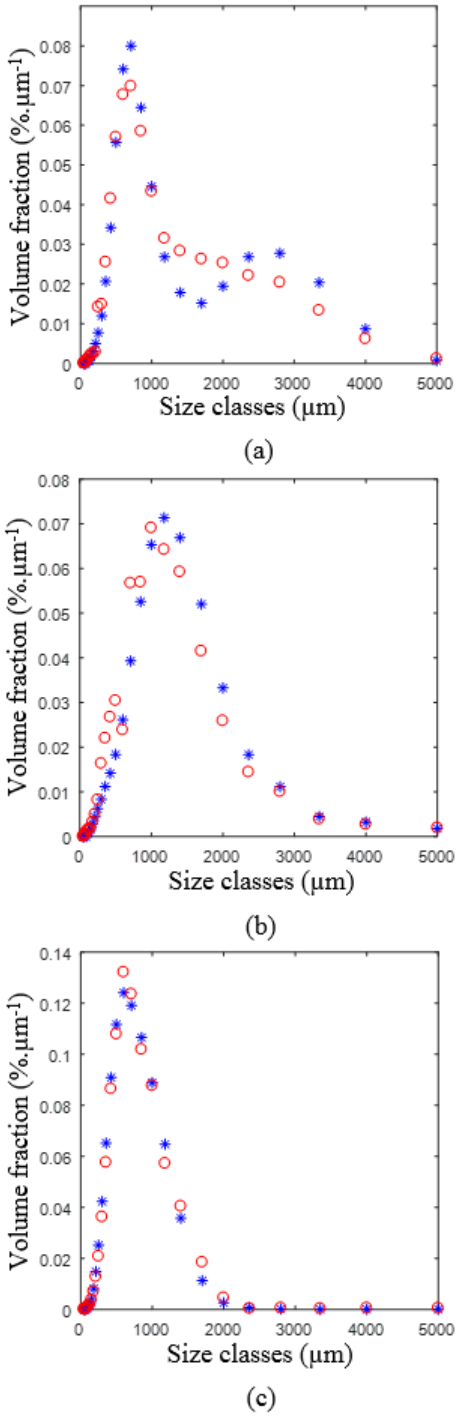

Figure 4.4. The T1FLS: the predicted (o) and the experimental (*) distributions for the size (a) using impeller type II, speed=2000rpm, L/S ratio (w/w)=14% and granulation time=10min, (b) using impeller type II, speed=6000rpm, L/S ratio (w/w)=15% and granulation time=15min.

Table 4.1. The overall performances of the fuzzy logic based models represented by R^2 and RMSE.

Model	T1FLS		T1FLS with bias compensation		IT2FLS		IT2FLS with bias compensation	
Output	R^2	RMSE	R^2	RMSE	R^2	RMSE	R^2	RMSE
Size	0.69	0.0081	0.73	0.0073	0.74	0.0071	0.79	0.0067
Binder content	0.44	1.2243	0.50	1.2009	0.48	1.1593	0.54	1.1017
Porosity	0.42	1.4547	0.47	1.3513	0.47	1.3086	0.56	1.2201

In a similar manner, the model was used to predict the whole size distribution of the granules. Figure 4.4 shows examples of the predicted and the experimental size distributions for three experiments, which were carried-out under varying operating conditions. Similarly, the T1FLS was used to predict the binder content and porosity values. The performance measures for all the investigated properties are summarized in Table 4.1. It is noticeable that the overall modelling performances for both the binder content and porosity are worse than the overall performance for the size. These performance measures indicate that the T1FLS on its own was not able to successfully predict the properties of the granules, in particular the binder content and porosity, and also it was not able to capture the complex input/output relationships and to deal with the uncertainties in a way that can lead to a good predictive performance. Thus, such a model by its own cannot be used to represent the granulation process. Therefore, these results reinforce the need to develop a model (*e.g.* a type-2 FLS (T2FLS)) that can tackle uncertainties more efficiently as compared to the T1FLS.

B. The Tabletting Process

A T1FLS was also developed to model the tabletting process and to predict the strength of the tablets. The collected data were divided randomly into two data sets: training (180) and testing (36). The granules' properties, namely; size, binder content

and porosity, and the strength of the tablets produced were used as the inputs and the output of the T1FLS, respectively, where all the inputs were dealt with as continuous variables. As mentioned above, the number of rules that was chosen corresponds to the minimum error between the predicted and the experimental output evaluated by the RMSE. The parameters of the T1FLS were initialized using the hierarchical clustering algorithm (Zhang and Mahfouf, 2011), followed by optimizing these parameters by employing the steepest descent algorithm with an adaptive back-propagation network (Mendel, 2001).

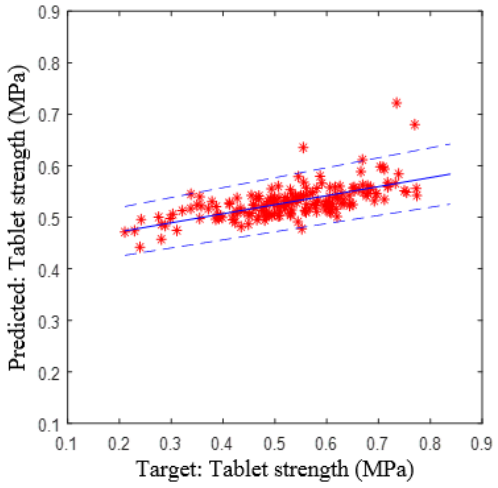

(a)

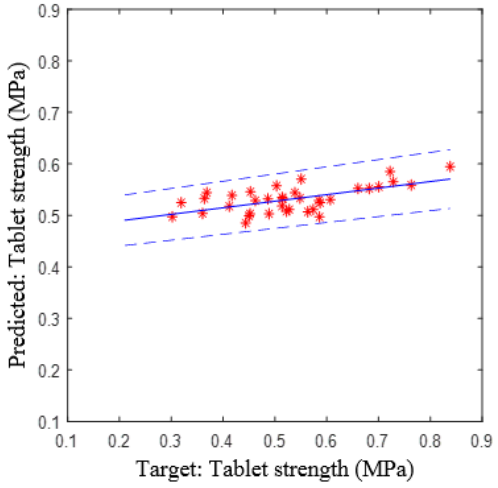

(b)

Figure 4.5. The T1FLS for the strength of the tablets:
(a) training, (b) testing (with 10% bands).

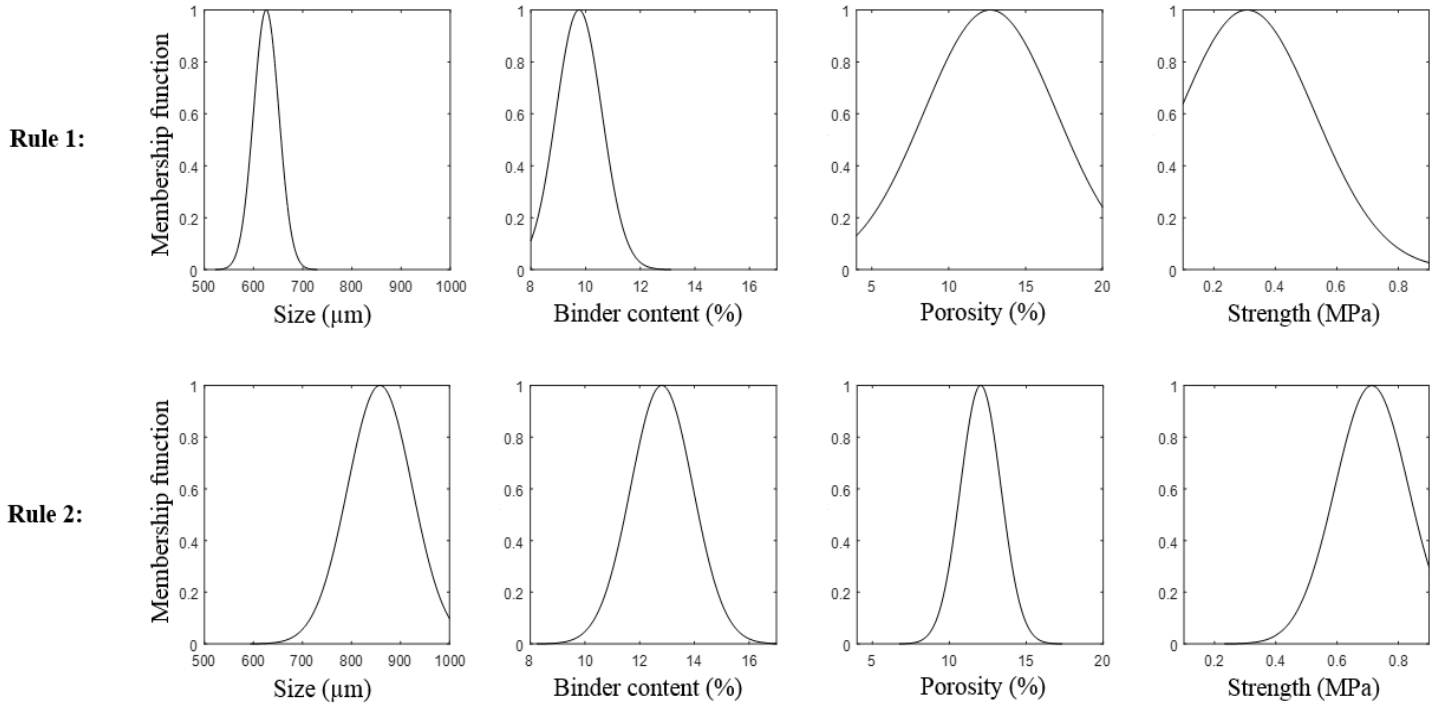

Figure 4.6. The rule base of the T1FLS for the strength of the tablets.

Figure 4.5 shows the modelling performance of the T1FLS for the strength of the tablets. The performance measures for the model presented by the RMSE (training, testing) and the R^2 (training, testing) values are [0.103 0.110] MPa and [0.41 0.39], respectively. Two sample rules out of a total of eight are presented in Figure 4.6, and their corresponding linguistic forms can be read as follows:

Rule 1: IF *the size is in the range of 500µm to 710µm and the binder content is small and the porosity is medium,* ***THEN*** *the strength is small.*

Rule 2: IF *the size is in the range of 710 µm to 1000µm and the binder content is medium and the porosity is medium,* ***THEN*** *the strength is large.*

The predictive performance for the strength of the tablets is much worse than the predictive performance for the size, and it is even worse than the ones for the binder content and porosity. Therefore, such a model cannot be utilized to accurately predict the strength of the tablets, and also the rules extracted may not reflect the tabletting process. Consequently, a T2FLS is utilized in this research work to predict the properties of the granules and the strength of the tablets. Such a choice was motivated by the fact that a T2FLS can deal with uncertainties more efficiently compared to its counterpart T1FLS.

4.3 The Interval Type-2 Fuzzy Logic System

4.3.1 The Interval Type-2 Fuzzy Logic System: Model Development

As mentioned previously, the most common types of the fuzzy sets are type-1 and type-2. A T1FLS, as described in details in Section 4.2, is the one whose rules' antecedents and consequent are completely described by type-1 fuzzy sets, whereas the system where at least one of its rules' antecedents or consequent is described by

type-2 fuzzy sets is called a T2FLS. In such a system, the membership functions are themselves fuzzy. Because of the extra degree of freedom, the T2FLS can typically tackle uncertainties more efficiently compared to its counterpart T1FLS. However, implementing such a paradigm is computationally expensive. Therefore, an interval type-2 FLS (IT2FLS) has been applied throughout instead (Mendel, 2001). Since the modelling results that were obtained by using the T1FLS indicated that such a model was not able to predict the properties of the granules and the strength of the tablets accurately, an IT2FLS is utilized in this research work to model both the granulation and the tabletting processes.

An interval type-2 fuzzy set can usually be given as follows (Mendel, 2001):

$$\tilde{A} = \int_{x \in X} \int_{u \in J_x \subseteq [0,1]} 1/(x,u) \tag{4.2}$$

where x, X and J_x stand for the primary variable, its measurement domain and its primary membership degree, respectively. The parameter u represents the secondary variable; $u \in J_x$ at each $x \in X$.

The IT2FLS structure is depicted in Figure 4.7. Although, it is quite different, such a structure seems to be similar to the structure of the T1FLS described in Figure 4.1. In the IT2FLS, the crisp inputs (x_1, x_2 …x_n) are usually fuzzified into input type-2 fuzzy sets ($\tilde{A}_j^i$) to determine the upper and lower membership functions $\left[\underline{\mu}_{\tilde{A}_j^i}, \overline{\mu}_{\tilde{A}_j^i} \right]$,

where $\tilde{A}_j^i$ is the i^{th} fuzzy set for the j^{th} variable and the Macron (diacritic) sign is used to distinguish some of the parameters that are used in the IT2FLS from the ones used in the T1FLS. The most commonly used membership function is the Gaussian one

with uncertain mean, this membership function can be expressed as follows (Mendel, 2001):

$$\mu_j^i(x_j) = \exp\left[-\frac{1}{2}\left(\frac{x_j - m_j^i}{\sigma_j^i}\right)\right], \quad m_j^i \in \left[m_{j1}^i, m_{j2}^i\right] \tag{4.3}$$

the parameters are as defined previously. It is worth mentioning that the lower (m_{j1}^i) and upper (m_{j2}^i) mean values are used to estimate the values of $\underline{\mu}_{\tilde{A}_j^i}$ and $\overline{\mu}_{\tilde{A}_j^i}$, respectively. The union of the membership functions that lie between the lower and upper ones is called the footprint of uncertainty.

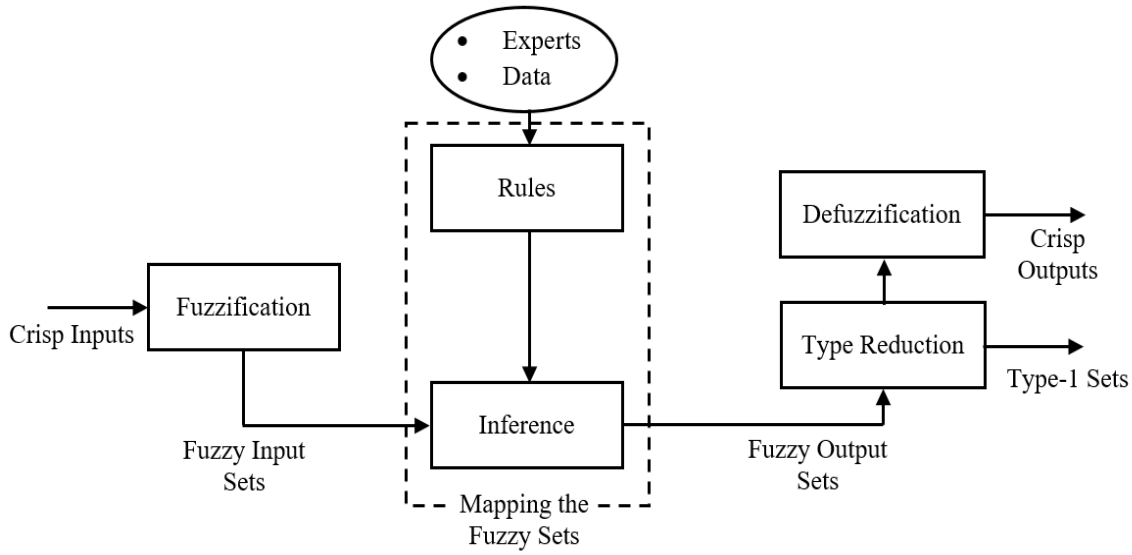

Figure 4.7. The structure of the IT2FLS.

As is the case in the T1FLS, the inference process combines the rules to map the input fuzzy sets to the output fuzzy sets. These rules have a similar form as that for T1FLS, the only distinction is associated with the nature of the membership functions, which is a type-2 fuzzy set in this case (Mendel, 2001). Finally, the type-2 output fuzzy

set is processed by two operations. The first operation is to reduce the type-2 fuzzy system into a type-1 one. Most of the computational effort of the IT2FLS is incurred by this step, where the left and right points of the interval are found using the Karnik-Mendel (KM) algorithm (Karnik and Mendel, 2001; Mendel, 2001). Such a step is usually followed by a defuzzification process of the output to get a crisp one, this operation can be simply performed by computing the average value (Obajemu *et al*., 2014; Mendel, 2001; Salomao *et al*., 2016).

4.3.2 The Interval Type-2 Fuzzy Logic System: Results and Discussion

A. The Granulation Process

To develop an IT2FLS for the HSG process, the collected data were divided into two sets; training (90) and testing (18). As mentioned previously, all the input parameters were considered as continuous except the impeller shape variable, which was dealt with as a crisp variable. The number of rules that corresponds to the minimum error value was selected. The steepest descent algorithm was utilized with an adaptive back-propagation network to tune the parameters of such a model. Such a model was written using Matlab software.

For D_{50}, two sample rules out of a total of five are illustrated in Figure 4.8, where the shaded area represents the footprint of uncertainty. The corresponding linguistic forms for these rules would read as follows:

***Rule 1**: **IF** the impeller type is Type II and impeller speed is medium and granulation time is small and the L/S ratio is small, **THEN** D_{50} is small.*

***Rule 2**: **IF** the impeller type is Type I and impeller speed is medium and granulation time is small and the L/S ratio is medium, **THEN** D_{50} is medium.*

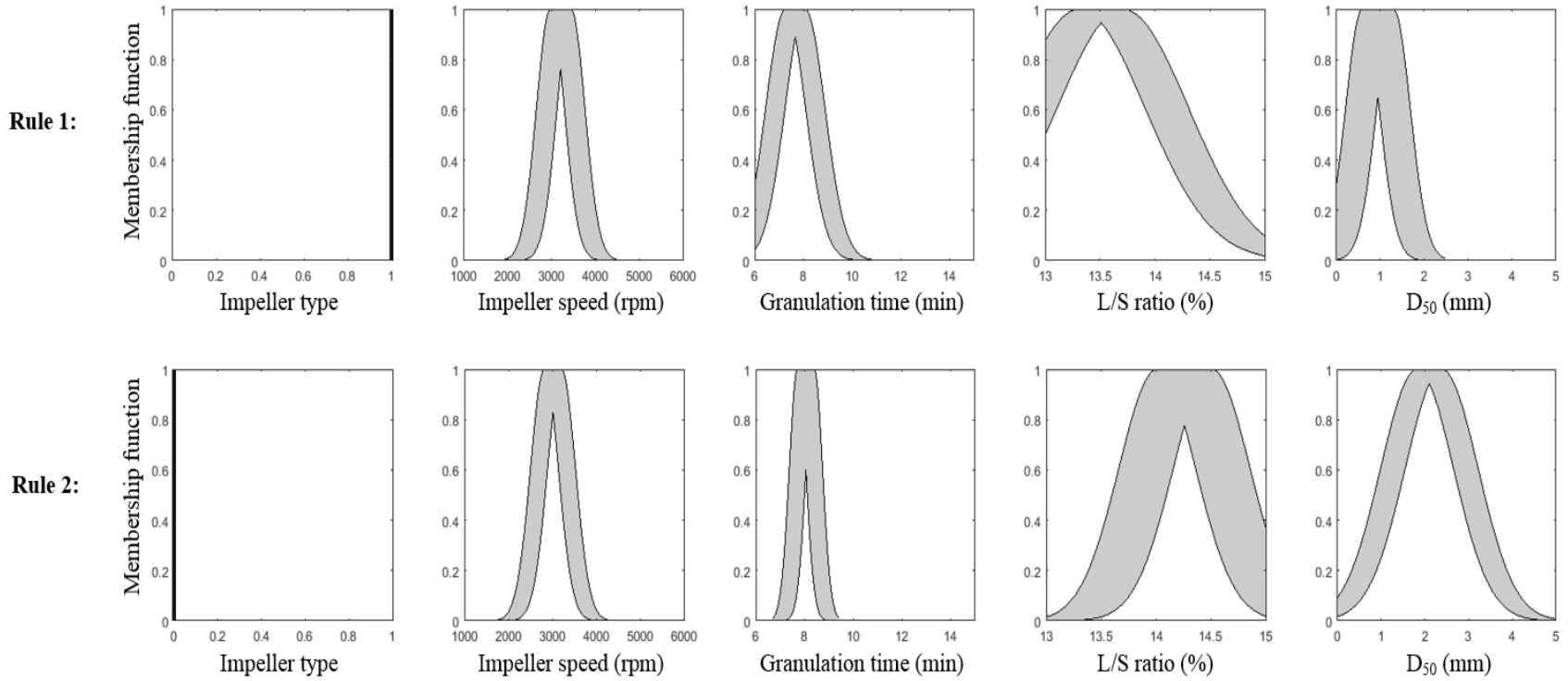

Figure 4.8. The rule base of the IT2FLS for D_{50}.

The model performance for D_{50} is shown in Figure 4.9, the R^2 values for the training and testing data sets are 0.76 and 0.74, respectively. It can be seen that most of the predictions fall within a 90% confidence interval. Similarly, the IT2FLS was utilized to predict the whole size distribution of the granules. Figure 4.10 shows examples of the predicted and the experimental size distributions for three experiments. Also, the overall modelling performance for the size is listed in Table 4.1.

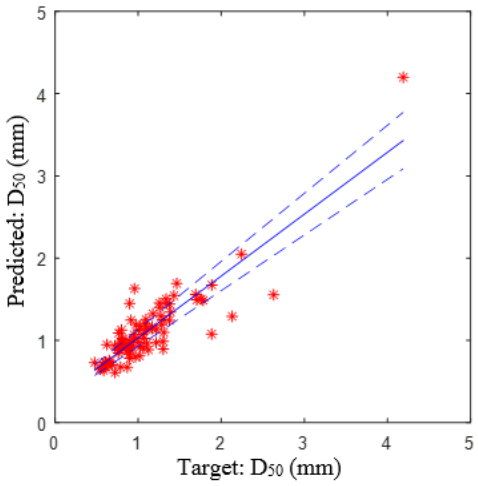

(a)

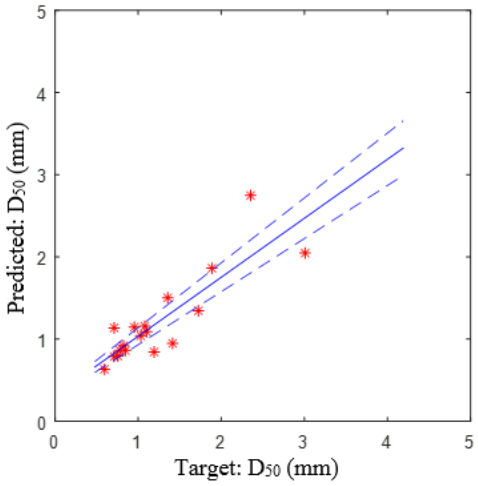

(b)

Figure 4.9. The IT2FLS model for D_{50}: (a) training and (b) testing (with 10% bands).

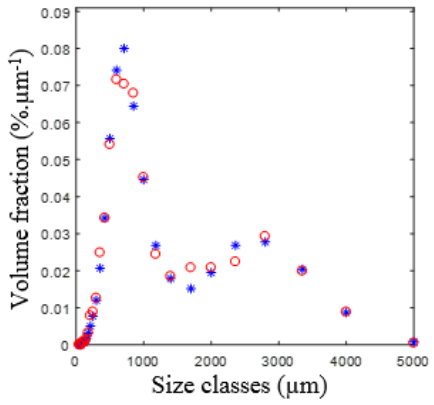

(a)

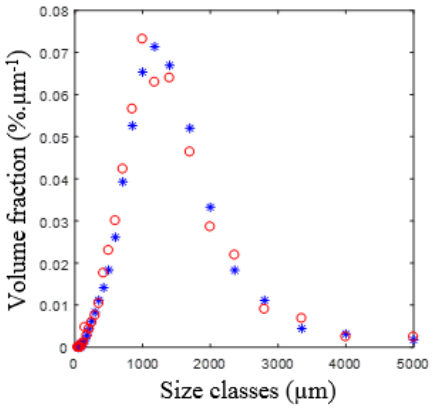

(b)

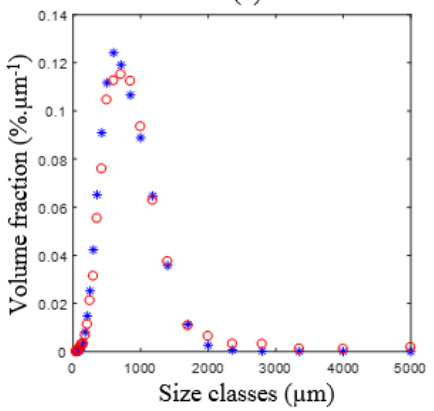

(c)

Figure 4.10. The IT2FLS model: the predicted (o) and the experimental (*) distributions for the size (a) using impeller type II, speed=2000rpm, L/S ratio (w/w)=14% and granulation time=10min, (b) using impeller type II, speed=6000rpm, L/S ratio (w/w)=15% and granulation time=15min.

As the IT2FLS is considered to be more computationally taxing as compared to the T1FLS, this raises the question as to whether it is this complexity that led to a superior model for the HSG process. For the size, the overall performance for the IT2FLS is $R^2 = 0.74$. This demonstrates that the prediction performance of the IT2FLS is superior to that of the T1FLS, with an overall improvement of approximately 7% in R^2. This indicates that the IT2FLS can handle the uncertainties more efficiently compared to it is counterpart T1FLS.

In a similar manner, the IT2FLS was utilized to predict the binder content and the porosity. The overall performances represented by the R^2 values for these properties are 0.48 and 0.47, respectively, as summarized in Table 4.1, where the RMSE for all the investigated properties are also presented. Although such performance measures are better than the ones obtained by implementing the T1FLS, they nevertheless demonstrate that such a model cannot be used to represent the granulation process. Therefore, there is a need to improve the performance of such a model further.

B. The Tabletting Process

An IT2FLS was developed for the tabletting process, the collected data were divided into two sets, as described above in Section 4.2.2 (B). As is the case in the T1FLS, the granules properties and the strength of the tablets were used as the inputs and the output of such a model, respectively. It is worth mentioning at this stage that all the inputs were considered as continuous variables.

By using 6 rules, the predictive performance of the IT2FLS for the strength of the tablets is shown in Figure 4.11, with a RMSE (training, testing) = [0.1038, 0.1099]

MPa. Two sample rules are presented in Figure 4.12, and their corresponding linguistic forms can be read as follows:

Rule 1: IF *the size is in the range of 500μm to 710μm and the binder content is small and the porosity is medium,* ***THEN*** *the strength is medium.*

Rule 2: IF *the size is in the range of 710μm to 1000μm and the binder content is medium and the porosity is medium,* ***THEN*** *the strength is large.*

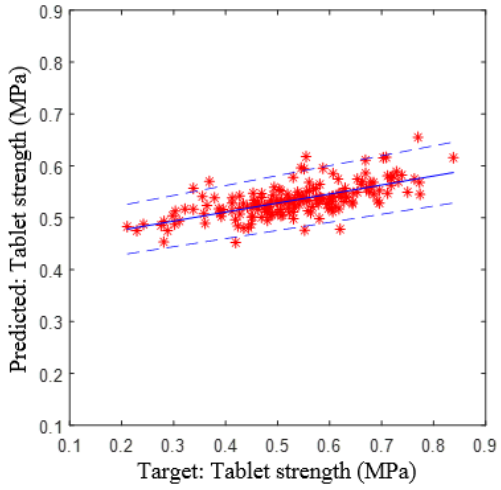

(a)

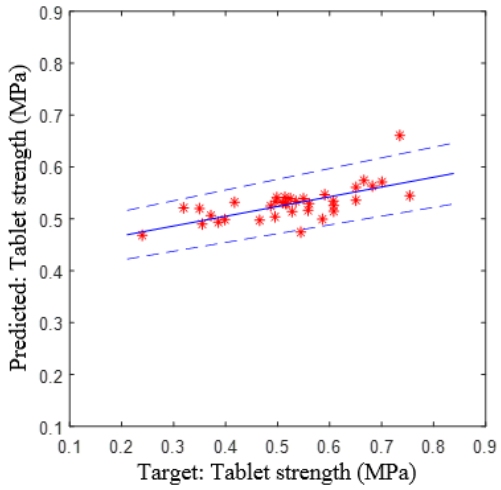

(b)

Figure 4.11. The IT2FLS for the strength of the tablets:
(a) training, (b) testing (with 10% bands).

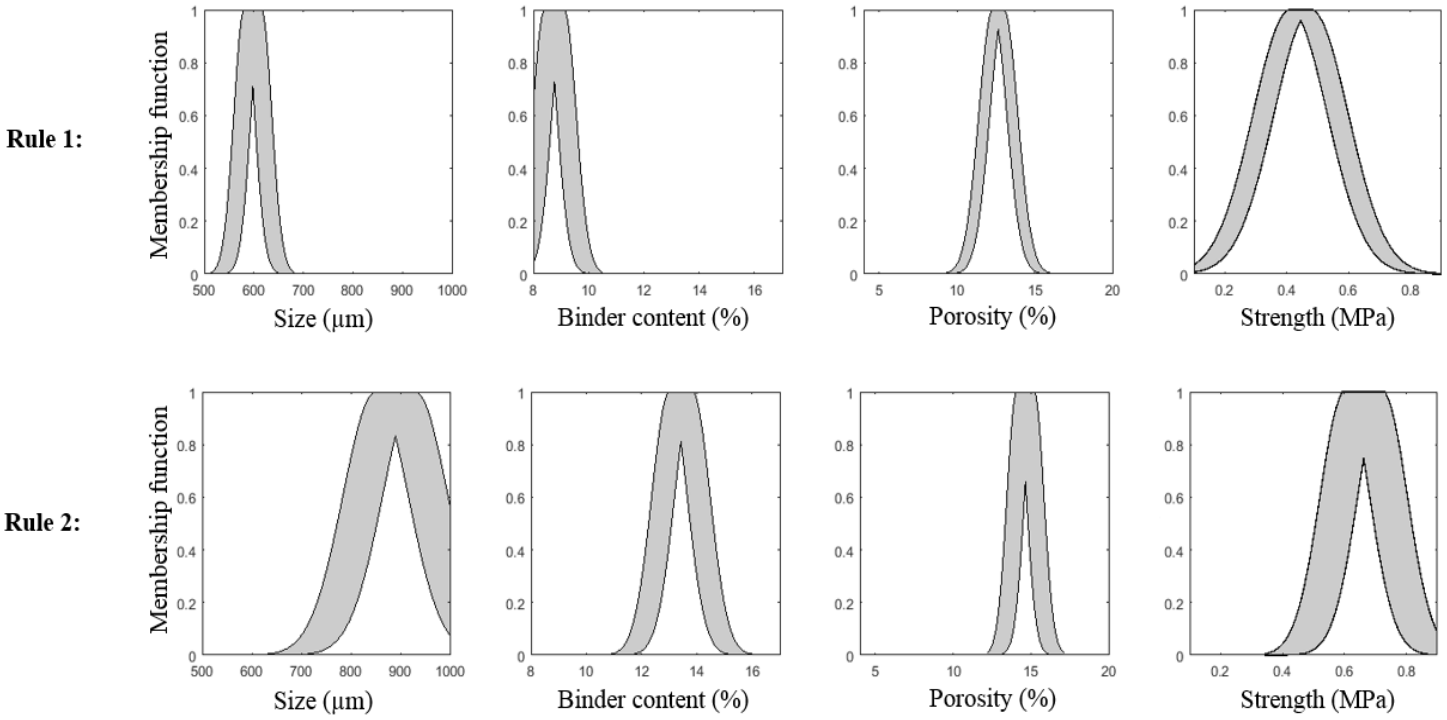

Figure 4.12. The rule base of IT2FLS for the strength of the tablets.

The predictive performance of the IT2FLS is superior to that of the T1FLS. However, such a performance indicates that the model cannot be utilized to represent the tabletting process. Consequently, the rules extracted may not reflect such a process. Therefore, in this research work, such a model will be improved by the incorporation of a modified GMM algorithm in the original modelling architecture for both T1FLS and IT2FLS.

4.4 The Gaussian Mixture Model

4.4.1 The Gaussian Mixture Model: Model Development

In general, the majority of the predictive modelling paradigms including fuzzy logic systems implicitly assume that the modelling error residuals follow a normal distribution (Yang *et al*., 2012), as stated previously in Chapter 3. In reality, such an assumption may not be valid, in particular, when the process to be modelled is complex and with measurable but noisy or non-measurable factors. In such a case, the normality assumption may result in losing useful information and, consequently, lead to a model with sub-optimal parameters (Yang *et al*., 2012). Hence, various modelling strategies have been presented to refine these models by extracting the information that may be hidden behind the error (Mauricio, 2008; Oliveira and Pedrycz, 2007; Yang *et al*., 2012). In Chapter 3, the GMM was utilized to refine the models presented by considering any potential bias in the predicted outputs. Such a choice was motivated by the fact that the GMM is able to provide a deeper insight into the density function, and it is also able to accurately approximate any density function using the optimal number of Gaussian components (Bishop, 2006). Therefore, such an algorithm can lead to the best model refinement (Yang *et al*., 2012). However, in fuzzy logic systems, using these paradigms, including the GMM, will change the rules extracted from the

process data, in other words, the rules cannot be accurately used to represent the process. Therefore, in this chapter, the GMM algorithm is modified to refine the rules of the fuzzy systems instead of the data points.

Some of the steps presented in this chapter are quite similar to the steps that were previously explained in Chapter 3. To illustrate, the GMM parameters (*e.g*. the mean and the covariance of each Gaussian component) are optimized by maximizing the log likelihood function, where the optimization problem is solved using the Expectation Maximization (EM) algorithm (McLachlan and Krishnan, 2008). In addition, BIC is adopted as a performance measure for choosing the optimal number of components (Simon and Girolami, 2012). Once the optimal parameters are defined, the calculated conditional mean is added to the consequent mean of the corresponding cluster; in order to compensate for the bias. This step is followed by defuzzifying and estimating the output. The steps of the modified error characterization algorithm are outlined in Figure 4.13.

4.4.2 The Gaussian Mixture Model: Results and Discussion

A. The Granulation Process

To improve the modelling performances of the FLSs, the error residuals were characterized using the modified GMM algorithm presented above. Since both the T1FLS and the IT2FLS considered the main effects of the investigated variables, two input variables out of four were included in the GMM. The combination of these variables that corresponds to the maximum error compensation was selected. Since the performance of the IT2FLS was superior to that of the T1FLS, the results of the former will be discussed in details, whereas the results of the latter will be briefly summarized in this chapter.

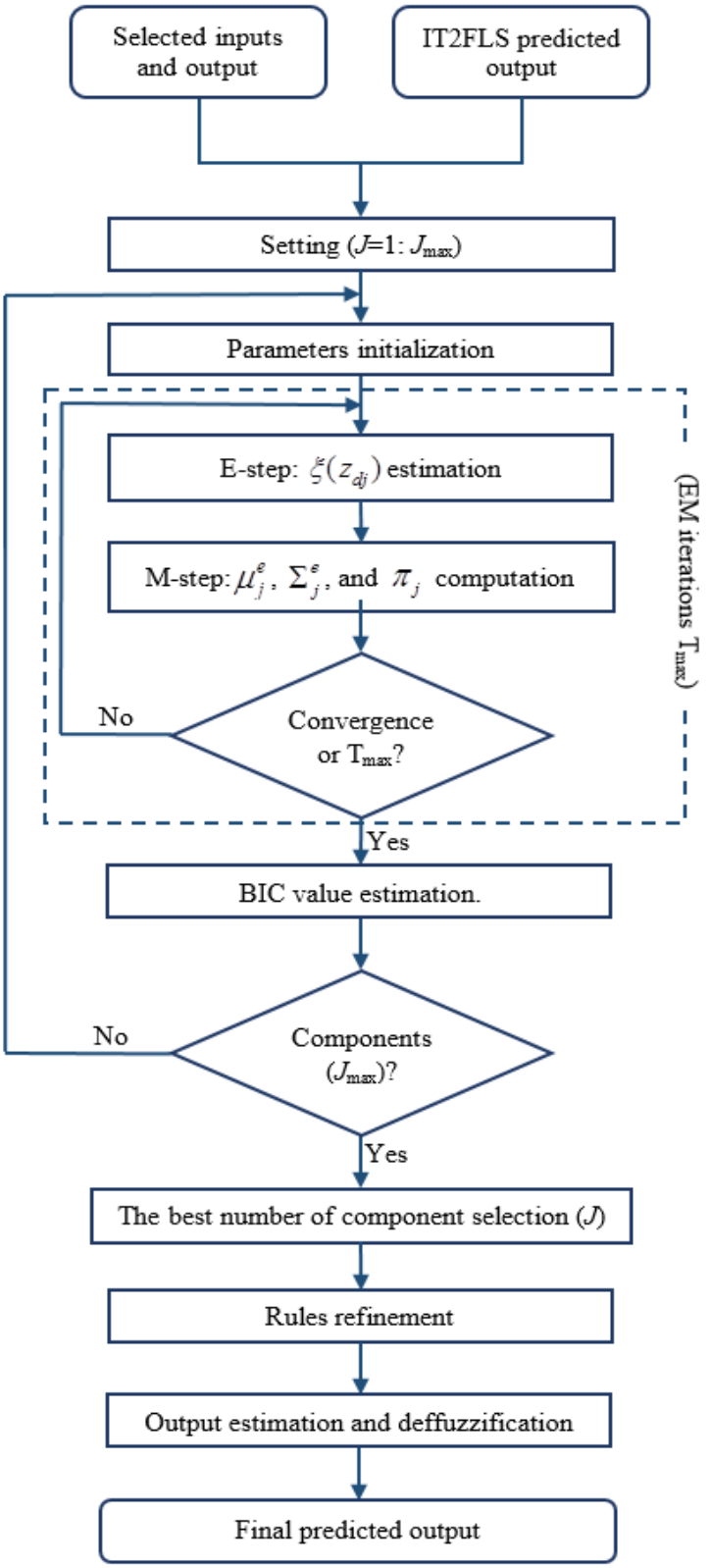

Figure 4.13. Flowchart of the modified error characterisation model (The parameters are as defined previously in Chapter 3).

The IT2FLS performance was refined by implementing the modified GMM algorithm illustrated in Figure 4.13. The combination of the input variables that was selected is the one that led to the minimum RMSE value (*i.e.* the maximum error compensation). Consequently, the impeller speed, the granulation time and the error residuals were utilized to develop the error characterization model. The GMM was trained using the training data set. By using 8 Gaussian components, Figure 4.14 shows the model performance for D_{50} after bias compensation, with a RMSE (training, testing) = [0.23, 0.24] mm.

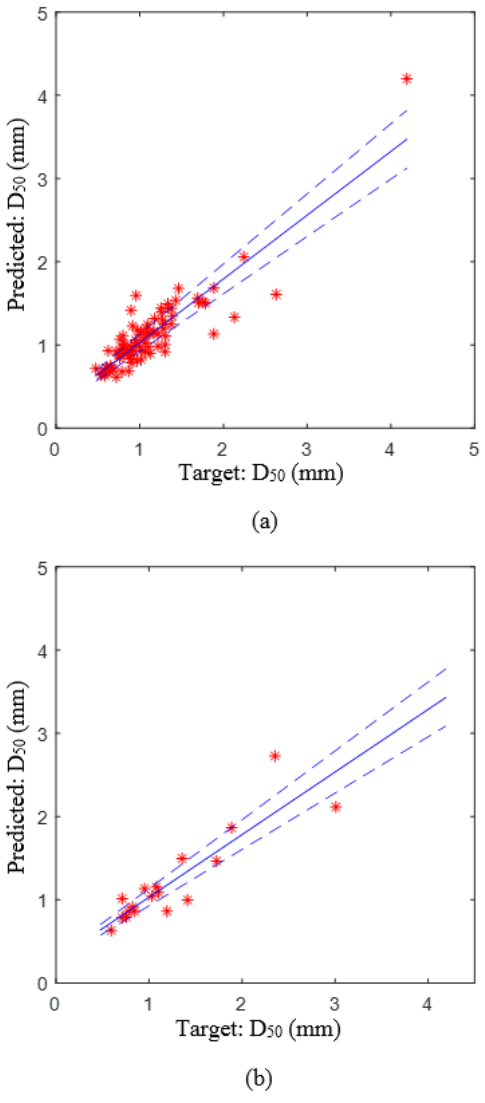

Figure 4.14. The prediction performance of the IT2FLS for D_{50} after bias compensation (with 10% bands).

For the granule size, the overall improvement achieved by applying the modified GMM algorithm is of approximately 6% in R^2. This demonstrates the ability of such an algorithm to compensate for bias by detecting the unmodelled (stochastic) behaviour. The rules after bias compensation are illustrated in Figure 4.15, where one can notice that the antecedents are similar to the ones presented in Figure 4.8 but the consequent is slightly different. The consequent mean values for Rules 1 and 2 were refined by approximately 0.24mm (to the left) and 0.32mm (to the right), respectively. Such slight changes in the mean values did not actually change the linguistic forms of these rules. It is worth mentioning at this stage that the prediction performance of the modified GMM algorithm is superior to that of the traditional GMM algorithm presented in (Yang *et al*., 2012), with an overall improvement of approximately 2% in R^2. Moreover, as stated previously, the rules extracted can be retained by such a modified algorithm.

The predicted and the experimental size distributions for the same three experiments presented above after bias compensation are shown in Figure 4.16. Different numbers of Gaussian components were assigned to the various size classes, these numbers were in the range of 4 to 9. Such a figure shows the ability of the proposed framework; the IT2FLS followed by the modified GMM algorithm, to satisfactorily predict the size distribution of the granules produced by the HSG process. Moreover, the IT2FLS provided users with a simple understanding of the process, such an understanding was retained during the error characterization model.

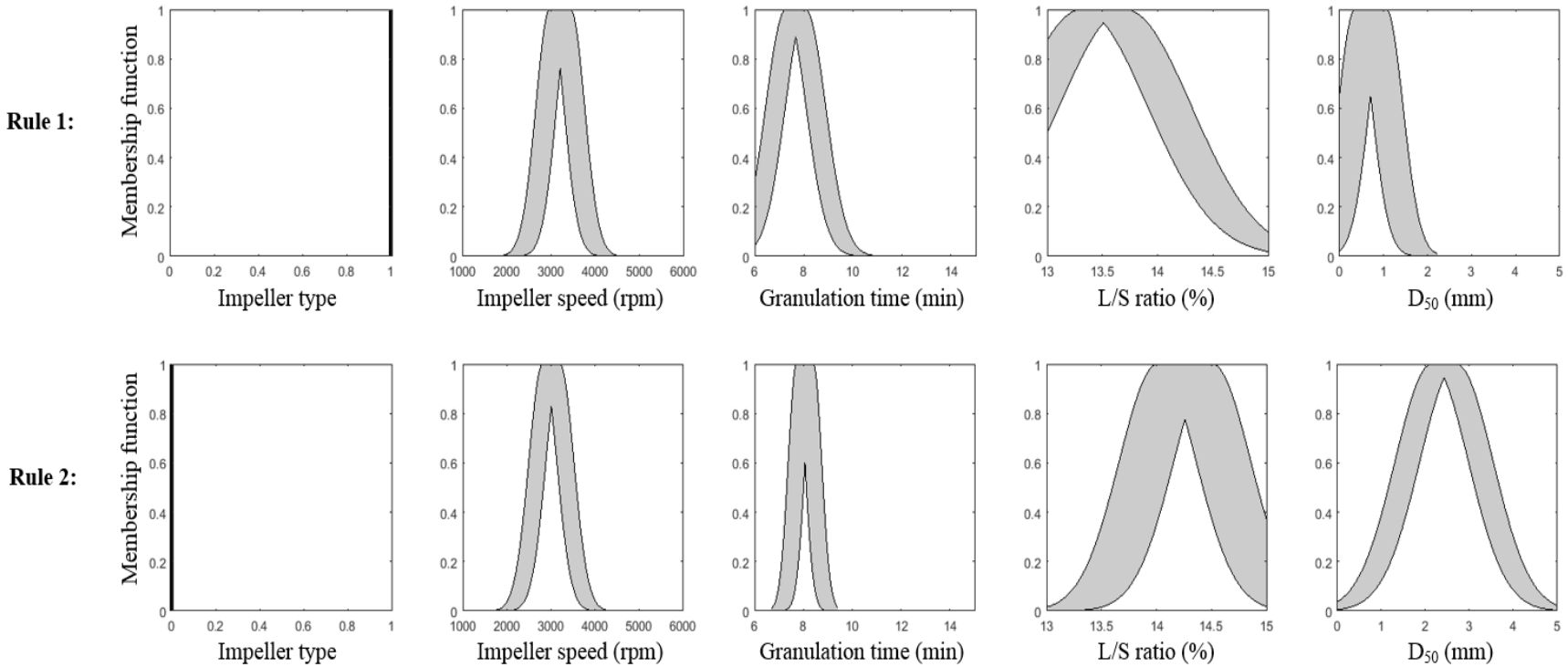

Figure 4.15. The rule base of the IT2FLS for D_{50} after bias compensation.

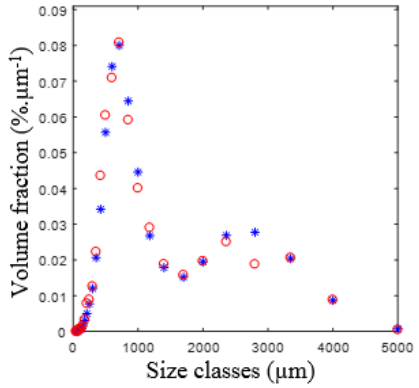

(a)

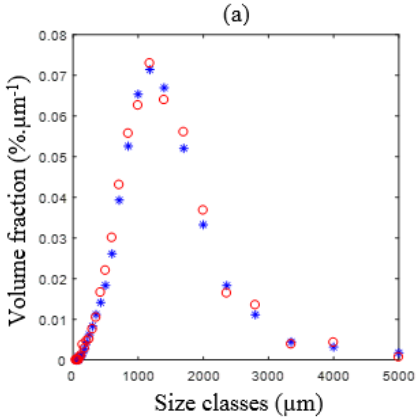

(b)

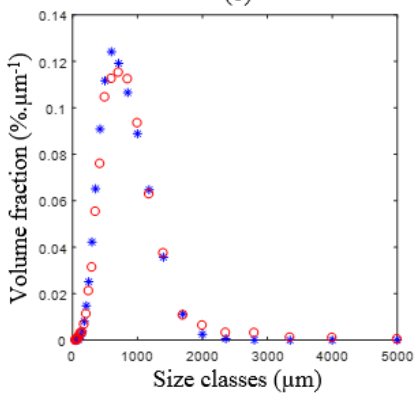

(c)

Figure 4.16. The IT2FLS after bias compensation: the predicted (o) and the experimental (*) distributions for the size (a) using impeller type II, speed=2000rpm, L/S ratio (w/w)=14% and granulation time=10min, (b) using impeller type II, speed=6000rpm, L/S ratio (w/w)=15% and granulation time=15min.

In a similar manner, the modified GMM algorithm was utilized to modify the IT2FLSs that were developed to predict the values of the binder content and the porosity of the granules. The performance measures for these properties are listed in Table 4.1. It is worth mentioning at this stage that different values for the number of Gaussian components were used. Although, the overall improvements that were gained by the modified GMM algorithm for the binder content and the porosity are 13% and 17% in R^2, respectively, the frameworks are still considered unable to predict these properties successfully. Consequently, these modelling frameworks cannot be used for the development of a *reverse-engineering* framework for the granulation process.

For comparison purposes, the modified GMM algorithm was adopted to refine the T1FLS, leading to a significant improvement, as summarized in Table 4.1. However, it is apparent that the model incorporating the IT2FLS and the modified GMM algorithm outperforms the one incorporating the T1FLS and the modified GMM algorithm for all the investigated properties. Therefore, such a framework cannot be utilized to successfully predict the properties of the granules and, consequently, it cannot be used for the development of a *reverse-engineering* framework for the granulation process.

B. The Tabletting Process

The modified GMM algorithm was also utilized to improve the performance of the IT2FLS that was developed to represent the tabletting process. The binder content, the porosity and the error residuals were used to implement such an algorithm. The selection of these two properties was expected since, as reported in literature and as it is well-known, they are heterogeneously distributed (Osborne *et al*., 2011;

Reynolds *et al*., 2004; Scott *et al*., 2000). The best number of Gaussian components is 9. The model performance for the strength is R^2 (training, testing) = [0.50, 0.50], as shown in Figure 4.17. The antecedents of the rules presented in Section 4.3.2 (B) are still the same but the consequents are slightly different. The consequent mean values for Rules 1 and 2 were refined by approximately 0.09 MPa (to the right) and 0.11 MPa (to the right), respectively. The overall improvement that was gained is of approximately 12% in R^2.

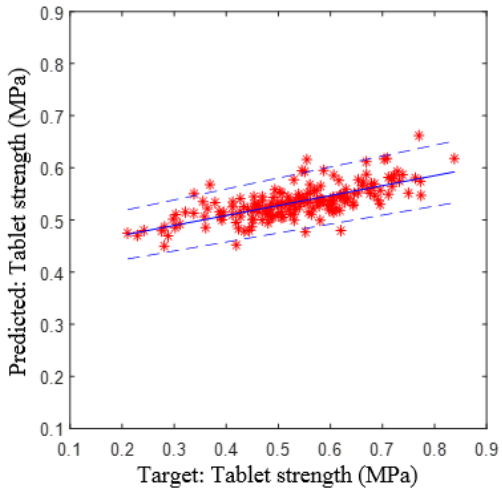

(a)

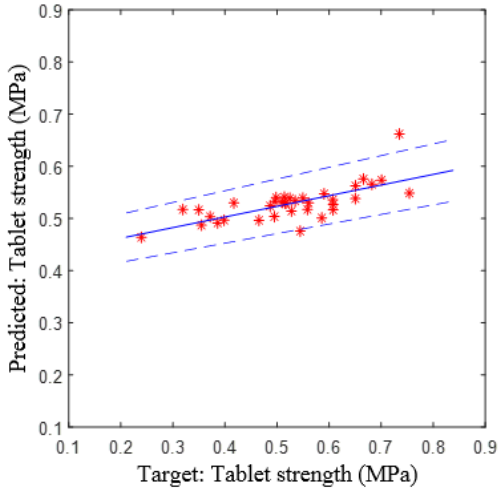

(b)

Figure 4.17. The model incorporating the IT2FLS and the GMM for the tablet strength: (a) training and (b) testing (with 10% bands).

For comparison purposes, the modified GMM was also adopted to refine the T1FLS that was developed for the tabletting process, leading to a significant improvement of approximately 8% in R^2. However, it is apparent that the model incorporating the IT2FLS and the modified GMM algorithm outperforms the one incorporating the T1FLS and the modified GMM algorithm. The traditional GMM algorithm was also utilized to refine both the IT2FLS and the T1FLS, the overall performances of the model that is based on the former and the one that is based on the latter are R^2 (training, testing) = [0.48, 0.49] and R^2 (training, testing) = [0.44, 0.44], respectively. Such performance measures demonstrate that the modified GMM algorithm is superior to that of the traditional one presented in (Yang *et al*., 2012).

4.5 Summary

In addition to successfully predicting the properties of the granules, providing a simple understanding of the granulation process is one of the objectives that researchers strive to achieve. However, such a process is surrounded by uncertainties that may limit the performance of some models such as an ANN. Furthermore, most of the modelling approaches presented previously assume that the error residuals follow a normal distribution, such an assumption may lead to a degradation in the performance of these approaches because of the presence of other non-deterministic behaviour. Therefore, in this chapter, FLSs, namely; type-1 and interval type-2, were utilized to model the HSG and tabletting processes. For the HSG process, these models mapped the input variables to the properties of the granules by extracting linguistic rules from the collected data set, whereas the granule properties and the strength of the tablets were used as the inputs and the output of the models that were developed for the tabletting process, respectively. The error residuals were then characterized using

the modified GMM algorithm, such an algorithm was implemented in such a way that extracted rules were refined in order to compensate for any potential bias, which would result from any unmodelled behaviour.

In this research work, the modelling performance of the IT2FLS was superior to that of the T1FLS, and, consequently, the model incorporating the IT2FLS and the modified GMM algorithm was also superior to the one incorporating the T1FLS and the modified GMM algorithm. However, significant improvements for both of them were gained by implementing the modified algorithm. It is worth mentioning at this stage that the performances for the binder content and porosity, which were not as good as expected, were generally worse than the ones for the size, and also the performance for the strength of the tablets was not satisfactory. Consequently, such models cannot be used to develop a *right-first-time* framework for the granulation and the tabletting processes. Therefore, there is a need to develop a model that can successfully predict the main properties of the granules, provide the required understanding of the process and its mechanisms at the micro-level, and be used efficiently by the pharmaceutical and other related industries. Thus, a modelling framework that integrates data-driven models and physical based ones will be presented in the next chapter.

Chapter 5

Integrating the Physics with Data Analytics for the Hybrid Modelling of the Granulation Process[5]

5.1 Introduction

In general, granulation is recognised as being a complex process with three distinct mechanisms taking place inside the granulator, namely; wetting and nucleation, growth and consolidation, and breakage and attrition (Benali *et al*., 2009; Litster, 2004). Various issues of the granulation process have been addressed in the related literature (Bjorn *et al*., 2005; Braumann *et al*., 2007; Darelius *et al*., 2010; Frikha and Moalla 2015; Litster, 2004; Liu *et al*., 2013; Mansa et al., 2008; Nguyen *et al*., 2014; Pinto *et al*., 2007; Ramkrishna, 2000; Sen *et al*., 2014). However, such a process remains a subject of active research. The reason behind this, as already stated in Chapters 3 and 4, can be attributed to the inherent complexity of such a process which results in the poor understanding of the process and its mechanisms and,

[5] The content of this chapter is published in "AlAlaween, W.H., Mahfouf, M., Salman, A.D., 2017. Integrating physics with data analytics for the hybrid modelling of the granulation process. AIChE. 63, 4761-4773".

consequently, leading to a high recycling ratio and significant wastes in the related industries (Walker, 2007). Consequently, recent studies have focused on the understanding, the modelling and the simulation of the granulation process. The various modelling paradigms that have been developed and applied are either data-driven (*e.g.* an ANN) or physical based models (*e.g.* a PBM) (Bjorn *et al*., 2005; Braumann *et al*., 2007; Mansa *et al*., 2008; Miyamoto *et al*., 1997; Westerhuis et al., 1997).

As discussed previously, these models have their own strengths and limitations. For instance, modelling the granulation process using the PBMs has hitherto provided a good understanding of the process at the micro-level (Poon *et al*., 2008). These models depend mainly on the impact velocity which is a function of the granule position from the impeller. They also depend on the overall flow pattern of the granules inside the mixer. However, such parameters cannot be extracted from these models (Yu *et al*., 2017). Moreover, one of the main difficulties that has been addressed is the representation of the interactions among the mechanisms which play a crucial role in shaping the properties of the granules (Litster, 2004). Thus, various stochastic and mechanistic models have been utilized to provide the necessary understanding of the flow pattern and the impact velocity of the granules (Sen *et al*., 2014; Yu *et al*., 2017). The discrete element method tracks every single particle in the mixer. In practice, such a method may however be computationally taxing since more than a billion particles have to be considered, which is the case for the HSG mixer (Sen *et al*., 2014). Recently, a CFD model has been utilized to model a multiphase flow (Yu *et al*., 2017), in particular, the so-called Eulerian multiphase model has been widely employed to simulate flow with both dispersed and continuous phases, and also to take account of the interactions between these phases (Darelius *et al*., 2010). In this model,

the mean diameter is used to represent the size distribution of the dispersed phase. Such an assumption may lead to inaccurate modelling results when the size distribution is multimodal or wide. Therefore, incorporating the CFD model with the PBM may circumvent the limitations of employing each model separately (Yu *et al*., 2017).

In the granulation process, the successful model is one that (i) can accurately predict the properties of the granules, (ii) can provide the required understanding of the process and its mechanisms, and (iii) can be used reliably and efficiently by the relevant industries. In fact, all of the above objectives may not be achievable by using one single data based or physical based model, this was demonstrated in earlier chapters. Therefore, in this research, a hybrid model integrating both data and physical based models is developed. Such a model integrates three separate but synergetic models through an iterative procedure. The hybrid model consists of three models, namely; a CFD model, the three-dimensional PBM and an RBF model. These models are integrated in such a way that the outputs from one of these models are used as inputs to the other model. In order to improve the modelling performance of the hybrid model, a new fusion model based on fuzzy logic theory and the DS theory is also proposed. The main idea behind this model is to combine the predicted outputs from different models to obtain more accurate predictions, which may not be obtainable using a single model. Thus, the predicted outputs from the hybrid model are combined with the ones from the model incorporating the integrated network and the GMM. As stated previously, this model will be from now on referred to as the incorporated model.

5.2 The Hybrid Model

5.2.1 The Hybrid Model: Model Development

Granulation is a complex process due to the different interactive mechanisms occurring inside the granulator. Such a process is also influenced by many controllable and uncontrollable factors which may possibly have conflicting effects. In addition to the ones mentioned in Chapter 3, these are some of the difficulties that may limit the performance of a single model. In this research work, a hybrid model consisting of both data and physical based models has been developed. Figure 5.1 illustrates the simple iterative scheme of the hybrid model. Based on the granulation input variables and the mixer geometry, a CFD model is developed to analyse the overall flow pattern of the granules, their distribution and the velocity inside the mixer. The output parameters from this model (*e.g.* impact velocity) are crucial to predict the main properties of the granules using a PBM such as the granule size. It is well-known that some empirical parameters are required to implement the PBM (Sanders *et al*., 2003). Therefore, an RBF model is included to estimate these parameters by mapping them directly to the granulation input variables. Such a model can implicitly compensate for the assumptions that have been made to simplify the computational efforts required by the physical models, for instance, the homogeneous mixing features of the overall flow of the granules. In addition, this model is used to express these parameters as a function of the input variables, therefore, a better knowledge relating the effects of the input variables on these parameters and on the final properties of the granules is gained. The size of the granules predicted by the PBM is then used to re-evaluate the parameters obtained from the CFD model, followed by re-estimating the outputs of the PBM and RBF model. The steps above are repeated until a satisfactory performance is reached,

or alternatively the difference between the predictions for two consecutive steps becomes asymptotically small. It is worth emphasising at this stage that the performance of the hybrid model depends on the performances of the models included.

The mathematics behind the single models presented have already been well-publicised. Readers may refer to various research papers and books for further readings, in particular references (Bishop, 1995; Bjorn *et al*., 2005; Braumann *et al*., 2007; Darelius *et al*., 2008; 2006; Frikha and Moalla 2015; Gidaspow, 1994; Immanuel and Doyle III, 2005; Immanuel *et al*., 2005; Iveson, 2002; Litster, 2004; Liu *et al*., 2013; Nguyen *et al*., 2014; Pinto *et al*., 2007; Poon *et al*., 2008; Ramkrishna, 2000; Sanders *et al*., 2003; Sen *et al*., 2014; Tu and Fletcher, 1995; Walker, 2007; Wen and Yu, 1966; Yu *et al*., 2017). In this chapter, only what are considered to be the key developments are included to in order to help the reader get to grips with the various algorithms used.

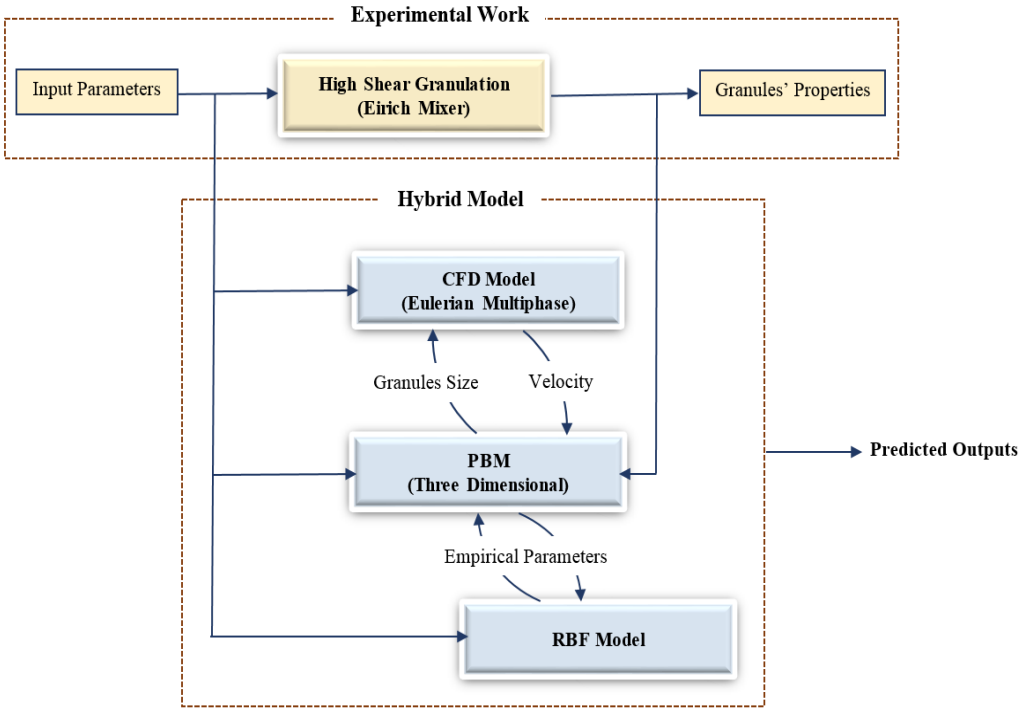

Figure 5.1. The hybrid model for the HSG process.

A. The Population Balance Model

As already stated, a three-dimensional PBM provides a deeper insight into the granulation process by representing its three main mechanisms. This is because it follows the evolution of the granules with time by virtue of the granule size, the binder content and the porosity. The three-dimensional population balance equation is usually written as follows (Ramkrishna, 2000):

$$\frac{\partial}{\partial t}F(s,l,g,t)+\frac{\partial}{\partial s}\left(F(s,l,g,t)\frac{ds}{dt}\right)+\frac{\partial}{\partial l}\left(F(s,l,g,t)\frac{dl}{dt}\right)+\frac{\partial}{\partial g}\left(F(s,l,g,t)\frac{dg}{dt}\right)=\Re_{Nucleation}+\Re_{Aggregation}+\Re_{Breakage} \quad (5.1)$$

where $F(s, l, g, t)$ represents the density function such that $F(s, l, g, t)ds\ dl\ dg$ is the mass of granules when solid (s), liquid (l) and gas (g) are in the ranges (s, $s+ds$), (l, $l+dl$) and (g, $g+dg$), respectively. The evolution of the mass is followed with time (t). The partial derivatives with respect to s, l and g account for layering, drying and re-wetting, and consolidation, respectively. The terms in the right hand-side of (5.1) stand for the rates of nucleation, aggregation and breakage. Various nucleation rates have been developed, however, the majority of these assume that one droplet forms a nucleus. However, the latter assumption is not always valid (Poon *et al*., 2008). Since the breakage of nuclei plays a significant role in the nucleation mechanism (Liu *et al*., 2013), an empirical nucleation rate was used in this study. The aggregation rate consists of two terms, formation and depletion, which can be written as follows (Poon *et al*., 2008):

$$\Re_{Aggregation} = \Re^{Formation}_{Aggregation} + \Re^{Depletion}_{Aggregation}$$

$$\Re^{Formation}_{Aggregation} = \frac{1}{2}\int_{s'=s_{nuc}}^{s-s_{nuc}}\int_{l'=0}^{l}\int_{g'=0}^{g}\beta(s',s-s',l',l-l',g',g-g')\times F(s',l',g',t) \times F(s-s',l-l',g-g',t)\,ds'\,dl'\,dg' \tag{5.2}$$

$$\Re^{Depetion}_{Aggregation} = F(s,l,g,t)\int_{s'=s_{nuc}}^{s-s_{nuc}}\int_{l'=0}^{l}\int_{g'=0}^{g}\beta(s',s,l',l,g',g) \times F(s',l',g',t)\,ds'\,dl'\,dg'$$

where s_{nuc} is the volume of the nucleus, and $\beta(s',s-s',l',l-l',g',g-g')$ is the aggregation kernel which governs the rate at which two granules with internal coordinates (s',l',g') and $(s-s',l-l',g-g')$ agglomerate. In fact, the coalescence of two granules depends on the granules size and the availability of the binder on their surfaces. The semi-mechanistic aggregation kernel that describes these two factors and the coalescence types has been already presented in (Immanuel and Doyle III, 2005). Such a kernel can be expressed as follows (Immanuel and Doyle III, 2005):

$$\beta = \varsigma\frac{4\pi u_0(R_1+R_2)^2}{W}$$

$$W = \begin{cases} (R_1+R_2)\int_{R=R_1+R_2}^{\infty}\frac{\exp\left(\frac{\psi}{kT}\right)}{R^2}dR, & \text{Type I coalescence} \\ (R_1+R_2)\left(\max\left(\int_{R=R_1+R_2}^{\infty}\frac{\exp\left(\frac{-\psi_{forward}}{kT}\right)}{R^2}dR, \int_{R=R_1+R_2}^{\infty}\frac{\exp\left(\frac{-\psi_{reverse}}{kT}\right)}{R^2}dR\right)\right), & \text{Type II coalescence} \end{cases} \tag{5.3}$$

where R_i is the radius of the i^{th} particle, u_0 and W are the initial velocity of the particle and the Fuch stability ratio, respectively. For simplicity, the parameter β is presented as a single variable in (5.3). The parameters k and T represent the Boltzmann constant and the temperature, respectively. The parameter ψ refers to the net attractive potential for coalescence, and ς is a tuneable parameter.

The consolidation mechanism takes into account the compaction process that increases the binder on the surface of granules and leads to a decrease in the porosity. The consolidation process has been empirically expressed by the following set of equations (Pinto *et al*., 2007; Sanders *et al*., 2003):

$$\varepsilon = \frac{l+g}{s+l+g}$$
$$\frac{d\varepsilon}{dt} = -c(\varepsilon - \varepsilon_{\min}) \tag{5.4}$$
$$\frac{dg}{dt} = -c\frac{s+l+g}{s(1-\varepsilon_{\min})}\left(l - \frac{\varepsilon_{\min} s}{1-\varepsilon_{\min}} + g\right)$$

where ε and $\varepsilon_{\min}$ are the porosity and its minimum value, respectively. The constant *c* is the compaction rate constant. The breakage rate was stochastically estimated based on the algorithm developed in (Pinto *et al*., 2007). Such an algorithm is based on determining the likelihood that a granule in a specific size class breaks to form a number of granules in smaller size classes.

B. Computational Fluid Dynamics

Generally, numerical simulation techniques of a system can be divided into two types; continuum and discrete. As the names indicate, the former views the system as a continuous flow (*i.e*. fluid), while the latter deals with an individual particle. An Eulerian multiphase model is used to simulate the particulate phase as a continuous flow (Nguyen *et al*., 2014). Two phases; solid and gas, are considered. The mass and momentum of these two phases are governed by the following set of equations (Darelius *et al*., 2008):

$$\begin{aligned}
&\frac{\partial(\alpha_g \rho_g u_g)}{\partial t} + \nabla.(\alpha_g \rho_g u_g u_g) = -\alpha_g \nabla P + \nabla.(\alpha_g \tau_g) - \gamma(u_g - u_s) + F \\
&\frac{\partial(\alpha_g \rho_g)}{\partial t} + \nabla.(\alpha_g \rho_g u_g) = 0 \\
&\frac{\partial(\alpha_s \rho_s u_s)}{\partial t} + \nabla.(\alpha_s \rho_s u_s u_s) = -\alpha_s \nabla P + \nabla P_s + \nabla.(\alpha_s \tau_s) - \gamma(u_g - u_s) + F \\
&\frac{\partial(\alpha_s \rho_s)}{\partial t} + \nabla.(\alpha_s \rho_s u_s) = 0
\end{aligned} \tag{5.5}$$

where α, ρ and u are the volume fraction, density and velocity, respectively. The subscripts are used to distinguish the parameters of the gas (*g*) phase from the ones of the solid (*s*) phase. The volume fractions must sum to unity. The parameters *P* and *F* represent the pressure and all the forces acting on the system under investigation, respectively. The interphase momentum exchange coefficient (γ) is calculated using the equation presented in (Wen and Yu, 1966). The viscous stress tensor (τ) can simply be written as follows (Darelius *et al*., 2008):

$$\tau_k = \left(\upsilon_k - \frac{2}{3} \nu_k \right) (\nabla.u_k) I + 2\nu_k S_k \tag{5.6}$$

where υ and ν represent the bulk and dynamic viscosity of the k^{th} phase, respectively. The parameter *S* represents the strain rate tensor derived in (Darelius *et al*., 2008), and *I* is the second invariant of the strain rate tensor.

By virtue of the extension of the kinetic theory of dense gas, one would develop the kinetic theory of the granular flow (KTGF) model. Such a theory depends on statistical mechanics to describe the velocity of a granular flow. As already outlined in (Gidaspow, 1994), the KTGF model assumes that particles interaction is binary as well as instantaneous. At a high solid fraction, this may result in high particles/granules stresses. Therefore, the frictional term, or the so-called frictional stress model, should

be taken into account when the pressure and the dynamic viscosity of the solid phase are evaluated: the model is further detailed in (Darelius *et al*., 2008). It is worth mentioning at this stage that, in this study, the angle of internal friction was 44^{o}.

Various boundary conditions have been used in the open literature (Darelius *et al*., 2008). In this research work, the 'no slip' boundary condition at the vessel, impeller and scraper wall was used for the gas phase. For the solid phase, the 'partial slip' model proposed in (Tu and Fletcher, 1995) was utilized. The coefficient of restitution was chosen to be 0.5. Such a model is a combination of both 'no slip' and 'free slip' conditions.

C. The Radial Basis Function Model

An RBF model usually maps a set of inputs to an output. Since the RBF model was discussed in Chapter 3, it will be briefly described in this section. In general, an RBF network consists of three layers: an input, hidden including basis functions, and an output layer. Such a mapping can be generally given as follows (Bishop, 1995):

$$y(x) = \sum_{i=1}^{I} w_i \phi_i(x) + w_0 \tag{5.7}$$

where w_i and w_0 denote the weights and bias, respectively. The parameter x is the input vector and y is the predicted output which is expressed as a linear combination of the basis functions. The RBF is a function of the radial distance from a centre. Because of its ability to approximate any function with a reasonable accuracy using a sufficient number of components, the Gaussian form is a popular choice for such a function (Bishop, 1995). The predicted outputs in this chapter are the empirical parameters that are required to implement the PBM. Typically, the available data are divided into

training and testing data sets. The training data are used for identifying the relationships between the inputs and the outputs, while the testing data are used to test good generalization capabilities measured via the RMSE. The model parameters (*e.g*. mean) were optimized using the SCG algorithm (Bishop, 1995). The best network structure (*i.e*. the number of basis functions) is the one that corresponds to the minimum RMSE, for instance.

5.2.2 The Hybrid Model: Results and Discussion

In order to study the flow of the granules inside the granulation vessel, two CFD models were developed using ANSYS software (ANSYS Inc., US, Release 16.1) for the simulation of the Eirich mixer with two impellers differing in shape, as shown in Figure 3.2. Accordingly, two fine-meshing schemes which differ in the number of cells were generated. For each model, three different meshing schemes were initially tested, the ones presented in this study are the schemes that led to acceptable solutions.

In each model, the gas-solid flow was analysed using a two-fluid model inspired from the KTGF model. The material properties were selected so as to reproduce as closely as possible the properties of air and the properties of the granules produced using 500gm of $CaCO_3$ and different mass values of PEG (1000). The vessel speed was kept constant during the simulation of all experiments (at 170rpm clockwise), while the values of the impeller speed were assigned corresponding to the operating conditions. The granules were assumed to have initially settled at the bottom of the granulation vessel. A second-order upwind scheme was utilized to solve all the partial differential equations, while the volume fraction equation was solved using a first-order scheme. The simulation was stopped once it converged, or alternatively a stable flow was observed.

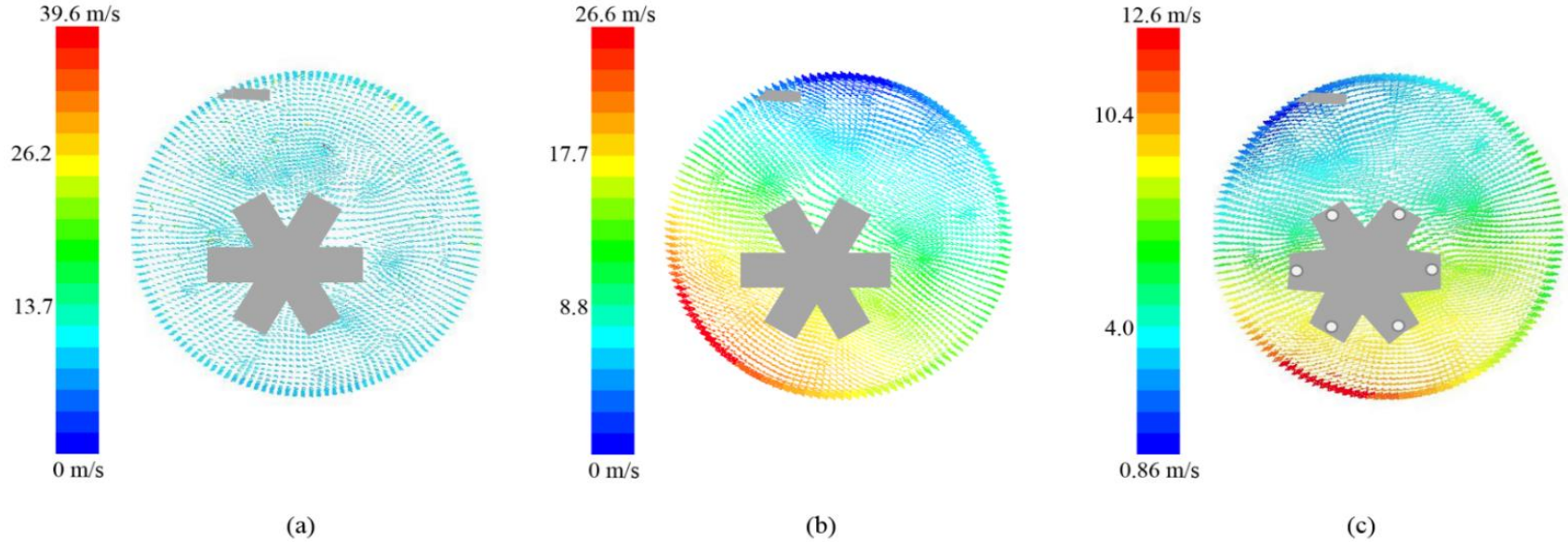

Figure 5.2. ANSYS based profiles: the velocity profiles of the granules (a) using impeller type II, speed=2000rpm, L/S ratio (w/w)=14%; (b) using impeller type II, speed=6000rpm, L/S ratio (w/w)=15%; (c) using impeller type I, speed=4000rpm, L/S ratio (w/w)=13%.

Figure 5.2 shows the velocity profiles of the granules for three different experiments. Although the vessel itself was rotating during the experiments, the highest velocities (*i.e.* radial and tangential velocities) and their gradients can be observed around the impeller area, specifically when the granules are close to both the impeller and the vessel, this being due to the values of the tip speed and also to the fact that both of them rotate in the same direction. Such a phenomenon was observed during experiments where the velocity of the impeller is high.

It was also observed that the velocity of the granules is still highly dependent on the spatial position of the granules from the impeller, similarly to what was previously reported in (Yu *et al*., 2017). Thus, different areas have different velocity values, as shown in Figure 5.2 (b) and (c). However, such a behaviour cannot be observed when the impeller speed is low, which can probably lead to relatively homogeneous mixing features (Yu *et al*., 2017), as presented in Figure 5.2 (a). It is worth noting that the velocity scale shown in Figure 5.2 (a) is wider compared to Figure 5.2 (b) and (c), however, the granule velocity value in (a) is smaller and it reflects the impeller and the vessel speed value (*i.e.* tip speed). Under the same operating conditions, the range of the velocity values for impeller type II model is wider than the one for impeller type I, which may be due to the difference in the geometry and contact area.

The concentration of the granules (volume fraction) inside the mixer is shown in Figure 5.3. The flow regime of the granules shows that the bed surface undulates as the granules are closer to the impeller. A similar behaviour was observed around the scrapper but the bed height is lower. A maximum bed height occurs when the impeller speed is high (at 6000rpm). Spikes in the concentration of the granules were observed

during the experiments, which were carried-out using impeller type I, as shown in Figure 5.3 (c). This may be due to the presence of pins on the upper surface of the impeller. As expected, a heterogeneous distribution of the granules is shown in the figure. It is worth noting at this stage that the concentration of the granules is relatively high around the scrapper area in some experiments, which can be explained if one considers the scrapper as a hindrance, especially, at low impeller speed.

A low concentration of the granules appears around the impeller; this is the result of the force that is applied by the impeller driving the granules towards the vessel wall. In addition, low concentration of the granules can also be observed in the upper volume of the vessel, where the gas phase dominates. Such a behaviour is noticeable when the impeller speed is relatively low. Moreover, such a low concentration appears around the centre of the vessel in some experiments as a result of the centrifugal force. In fact, this should be in the centre of the vessel, however, the presence of the impeller, which is not in the centre, and the scrapper may have shifted the force effect.

The initial results obtained from running the CFD model prove that the velocity and the concentration of the granules and, accordingly, the granulation rates (*e.g.* growth and breakage) are indeed dependent on the spatial position of the granules themselves, as also previously reported in the literature (Yu *et al.*, 2017). A compartmental model has already been developed for similar cases in the literature. This model can lead to better results if a sufficient number of compartments is used. However, it is considered to be a computationally-taxing model (Yu *et al.*, 2017). Therefore, the average velocity was instead used to evaluate the parameters of the PBM in this study. In fact, such an assumption may have a negative effect on the final predictions of the granule properties if the empirical parameters were not

systematically estimated. However, in this research work, this did not seem to have a significant effect since the RBF-based model will internally compensate for this.

A three-dimensional PBM was also developed, as discussed in Section 5.2.1 (A). In order to solve the integro-differential equations, a hierarchical algorithm presented in (Immanuel and Doyle III, 2005) was employed in this research work. This algorithm is based on discretising the three-dimensional population into a number of bins represented as finite volumes. This hierarchical framework enables the user to pre-calculate the time-independent terms of the kernels. As stated previously, estimating the kernels (*e.g.* aggregation kernel) depends on empirical parameters. These parameters were evaluated to match the experimental results, followed by mapping the parameters to the granulation input variables by using the RBF model.

A single RBF model was developed to represent the relationships among all the input variables (*i.e.* operating conditions) and the empirical parameters of the PBM. For the empirical parameter (ς) that is used to estimate the size dependent aggregation kernel presented in (5.3), 8 RBFs, which correspond to the minimum error calculated using the RMSE, were selected. The prediction performance is presented in Figure 5.4. The RMSE values (training=0.055, testing=0.035) indicate that the model can be used successfully to predict this parameter. Similarly, the model led to a good performance for all the empirical parameters considered. Using the estimated empirical parameters, the properties of the granules were predicted. Since the granule size has a significant effect on the granule velocity and its distribution, the predicted size was then used to update the parameters of the CFD model. These steps were repeated until the difference between the predictions for two consecutive steps became very small.

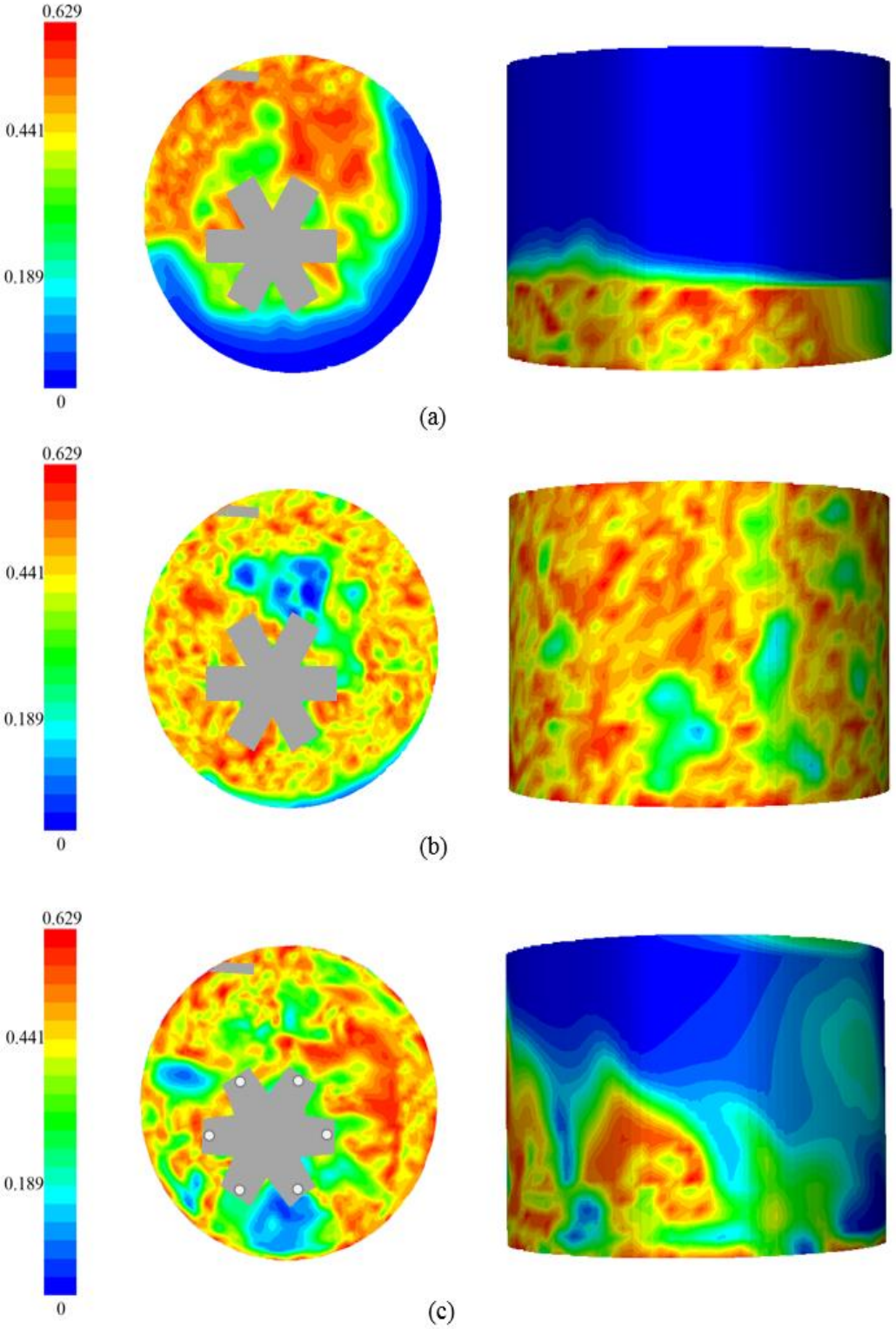

Figure 5.3. ANSYS based profiles: the concentration of the granules: top (at approximately 3cm from the base) and side view (a) using impeller type II, speed=2000rpm, L/S ratio (w/w)=14%; (b) using impeller type II, speed=6000rpm, L/S ratio (w/w)=15%; (c) using impeller type I, speed=4000rpm, L/S ratio (w/w)=13%.

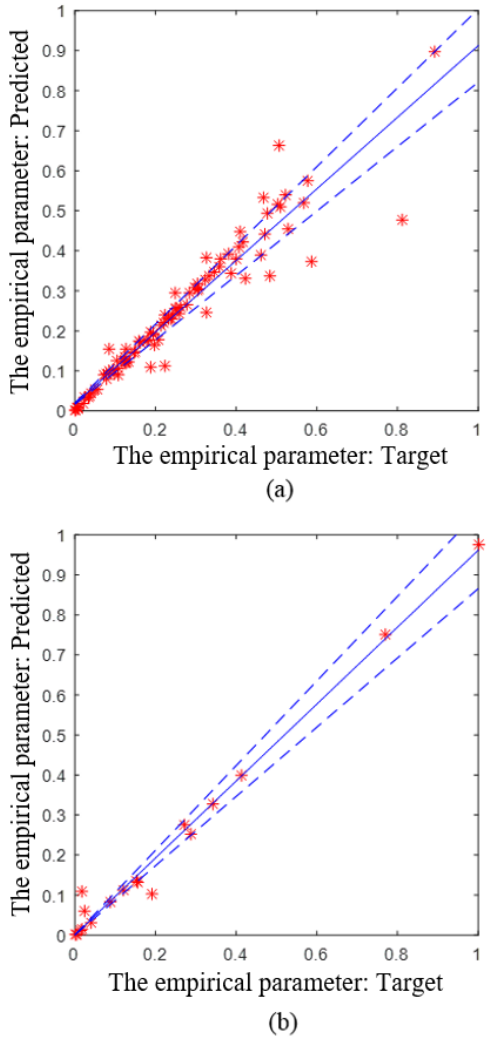

Figure 5.4. The RBF model for the empirical parameter that is used to estimate the aggregation kernel (normalized): (a) training, (b) testing (with 10% bands) (RBF Network Weights= [1 0.5 0.4 1.5 0.8 1.3 1.3 0.9], and Bias=0.58).

Figure 5.5 shows the prediction results for the three experiments which were carried-out under varying operating conditions. In a similar manner, the properties of the granules were predicted for all experiments. The number of iterations for the experiments varied, and generally this number was in the range of 6 to 10. The predictive performances for all experiments demonstrate the ability of the hybrid model to predict the properties successfully and to implicitly compensate for the

assumptions that have been made about the granulation process. Moreover, the presented model outperformed the three-dimensional PBM. Figure 5.6 shows an example of the predictive performance of the PBM. The PBM performances for the binder content and porosity are not as good as the hybrid model ones, and it is apparent that these performances are worse than the ones for size.

Although, the hybrid model satisfactorily modelled the granulation process, it can be further improved. This model initiated the simulation process using the nuclei instead of the particles, this being due to the difficulty in taking account of three phases in the CFD model. Therefore, the hybrid model can be implemented in two stages; the first stage considers the binder and the particles, whereas the second stage considers the granules and gas, followed by integrating the two stages together. Moreover, further investigations will need to be performed to explore the advantages and the limitations of developing such a complex model.

5.3 Fusion Model

5.3.1 Fusion Model: The Basic Idea

One of the basic concepts of cognitive process used by human is information fusion. In simple terms, fusion is integrating information from various sources to realise effective inferences and generate optimal decisions (Frikha and Moalla, 2015). The motivation for this process lies in the fact that the information provided from one source are, more often than not, limited and with limited accuracy (Frikha and Moalla, 2015). Therefore, information fusion has been extensively applied in many areas, including marine technology, manufacturing as well as health care, to ultimately improve the reliability of information (Boudraa *et al*., 2004).

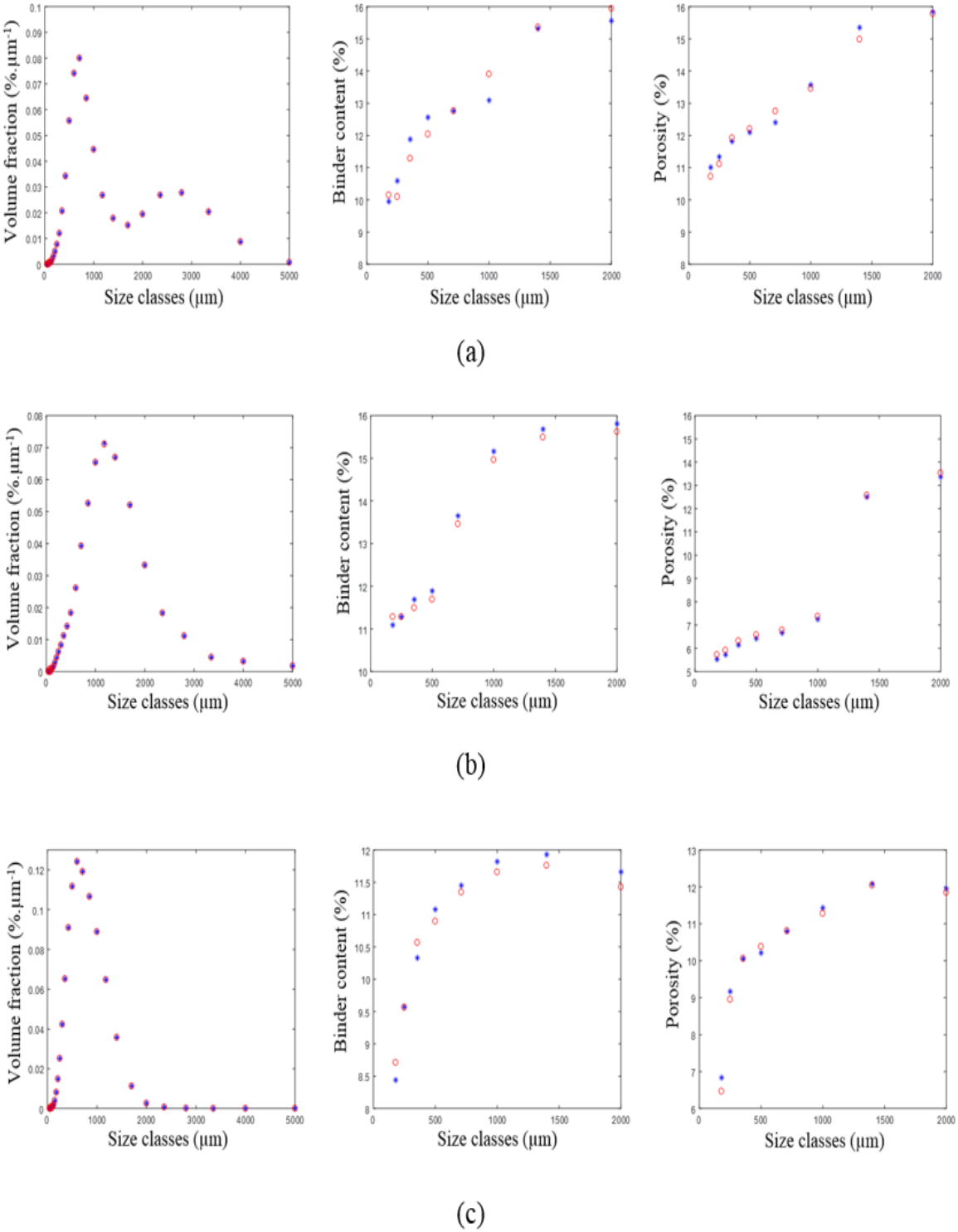

Figure 5.5. The hybrid model: the predicted (o) and the experimental (*) distributions for the size, binder content and porosity (a) using impeller type II, speed=2000rpm, L/S ratio (w/w)=14% and granulation time=10min; (b) using impeller type II, speed=6000rpm, L/S ratio (w/w)=15% and granulation time=15min; (c) using impeller type I, speed=4000rpm, L/S ratio (w/w)=13% and granulation time=6min.

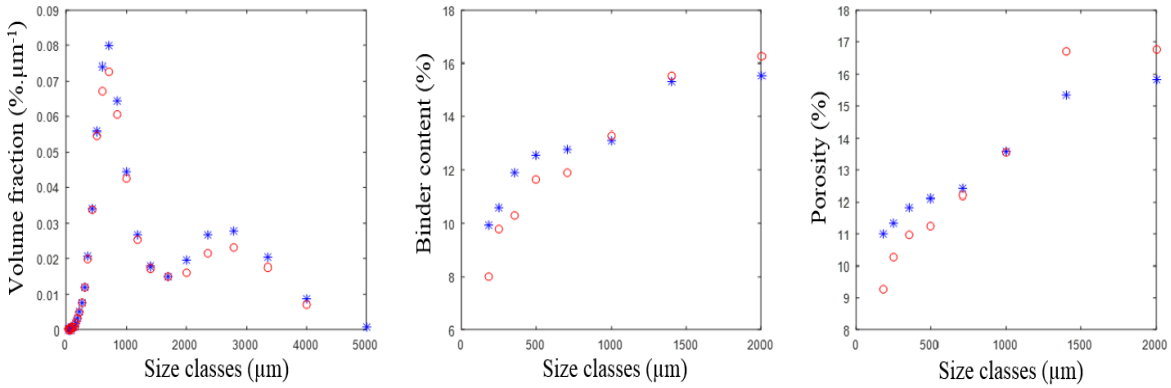

Figure 5.6. The PBM: the predicted (o) and the experimental (*) distributions for the size, binder content and porosity using impeller type II, speed=2000rpm, L/S ratio (w/w)=14% and granulation time=10min.

Various approaches have been developed and used such as Bayesian inference, neuro-fuzzy and the DS theory (Dempster, 1967; Maseleno *et al*., 2015). The latter approach has attracted a lot of interest; this being due to its ability to explicitly estimate imprecision and conflict that may exist between two or more sources of information. However, in order to develop a more reliable fusion model, one should consider three types of uncertainties; uncertainty due to probabilities, uncertainty due to lack of specification and uncertainty due to fuzziness (Boudraa *et al*., 2004). The first two types can usually be tackled via the DS theory, while the third type can be successfully handled using fuzzy logic. Therefore, a new approach that integrates both the DS theory and fuzzy logic has been presented in this research work. The motivation for such an algorithm stems from the strong need to improve the output predictions of the granulation process which is considered to be one of the complex processes to be modelled and predicted. The proposed algorithm integrates the predicted outputs from both the hybrid model and the incorporated model. The fusion model was developed not only to obtain more accurate predictions, which may not be obtainable by using a

single model, but also to resolve any conflict that may exist between the two models. Figure 5.7 summarises the main steps of the proposed model.

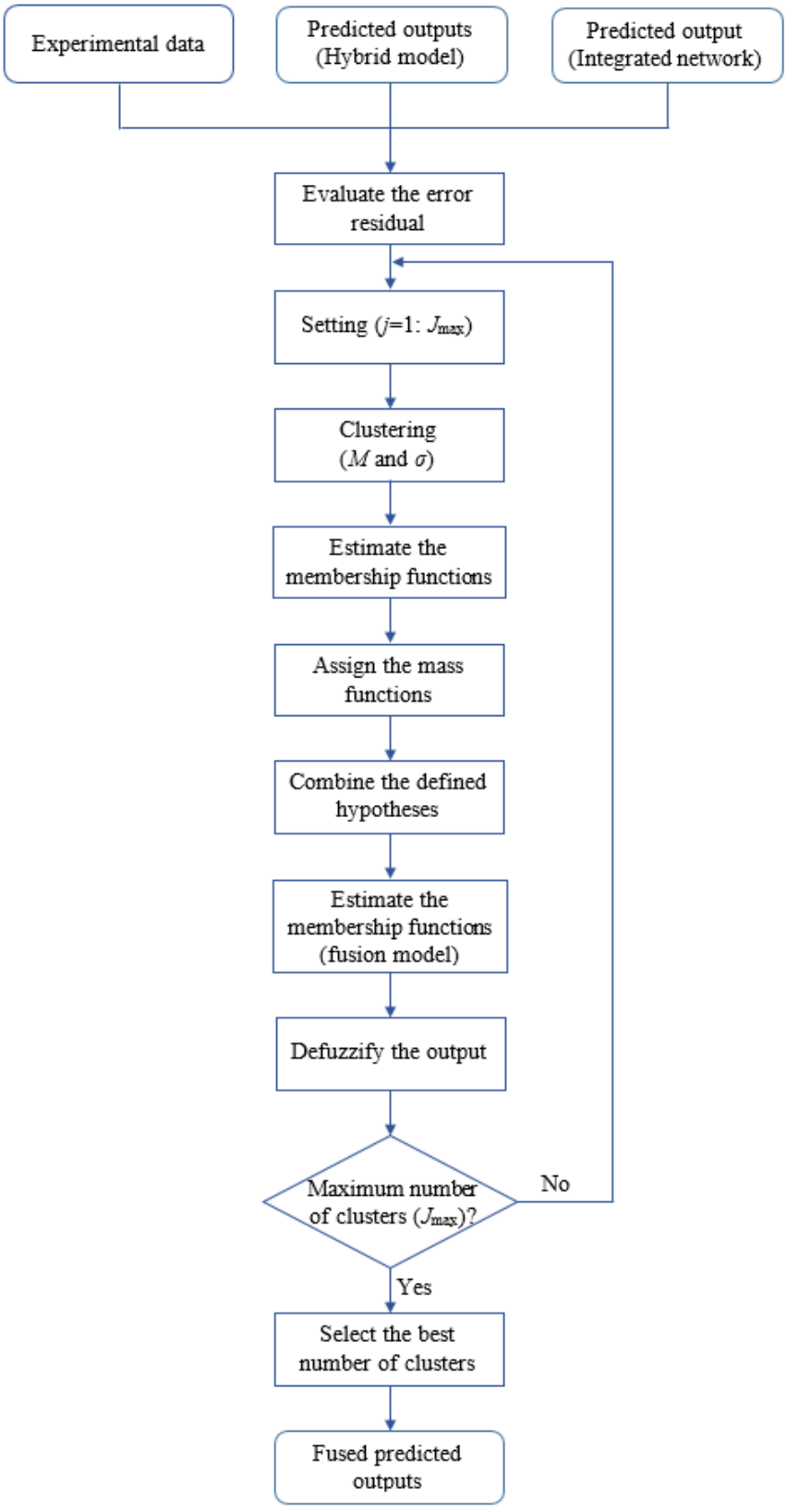

Figure 5.7. Flow chart of the fusion model.

First of all, the number of clusters is defined. Generally, clustering is an unsupervised learning process that aims to discover groups of similar data points within the data set. The optimal number of clusters is subjective, in other words, it depends on the application. In this study, the best number of clusters is the one that corresponds to the maximum improvement in the predictive performance (*i.e.* the minimum RMSE). This step is followed by clustering the input variables and the error residuals that result from both the hybrid model and the incorporated model. The membership function value is defined for each data point as follows (Mendel, 2001):

$$\mu_i^e = \exp\left(\frac{-(x_i^e - M^e)^2}{2(\sigma^e)^2}\right) \tag{5.9}$$

where μ_i^e is the membership function of the i^{th} data point. The parameters M^e and σ^e represent the mean and the standard deviation of a cluster, respectively, and x_i^e is the residual error. The superscript letter (e) is used to distinguish the parameters of the fusion model from the ones used previously in Chapter 4.

In order to combine the predicted outputs of the hybrid model with the ones of the incorporated model, the DS theory is utilized. One of the main challenges in implementing the DS theory is assigning the mass function for all the examined hypotheses. In fact, the mass function can be derived using different algorithms such as probabilities or distance from the centre of a cluster (Bloch, 1996). In this research, the mass function is evaluated using the fuzzy membership function, which is calculated in (5.9). The mass function is generally governed by the following set of equations (Boudraa *et al*., 2004):

$$m_t^f = \left(1 - \sum_{\substack{j=1 \\ j \neq t}}^{J_{\max}} \mu_j^e \times (\eta - \mu_j^e)\right) \times \mu_t^e \qquad (5.10)$$

$$\eta = \arg \max_{1 \le j \le J_{\max}} \mu_j^e$$

where m_t^f is the mass function for the t^{th} hypothesis, and η is the maximum membership function. If the number of clusters is less than or equal to three, then special cases are considered (Boudraa *et al*., 2004). The hypotheses are merged using the Dempster's rule of combination as follows (Dempster, 1967):

$$m_{FM}^f = \frac{1}{1-K} \sum_{HM \cap IM \neq \phi} m_{HM}^f \, m_{IM}^f$$

$$K = \sum_{HM \cap IM = \phi} m_{HM}^f \, m_{IM}^f , \; K \neq 1 \qquad (5.11)$$

where the mass functions for the hypotheses of the fusion, hybrid and incorporated models are distinguished by the subscripts FM, HM and IM, respectively. The parameter *K* measures the conflict between two sources, and it is also used to estimate the normalization factor, which is equal to (1-*K*). A hypothesis of the hybrid model is usually combined with the hypotheses of the incorporated model that have the same or better degree of accuracy, and vice versa. To elucidate, assume that the number of clusters for both models is three (*i.e*. good, satisfactory and bad), as presented in Figure 5.8. To estimate the mass function for the 'satisfactory' hypothesis of the fusion model, the 'satisfactory' hypothesis of the incorporated model should be combined with the 'good' and 'satisfactory' hypotheses of the hybrid model, and the 'satisfactory' hypothesis of the hybrid model should be combined with the 'good' one of the incorporated model, note that the combination of the 'satisfactory' hypotheses has already been considered. A high degree of conflict between a hypothesis and another

less accurate one is assumed, thus, the fusion model can lead to a better performance compared to both the hybrid model and the incorporated model.

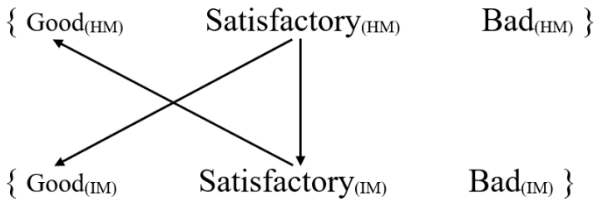

Figure 5.8. Example of combining the clusters.

Once the mass functions of the fusion model are estimated, the membership functions can be calculated by solving the set of equations in (5.10), which is reversed to calculate the membership functions, which need to be weighted and normalized (Boudraa *et al*., 2004). Finally, the height defuzzifier is utilized to evaluate the outputs of the fusion model (Mendel, 2001).

5.3.2 Fusion Model: Results and Discussion

The algorithm relating to the fusion model was implemented to improve the performance of the two models; the hybrid model and the incorporated model, especially, in those areas where the performance of one of the models or both was not as close to the target as desired. Thus, the granulation input variables and the error residuals were used to identify these areas. For instance, Figure 5.9 shows how the hybrid model performs in one of the space areas (*i.e*. clusters) of the binder content. Such a figure indicates that the hybrid model performance measured via the error residuals is satisfactory when the impeller is of type I, the impeller speed is medium, the granulation time is small and the L/S ratio is medium.

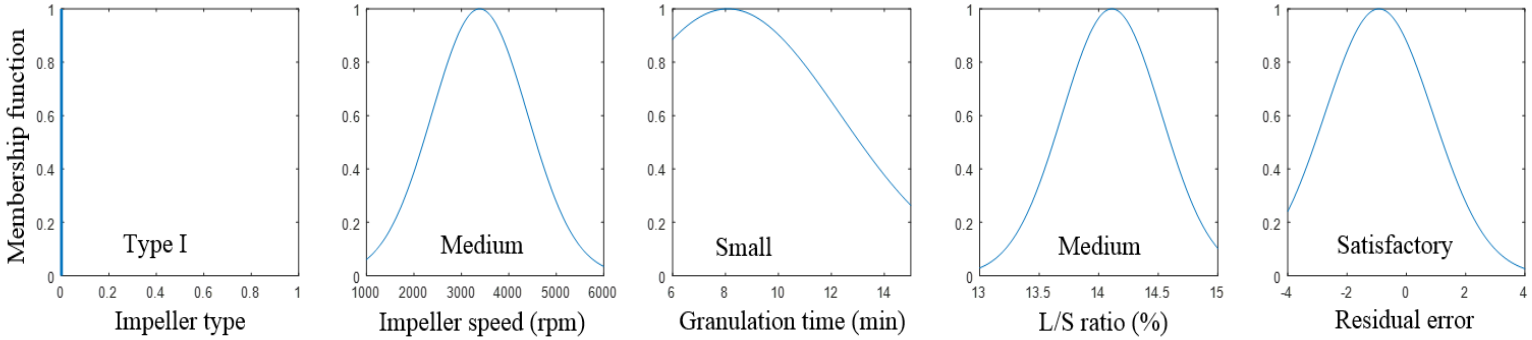

Figure 5.9. An example of the hybrid model performance in the space area of the binder content.

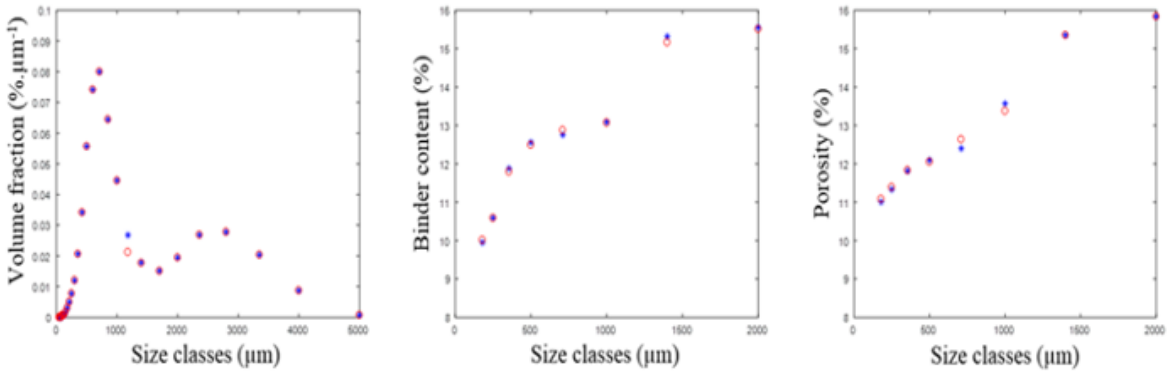

(a)

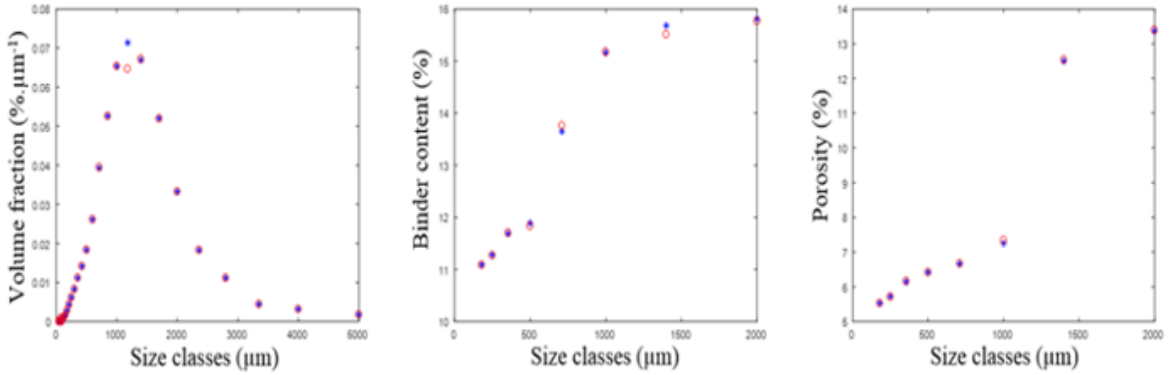

(b)

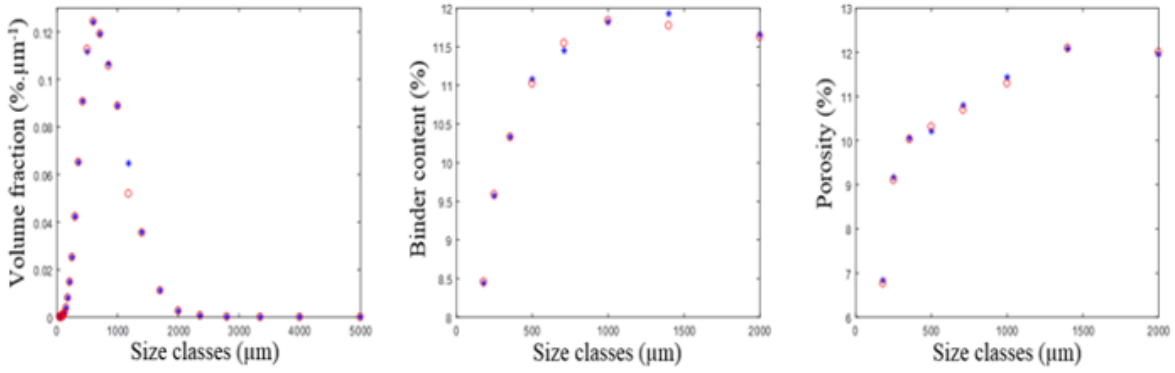

(c)

Figure 5.10. The fusion model: the predicted (o) and the experimental (*) distributions for the size, binder content and porosity (a) using impeller type II, speed=2000rpm, L/S ratio (w/w)=14% and granulation time=10min; (b) using impeller type II, speed=6000rpm, L/S ratio (w/w)=15% and granulation time=15min; (c) using impeller type I, speed=4000rpm, L/S ratio (w/w)=13% and granulation time=6min.

As summarised in Figure 5.7, the estimated membership functions were used to assign the mass functions for the hypotheses of both models. Next, the mass functions were combined using the set of equations in (5.11). This led to the mass functions for the hypotheses of the fusion model. To estimate the membership functions of the fusion model clusters, the set of equations in (5.10) were solved numerically, since the analytical solution (*i.e*. closed form solution) may be computationally taxing, in particular, when the number of clusters is large. After the defuzzification step, the outputs from the fusion model for three experiments are shown in Figure 5.10, where different numbers of clusters were assigned to the various size classes, these numbers laying in the range of 5 to 9.

The predictive performance of the fusion model for all experiments is similar to the one presented in Figure 5.10, which shows a good performance. In the size class (1180μm), the predictive performance is not as good as the one for the other size classes, because the performance of the incorporated model was slightly lower for this size class. However, the overall improvement is noticeable.

Table 5.1 includes the average R^2 and the RMSE performance values of the RBF model (standalone model), which was used here to predict the properties of the granules, as explained previously in Chapter 3, the PBM (standalone model), the previous model presented in Chapter 3, referred to in the table as 'the incorporated model', the hybrid model presented in Section 5.2, and the fusion model described in Section 5.3.

Table 5.1. The performances of the models represented by R^2 and RMSE.

Model	RBF[1]		PBM[2]		Incorporated Model[3]		Hybrid Model[4]		Fusion Model[5]	
Output	R^2	RMSE	R^2	RMSE	R^2	RMSE	R^2	RMSE	R^2	RMSE
Size	53.65	0.0098	75.84	0.0076	87.83	0.0055	88.49	0.0017	91.28	0.0008
Binder Content	46.80	1.2792	67.53	1.0252	74.04	0.9352	76.06	0.6316	80.30	0.5577
Porosity	36.99	1.6457	65.49	1.23	74.02	1.0879	75.67	0.9208	79.54	0.5508

1. The RBF standalone model was utilized to predict the granule properties using different number of basis functions.
2. The PBM was used as a stand-alone model.
3. The incorporated model includes the integrated network and the Gaussian mixture model as presented in Chapter 3.
4. The hybrid model as presented in Section 5.2.
5. The fusion model as described in Section 5.3.

As shown in this table, the fusion model outperformed both the incorporated and the hybrid models. Furthermore, this table shows that the predictive performance for the size was better than that for the binder content and porosity. This may be due to the heterogeneity and the high uncertainties in the measurements of these properties. However, most of the predictions from the incorporated, hybrid and fusion models lay within the 95% confidence interval.

Assessing the generalization capabilities of the developed models is an important step to prove their effectiveness and efficiency. Thus, the hybrid model has been utilized to predict the properties of the granules produced using different operating conditions but within the investigated ranges. Figure 5.11 (a) shows the predicted outputs for a new experiment. The predictive performance values for the three properties are comparable to the ones that obtained using the training data. Similarly, the fusion model has been validated using the operating conditions of the new experiment and the predictions from both the hybrid and the incorporated models. The predicted outputs obtained by the fusion model are presented in Figure 5.11 (b). The predictive performance and the generalization capabilities prove the abilities of the hybrid and the fusion models to be used successfully to understand the granulation process and to accurately predict the properties of the granules produced by the HSG process.

The proposed modelling framework, *i.e.* the hybrid model followed by the fusion model architecture, successfully modelled the granulation process. This has been achieved by providing good predictions for the properties of the granules and an understanding of the process and its mechanisms. Generally, one develops models either to predict properties/behaviours or to control a process. The former, which is

one of the main aims of this research, paves the way for the latter. In the future, the developed framework will be exploited in a *reverse-engineering* framework to identify the optimal operating conditions for granules with predefined properties. This can be achieved by, for instance, embedding the multi-objective optimization paradigms to ensure the *right-first-time* production.

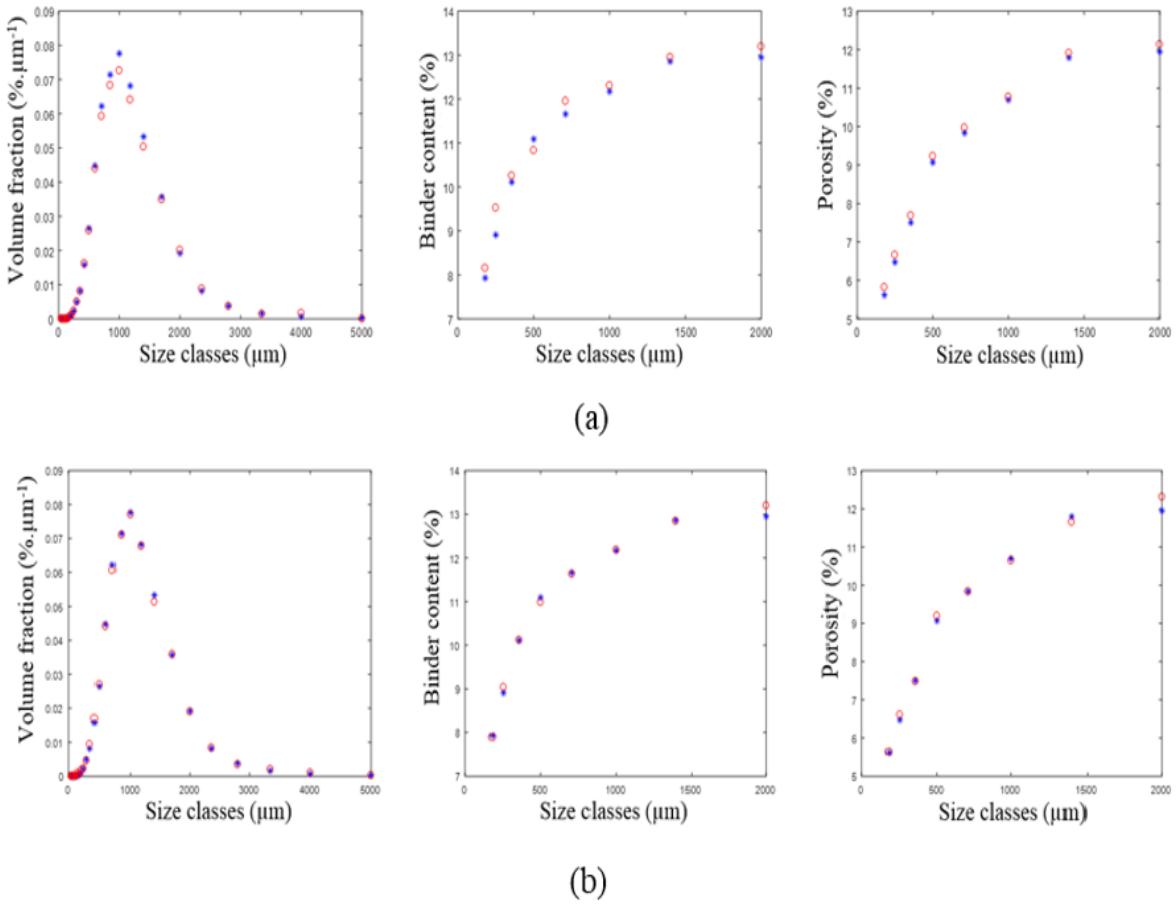

Figure 5.11. The validation experiment: the predicted (o) and the experimental (*) distributions for the size, binder content and porosity using impeller type I, speed=4400rpm, L/S ratio (w/w)=13.6% and granulation time=12min (a) the hybrid model and (b) the fusion model.

5.4 Summary

In this chapter, a hybrid model based on both physical and data based models was presented to model the high shear granulation process only. The model consisted

of three components, namely, a CFD model, a PBM and an RBF model. These models were integrated through an iterative procedure, where the outputs from one of these models are used as inputs to the model architecture. The hybrid model combined the strengths of the single models involved in a way that any potential limitations may be circumvented. Consequently, this model was able to provide a deeper insight into the granulation process and its mechanisms, and also the flow of the granules. It was also capable of interpreting the relationships between the inputs and the outputs, hence it can be used to predict the properties of the granules with a good degree of accuracy. In addition, the model was able to implicitly compensate for some of the basic assumptions normally used in physical based models, which were previously reported in the literature. Furthermore, the new model expressed the empirical parameters as a function of the granulation input variables. Although, the RBF model cannot physically interpret the relationship between the inputs and the outputs, these parameters can easily be predicted if one knows the operating conditions of the experiment. The effectiveness and efficiency of the hybrid model was demonstrated and validated by predicting the properties for the training experimental data and subsequently newly acquired data successfully. By utilizing the scaling-up methods presented in the related literature (Watano *et al*., 2005) and by training the RBF network, the hybrid model can be exploited on a relatively larger scale. However, many aspects need to be considered (*e.g*. mixer geometry) to ensure that it will be implemented correctly.

Accurate predictions of the properties of the granules are more often than not required. Accordingly, a new fusion model based on integrating fuzzy logic theory and DS theory was developed. This model combined the predicted outputs from the hybrid model with the corresponding ones from the model incorporating the integrated

network and the GMM; such a model is a data-based model that had been developed previously in Chapter 3. The main motivation behind such a model was, in addition to accurate predictions, to resolve any conflict(s) that may exist between the various model formalisms. Significant improvements were achieved by using this new approach over the hybrid and the incorporated models.

In summary, a good modelling performance was achieved by the hybrid model, followed by the fusion model. Such a framework is considered to be a promising development in those industries where the granulation process is considered to be one of the most crucial unit operations that determine the quality of the final product. Since a good modelling performance was already achieved, the modelling paradigms presented in Chapters 3 and 5 can now be inverted to identify the optimal operating conditions and the optimal granules' properties to produce a tablet with predefined properties. Therefore, a *reverse-engineering* framework will be proposed in Chapter 6 in order to achieve the concept of *right-first-time* production of the granules and the tablets.

Chapter 6

When Swarm Meets Fuzzy Logic: *Right-First-Time* Production of Pharmaceuticals Using Multi-Objective Optimisation[6]

6.1 Introduction

In the pharmaceutical industry, the granulation process is used as a unit operation in the tablet production line. Although good powder properties (*e.g.* flowability and homogeneity) are usually obtained and maintained, the inclusion of such a process, which, as a single operation, can ultimately determine the outcome for the final tablets produced, makes it difficult to control the production line, leading, as a result, to high recycling ratios and inefficient operations (Walker, 2007). Recently, as mentioned in the previous chapters, a good number of books and research papers has been devoted to modelling and control the granulation process (Barrasso *et al*., 2015; Benali *et al*., 2009; Braumann *et al*., 2007; Darelius *et al*., 2006; Frikha and Moalla 2015; Immanuel *et al*., 2005; Iveson, 2002; Liu *et al*., 2013; Nguyen *et al*.,

[6] The content of this chapter is to be submitted to "AlAlaween, W.H., Mahfouf, M., Salman, A.D. When swarm meets fuzzy logic: right-first-time production of pharmaceuticals using multi-objective optimization. Applied Soft Computing".

2014; Sen *et al*., 2014; Yu *et al*., 2017). For instance, the Quality by Design (QbD) concept has been implemented in order to control the process and the variables affecting it. However, such an implementation was based on experimental studies (Barrasso *et al*., 2015). Therefore, as discussed in earlier chapters, developing a model that provides a better understanding of the granulation process and its mechanisms, and predicts the granule properties accurately is necessary to systematically control such a process.

Various modelling approaches have been developed to model the granulation processes. These paradigms are either physical based models, data-driven models or models that integrate both topologies; such as the one that was developed in Chapter 5 (Frikha and Moalla 2015; Iveson, 2002; Liu *et al*., 2013; Mansa *et al*., 2008; Nguyen *et al*., 2014; Sanders *et al*., 2003; Yu *et al*., 2017; 2015). These modelling paradigms have successfully modelled the granulation process and provided a good understanding of the process at different levels. However, to the best of the knowledge of this thesis author, none of these modelling paradigms was exploited in a *right-first-time* (*i.e*. *reverse-engineering*) framework to systematically control the granulation process, or to achieve *right-first-time* production in those industries where such a process is considered to be a unit operation in their production cycle. The reason for this may be due to the fact that it is not necessarily straightforward to invert nonlinear high dimensional models to obtain a unique solution. In this chapter, the modelling paradigms; the model presented in Chapter 3, which will be referred to as the incorporated model, the hybrid model presented in Chapter 5, and the fusion model, which integrates the predictions from the incorporated model with the ones from the hybrid model, as described in Chapter 5, are exploited within a *right-first-time* framework to determine the optimal operating conditions for both the granulation and

the tableting processes as well as the optimal granule properties to produce a tablet with the desired properties. Since inverting these models may lead to more than one possible set of operating conditions (Mahfouf *et al*., 2008), especially when multiple conflicting objective functions need to be taken into consideration, powerful optimization algorithms are commonly utilized to define such an optimal set of operating conditions (Mahfouf *et al*., 2008).

Various multi-objective optimization algorithms, including but not limited to evolutionary and genetic algorithms, have hitherto been developed and applied to define a set of optimal points, the so-called *Pareto* optimal set, which may also be called non-inferior or non-dominated set (Kennedy *et al*., 2001). In particular, PSO, as a stochastic population based approach, has been successfully and extensively implemented in many research areas, such as those associated with industrial, academic and medical applications (Shanmugavadivu and Balasubramanian, 2014; Unler and Murat, 2010), this being due to its computational simplicity and efficiency (Kennedy *et al*., 2001). Despite the huge body of research that addresses different issues of the multi-objective optimization, it remains a subject of active research. The reason behind this is that there are still many open questions that need to be addressed. One of these issues is the definition of the single optimal solution. Various algorithms have been proposed in the open literature (*e.g*. the weighted sum method) (Vu *et al*., 2017), however, there is hitherto no universally accepted algorithm that can be used to define a single optimal solution for the MOPs, instead the concept of *Pareto* optimal is used to propose a set of non-dominated solutions which the user normally select one or more pragmatic alternative solutions.

In this research work, a new approach that integrates a multi-objective PSO (MOPSO) algorithm with a FLS is proposed. First, a MOPSO algorithm is implemented to find the *Pareto* optimal set. A FLS is then utilized to determine the membership function values for each solution in the set, the estimation of these values being based on user-defined criteria. The predictive performance of a forward model is considered to be a good criterion for the development of the *right-first-time* modelling framework. This choice is motivated by the fact that the proposed *right-first-time* framework will be accurate and reliable only when the predictive performances of the forward modelling frameworks are acceptable. Such a step is followed by applying the set of fuzzy logic operations to define the single optimal solution, which corresponds to the maximum membership function value.

6.2 *Right-First-Time* Framework

6.2.1 *Right-First-Time* Framework: Model Development

Recently, nature-inspired optimization algorithms have attracted a great deal of interest (Kennedy *et al*., 2001; Mahfouf *et al*., 2008; Shanmugavadivu and Balasubramanian, 2014). Several algorithms, such as Genetic and Evolutionary Algorithms, have been proposed and applied to tackle nonlinear, multimodal and discontinuous real-world problems (Shanmugavadivu and Balasubramanian, 2014; Unler and Murat, 2010; Vu *et al*., 2017). In particular, PSO algorithms, which mimic the competitive and cooperative behaviours of fish schooling and bird flocking, have been widely used, this being due to their computational efficiency (*i.e.* fast convergence speed) and, more often than not, their effectiveness in locating the global optima (Kennedy *et al*., 2001). Various PSO algorithms have been presented in the related literature to solve single optimization problems (SOPs) (Kennedy *et al*., 2001).

The promising results that were obtained via such algorithms were the main motivation behind extending the PSO to deal with MOPs (Unler and Murat, 2010; Vu *et al*., 2017).

Unlike SOPs, solving MOPs leads to a set of alternative solutions. Such a set is optimal, in the wider sense, no other set of solutions is superior to it when all the objective functions are taken into consideration (Mahfouf *et al*., 2008). Many algorithms, such as ranking objective functions and weighted sum methods, have been utilized to identify a single optimal solution for the MOPs (Kennedy *et al*., 2001; Vu *et al*., 2017). In this research work, a new algorithm that integrates the PSO with a FLS is proposed to solve MOPs.

Generally, a continuous and unconstrained MOP can simply be written as follows (Kennedy *et al*., 2001):

$$\underset{x\in\Omega}{Min}\ F(x)=\left(f_1(x),\ f_2(x),\ldots f_N(x)\right) \tag{6.1}$$

where x is a k-dimensional vector of decision variables, which are usually bounded by the decision space (Ω). In many cases, the decision vector must satisfy a set of equality and inequality constraints (Mahfouf *et al*., 2008; Vu *et al*., 2017).

To identify the set of *Pareto* optimal solutions, a PSO algorithm is utilized. In the PSO, particles are randomly initialized within the feasible (*i.e*. search) space. Each particle represents a potential solution. A particle i is usually described by its position, $x_i=(x_{i1}, x_{i2}, \ldots, x_{ik})$, and velocity, $v_i=(v_{i1}, v_{i2}, \ldots, v_{ik})$. During the search, the position and the velocity of each particle are updated according to the particle's experience and the experience of the neighbour particles. For the i^{th} particle, these parameters can be updated using the following set of equations (Unler and Murat, 2010):

$$v_{ij}^{t+1} = v_{ij}^{t} + c_1 r_1 \left(p_{ij}^{t} - x_{ij}^{t} \right) + c_2 r_2 \left(p_{gj}^{t} - x_{ij}^{t} \right) \tag{6.2}$$
$$x_{ij}^{t+1} = x_{ij}^{t} + v_{ij}^{t+1}$$

where r_1 and r_2 are random numbers generated uniformly in the range of 0 to 1. The parameter t stands for the iteration number. The parameters c_1 and c_2, the so-called learning factors, represent the degree of influence of the local and global best solutions, respectively. The velocity value is usually bounded within a predefined range of $v_{\min}$ to $v_{\max}$ to prevent the particles from flying out of the feasible space (Kennedy *et al*., 2001).

The set of equations in (6.2) is only applicable when the decision variables are continuous. For discrete variables, the velocity vector is first transformed into a probability one through the sigmoid function as follows (Unler and Murat, 2010):

$$\lambda_{ij}^{t} = \frac{1}{1 + e^{-v_{ij}^{t+1}}} \tag{6.3}$$

where λ_{ij}^{t} represents the probability that the value of the j^{th} element of the position vector is 1. Hence, the position of the discrete particle can be updated as follows (Unler and Murat, 2010):

$$x_{ij}^{t} = \begin{cases} 1 & \text{if } RN < \lambda_{ij}^{t} \\ 0 & \text{otherwise} \end{cases} \tag{6.4}$$

where RN is a uniform random number in the range of 0 to 1.

Once the *Pareto* optimal set is defined, the single optimal solution can be found using the fuzzy logic. First of all, and based on predefined criteria (*e.g*. the predictive performance of a model), a number of clusters can be defined in the feasible space.

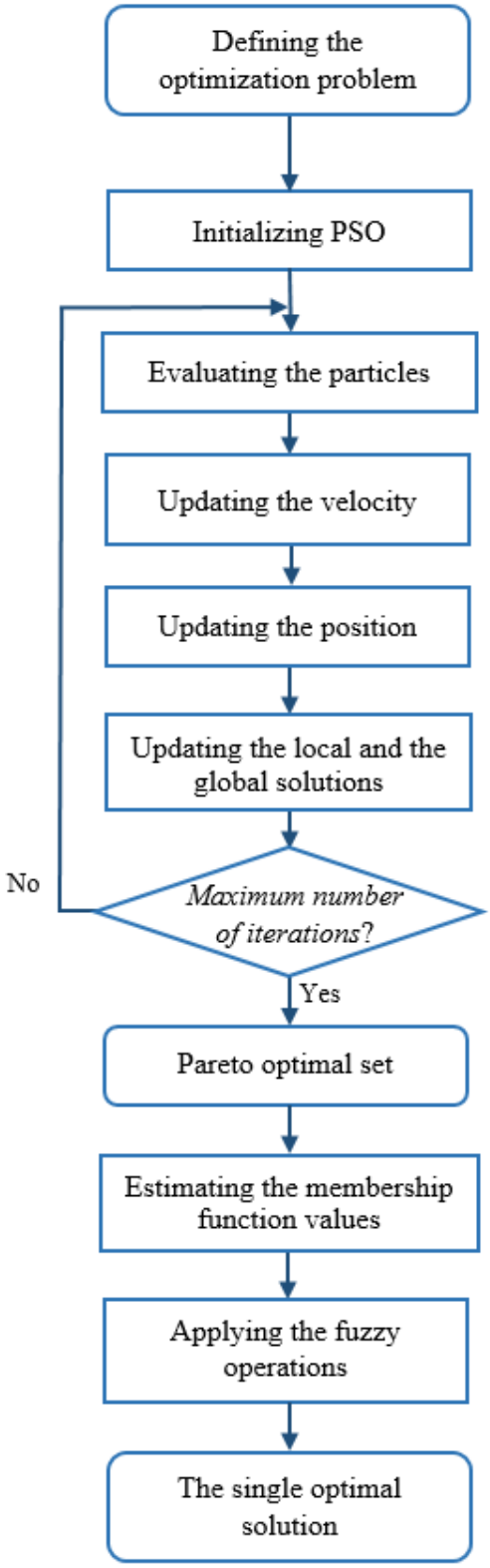

Figure 6.1. Flow chart of the optimization algorithm.

The membership function values for each point in the set can then be estimated using the equation presented previously, such an equation is presented here in order to help the reader get to grips with the algorithm presented (Mendel, 2001):

$$\mu_i = \exp\left(\frac{-(P_{x_i} - M)^2}{2\sigma^2}\right) \tag{6.5}$$

where the parameters are as defined previously. The parameter P_{x_i} represents the performance of the i^{th} solution estimated using the predefined criteria. It is worth noting at this stage that the number of criteria may not necessarily be equal to the number of the objective functions considered.

Once the membership function values are calculated, they can be combined for each solution using the set of fuzzy logic operations. Various operations, such as minimum and product, can be used for this purpose. Selecting the appropriate set of operations depends on the problem under investigation. The main steps of the optimization algorithm are summarised in Figure 6.1.

6.2.2 *Right-First-Time* Framework: Model Implementation and Results

The models, which were introduced previously in Chapters 3 and 5, were exploited within a *right-first-time* framework that was used to facilitate the implementation of the proposed optimization algorithm. Figure 6.2 illustrates the development of the *right-first-time* framework for the granulation and tabletting processes. As shown in Figure 6.2, the *right-first-time* framework was implemented in two stages. In the first stage, the target properties of the tablets were used to define the best granule properties, which were utilized to identify the optimal operating conditions of the HSG process in the second stage of the framework.

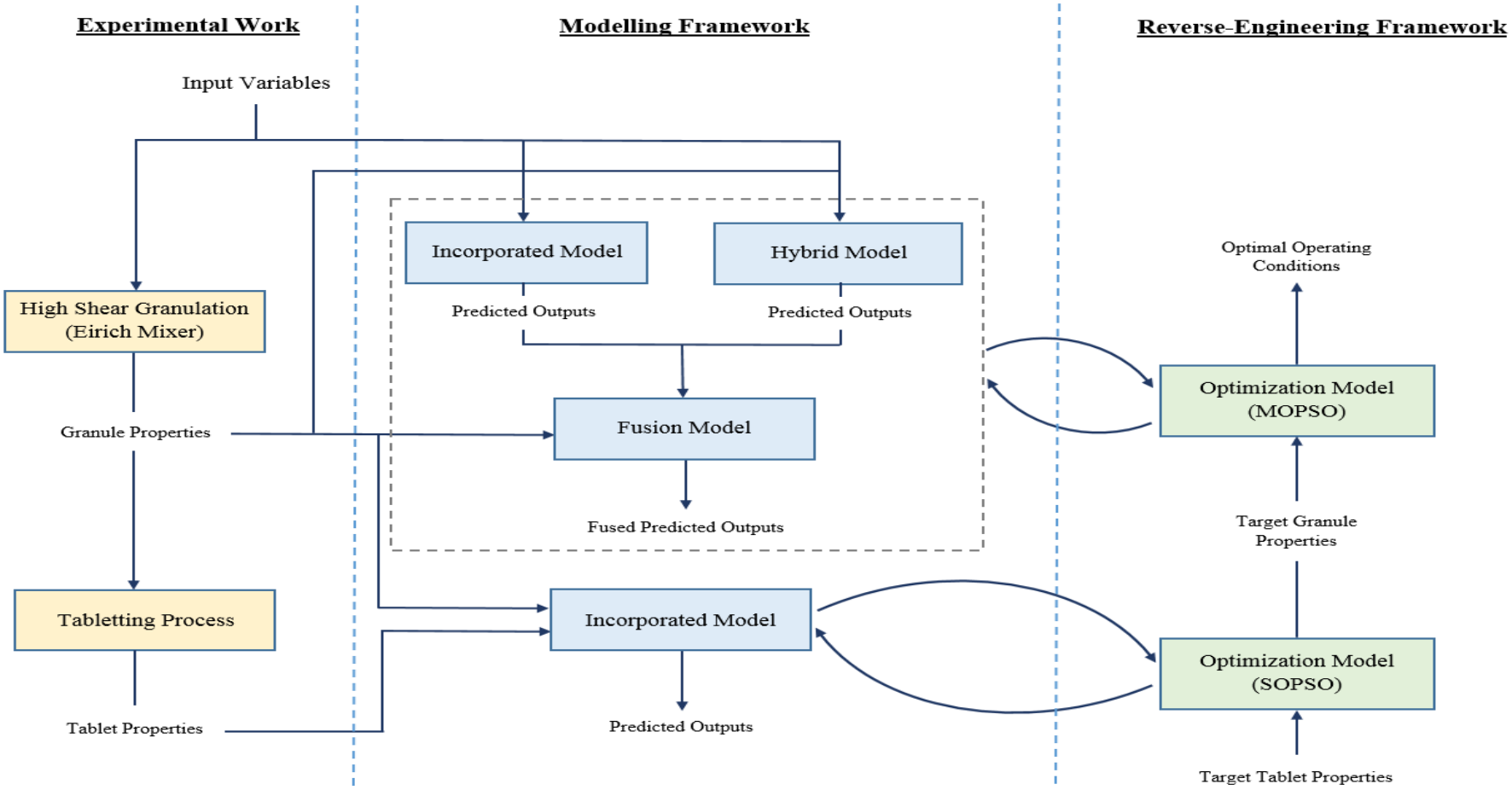

Figure 6.2. Modelling and optimization frameworks for right-first-time production of the granules and tablets.

Since the main property of the tablet that was considered in this research work is the strength, the input parameters for the tabletting process (*i.e*. the properties of the granules produced) were identified using a single objective PSO (SOPSO) method. The optimization problem for the tabletting process can be written as follows:

$$\begin{aligned} &Minimize \quad J_{Tablet} = \left| \frac{S_P}{S_T} - 1 \right| \\ &Subject\,to: \\ &\qquad x_{ij}^{\min} \le x_{ij} \le x_{ij}^{\max} \qquad \forall j \end{aligned} \tag{6.6}$$

where S represents the strength of the tablet, and x_{ij} represents the j^{th} element of the position vector of the i^{th} particle. These subscripts are used to distinguish the predicted strength value (P) from the target (*i.e*. desired) one (T). The inclusion of constraints ensures that all the granule properties, namely, size (500-1000μm), binder content (8-17%) and porosity (4-20%), are located between their minimum and maximum values. To elucidate, suppose that the target strength value of the tablet is 0.75 MPa. The optimization problem in (6.6) was solved using a SOPSO algorithm, where 300 particle solutions were randomly initialized. The optimal granule properties are: the granule size is in the range of 710 to 1000μm, the binder content is 11.75% and the porosity is 10.53%. Such properties were used as target properties that need to be obtained from the granulation process.

For the granulation process, two objective functions should be considered; minimizing the difference between the target and the predicted values for both the binder content and the porosity, and maximizing the amount of the granules in the desired size range, in other words, minimizing the waste and the recycling ratio. The optimization problem for such a process can be mathematically described as follows:

$$
\begin{aligned}
&\textit{Minimize} \quad J_{properties} = \sum_{i=1}^{I} \left| \frac{\gamma_P^i}{\gamma_T^i} - 1 \right| \\
&\qquad\qquad J_{waste} = 1 - \upsilon_T \\
&\textit{Subject to}: \\
&\qquad\qquad x_{ij}^{\min} \le x_{ij} \le x_{ij}^{\max} \qquad \forall j,\ j \ne 1 \\
&\qquad\qquad x_1 = \begin{cases} 0 & \textit{if impeller type I is used} \\ 1 & \textit{if impeller type II is used} \end{cases}
\end{aligned}
\tag{6.7}
$$

where γ^i represents the i^{th} property of the granules, and x_{ij} represents the j^{th} element of the position vector of the i^{th} particle. Similarly to above, such subscripts should distinguish the predicted (P) from the target (T). The parameter υ_T represents the volume fraction of the granules that are in the required size range. The first set of constraints ensures that all the input variables of the granulation process are within the investigated ranges, as listed in Section 2.3.1, whereas the second constraint ensures that the impeller type is considered as a discrete or binary variable. Figure 6.3 and 6.4 show the behaviour of the two objective functions in the search area of the three continuous parameters, namely, impeller speed, granulation time and L/S ratio. It is noticeable that the two objectives are in conflict, in other words, any improvement in one of the objectives leads to a deterioration in the other one. For instance, when both the impeller speed and the granulation time are medium, the first objective function is increasing while the second one is decreasing.

The optimization approach presented in this chapter was implemented to find the single optimal solution. First, the MOPSO algorithm was applied to find the *Pareto* optimal set for the model presented in (6.7). The MOPSO process was run using 300 particles, which were initialized randomly, for 300 iterations.

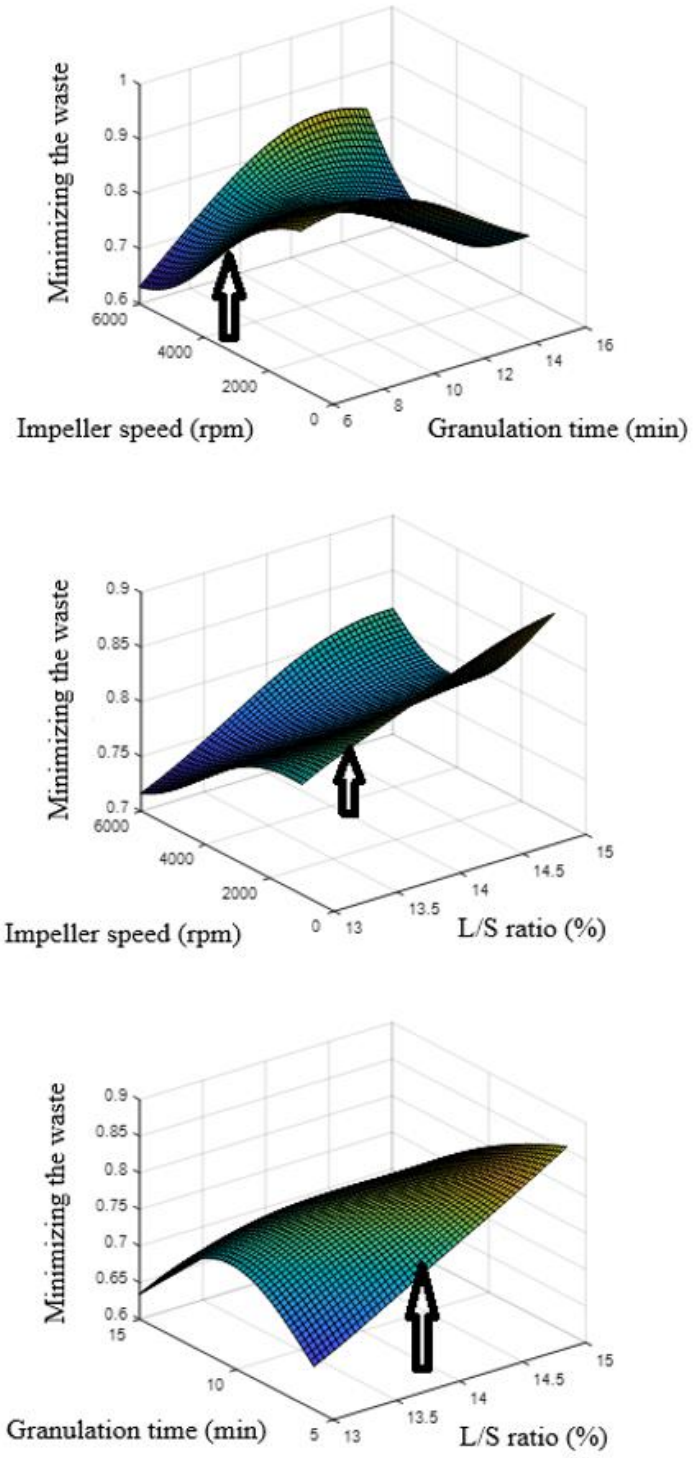

Figure 6.3. The 3D surfaces relating to the objective function: Minimizing the waste and recycling ratio (the arrows show the location of the optimal solution for a tablet with a 0.75 strength value).

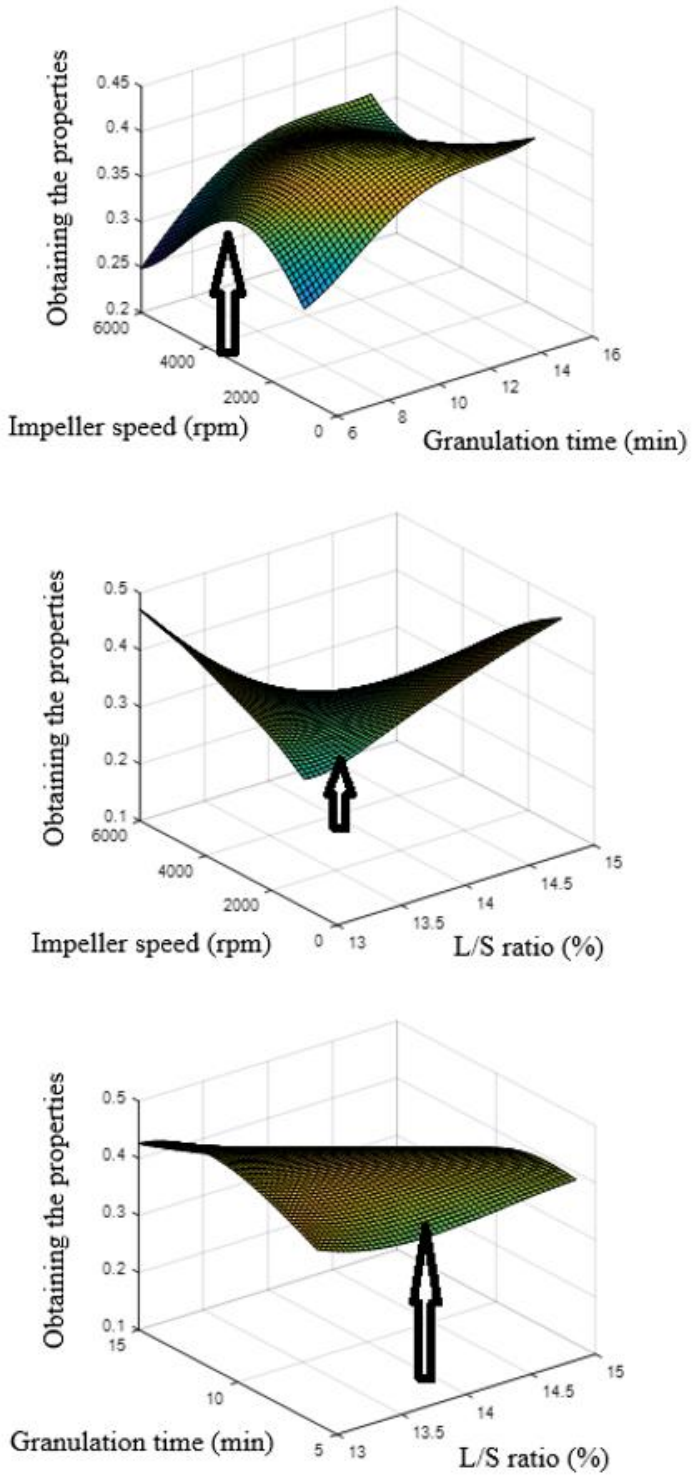

Figure 6.4. The 3D surfaces relating to the objective function: Obtaining the pre-defined properties (the arrows show the location of the optimal solution for a tablet with a 0.75 strength value).

It is worth mentioning at this stage that the incorporated model was used to estimate the objective function values for the 300 iterations, whereas the hybrid and the fusion models were used on the last iteration only, this being due to the computational effort that is required by the hybrid model, as mentioned previously in Chapter 5. Since the size of the *Pareto* optimal set can be potentially large, the results are rather displayed on a Cartesian plot, such a set being shown in Figure 6.5. This figure proves that the two objectives are indeed conflicting.

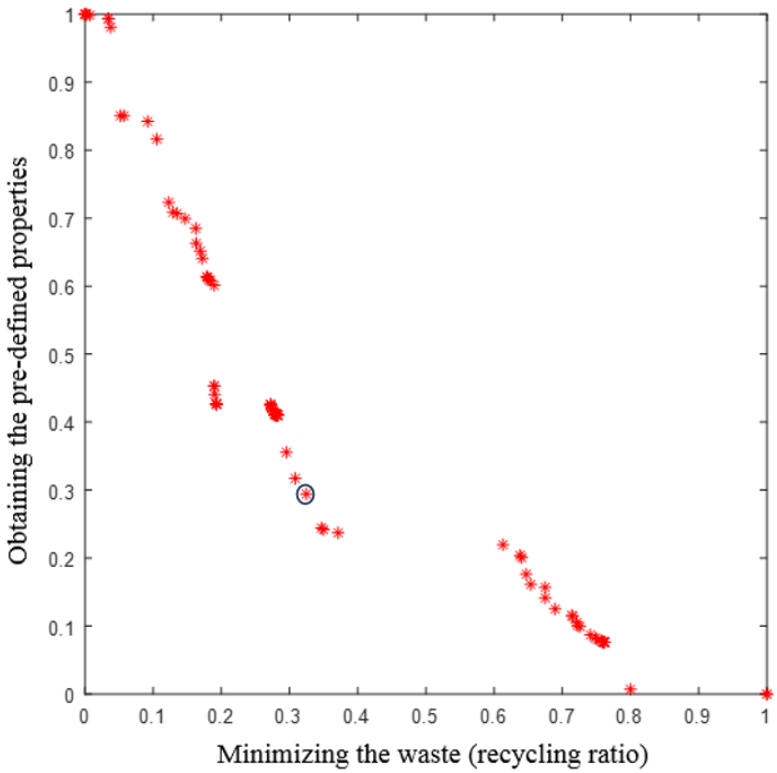

Figure 6.5. The normalized best performance obtained by the MOPSO algorithm (Tablet strength is 0.75 MPa, the single optimal solution is highlighted (o)).

Defining the *Pareto* set was followed by selecting the single optimal solution. Various criteria can be selected based on the designer's priorities and preferences. However, in the *right-first-time* modelling framework, one may consider the

performance of the predictive models and their behaviours at different areas in the feasible space. In this research work, the predictive performances of the fusion model for the three granule properties were chosen as criteria. Therefore, the granulation input variables and the error residuals that resulted from the fusion model were utilized to determine the predictive performance of such a model in the optimization feasible space. For example, and based on the number of clusters that was defined previously in Chapter 5, Figure 6.6 illustrates how the fusion model performed in one of the space areas of the binder content. Such a figure shows that the performance of the fusion model is good when the impeller is of type I, the impeller speed is medium, the granulation time is small and the L/S ratio is medium.

The membership function values for each point in the *Pareto* optimal set were estimated. For each cluster, each solution had membership function values for the size, binder content and porosity. These values were combined using the set of fuzzy logic operations. The minimum operation was used to combine the binder content and porosity. The product operation was then utilized to combine the minimum value with the membership function value for the size. The solution that corresponds to the maximum membership function value was selected. The best set of the operating conditions for the granulation process is: impeller type is of type I, impeller speed is 3879 rpm, granulation time is 6 minutes and L/S ratio is 13.74%. The single optimal point is highlighted in Figure 6.5. The location of this point is also highlighted by arrows in Figures 6.3 and 6.4, where it can be seen that any shift of this point may lead to a significant degradation of one of the objective functions.

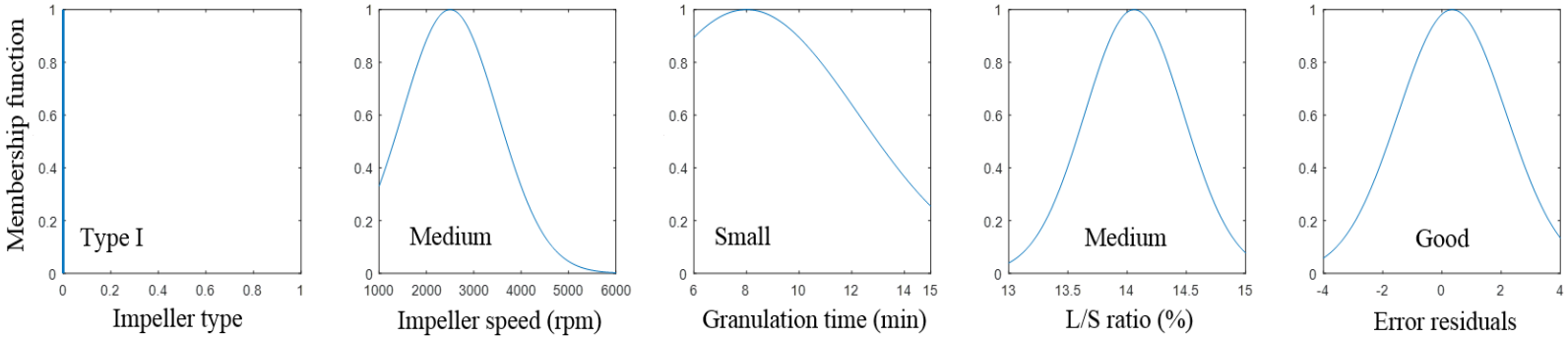

Figure 6.6. An example of the fusion model performance in the space area of the binder content.

Table 6.1. The target and the predicted values of the granule and tablet properties.

	Target tablet strength (MPa)		**0.45**		**0.6**		**0.75**	
			PSO and FLS	PSO	PSO and FLS	PSO	PSO and FLS	PSO
Operating conditions	Impeller shape		Type I	Type I	Type II	Type I	Type I	Type II
	Impeller speed (rpm)		5978.88	3363.57	1878.15	5237.32	3879.45	5832.24
	Granulation time (min)		6.06	15	12.69	6.17	6	6.02
	L/S ratio (%)		14.03	13.84	14.8	14.65	13.74	13.27
Granule properties	Binder content (%)	**Target**	**13.71**		**8.75**		**11.75**	
		Experimental	12.86±0.53	11.81±0.42	9.72±0.95	10.44±0.48	11.63±0.37	12.88±0.34
	Porosity (%)	**Target**	**8.58**		**10.94**		**10.53**	
		Experimental	9.24±0.91	9.44±0.95	10.04±0.63	13.02±0.43	9.72±0.66	11.80±0.71
Experimental Tablet strength (MPa)		**Experimental**	0.412 ±0.03	0.407±0.03	0.533±0.07	0.68±0.04	0.814±0.05	0.858±0.03

An actual granulation experiment was conducted, where the input variables were assigned to be as close as possible to the optimal set of the operating conditions. The granules produced were characterized in terms of size, binder content and porosity. This was followed by producing tablets from the granules in the size range of 710 to 1000µm, and measuring the strength of these tablets. The target and the experimental properties of the granules and the tablets are summarized in Table 6.1. It is noticeable that the experimental values of these properties are close to the target values.

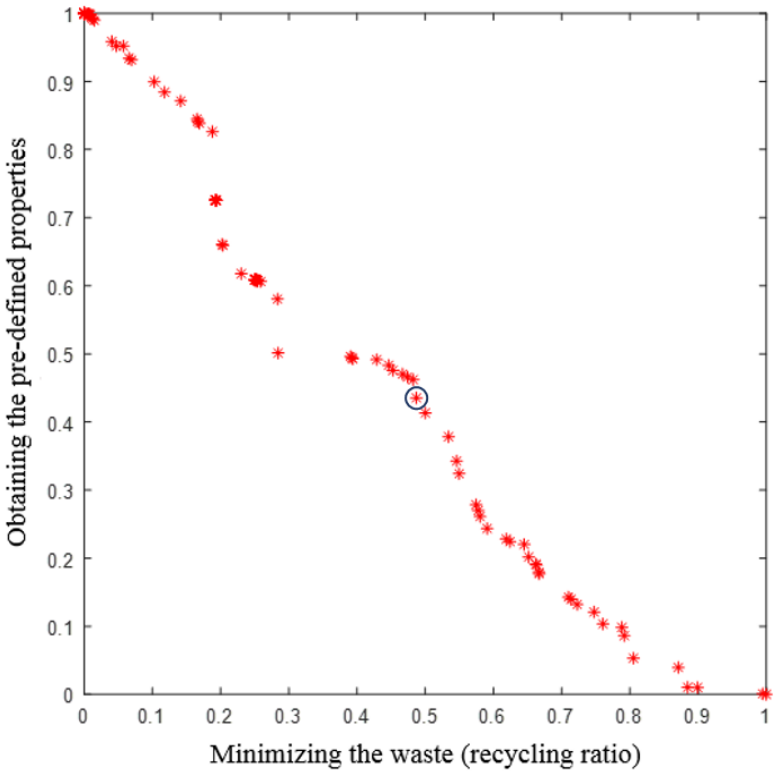

Figure 6.7. The normalized best performance obtained by the MOPSO algorithm (Tablet strength is 0.45 MPa, the single optimal solution is highlighted (o)).

To prove the efficiency and the effectiveness of the proposed algorithm at different areas of the feasible space, two strength values; 0.45 MPa and 0.6 MPa, were also used to test the *right-first-time* framework. Following the same algorithm which

was discussed in Section 6.2.1, the *Pareto* optimal sets for the MOPSO are shown in Figures 6.7 and 6.8. The single optimal solution for each model is highlighted in the corresponding figure. The experimental and the target values of the properties are listed in Table 6.1.

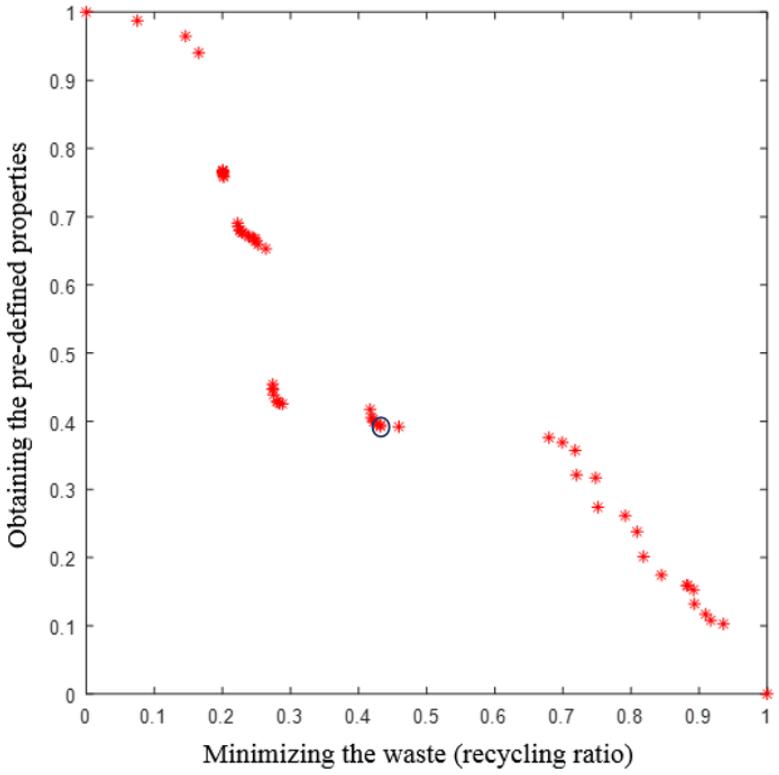

Figure 6.8. The normalized best performance obtained by the MOPSO algorithm (Tablet strength is 0.6 MPa, the single optimal solution is highlighted (o)).

It is worth noting that there is a difference between the target and the predicted values for all the investigated properties. Such a difference is relatively high for the strength of the tablet (approximately 10%) when compared to the differences for the granule properties. The reasons behind this can be attributed to one or more of the following reasons:

- The heterogeneity of the granules: It has been demonstrated in the open literature that the granules from the same batch but different size classes are heterogeneous (Reynolds *et al*., 2004; Scott *et al*., 2000). In addition, the granules from the same size class may not be homogeneous, particularly when the size class is wide.
- Measurement uncertainties: Laboratory apparatus and techniques, which were used to characterize the granules and the tablets, involved uncertainties. Although each measurement was repeated a number of times, such uncertainties could not be eliminated. Moreover, the propagation of uncertainties might affect the developed models, in particular, the model that was developed for the tabletting process.
- Simplifying the optimization model: As mentioned previously, only the incorporated model was used to estimate the objective function values for the 300 iterations, whereas the hybrid and the fusion models were used on the last iteration only. Since the predictive performances of the incorporated model for the binder content and porosity were not as good as the ones for the hybrid and the fusion models, this assumption might negatively affect the performance of the *right-first-time* framework.

For comparison purposes and in order to prove the effectiveness and efficiency of the proposed algorithm, the well-known standard PSO algorithm was utilized to identify the optimal granules' properties and the optimal operating conditions for the granulation process to produce tablets with the same predefined strength values. Then, actual granulation and tabletting experiments were carried-out, and the granules' properties and the strength of the tablets were measured. The target and the experimental results are summarized in Table 6.1, where it is obvious that the proposed

algorithm outperforms the PSO one, this is being due to its ability to take account of the predictive performance of the modelling framework.

In summary, the MOPSO algorithm and the FLS play complementary roles in the optimization process, where the former was utilized to define the set of Pareto optimal solutions and the latter was used to identify the single optimal solution by considering the predictive modelling performances of the forward models. It is worth mentioning at this stage that the FLS alone cannot be used to identify the Pareto optimal solutions for an MOP. On the other hand, the PSO algorithm was not able to consider the predictive performances of the forward models. Therefore, integrating these two approaches has combined their respective strengths in a way that the single optimal solution can be successfully identified. The proposed approach was successfully implemented to produce granules and tablets right from the first time. Such an approach can be further improved to be more robust to the uncertainties and the propagation of uncertainties. A type-2 fuzzy set can be integrated with the PSO algorithm. The choice of such a set is motivated by the fact that the type-2 fuzzy set can deal with uncertainties more efficiently compared to its counterpart type-1 fuzzy set. However, it is well known that a type-2 fuzzy system is computationally demanding when compared to type-1. Therefore, further investigation should be performed to explore the advantages and the potential limitations of integrating such a more complex topology.

6.3 Summary

In the pharmaceutical industry, producing granules and tablets right from the first time is a tricky target that researchers in both academia and industry strive to ascertain. Indeed, achieving such a target is not a trivial task, this being due to the

complex nature of the many processes involved, namely, granulation and tabletting processes, which are key to the production line of these pharmaceutical tablets, and also due to the uncertainties and challenges that surround these processes, including access to measurement points. Therefore, in this research work, a new approach that integrated a PSO algorithm with a FLS was proposed. The ultimate aim of this new approach was to facilitate the development of the *reverse-engineering* framework by which the concept of *right-first-time* production was ascertained. This framework was employed to invert the models that were previously introduced in Chapters 3 and 5 to represent the HSG and the tabletting processes. By implementing such a framework, the optimal granule properties and the optimal operating conditions to produce a tablet with predefined properties (*e.g*. strength) were successfully defined. Moreover, waste and recycling ratios were significantly minimized. This *right-first-time* optimization framework is original in that: (i) It circumvented the direct mathematical inversion of the complex models (via multi-objective optimization) which, more often than not, is not possible due to the fact that such inverse does not exist or simply is not unique; (ii) It considered more than one objective function which made the definition of optimality not so straightforward and instead the concept of *Pareto-optimality* was relied upon whereby a set of non-dominated solutions was obtained. The user usually selects from this 'golden' set what is thought to be a pragmatic outcome for the product/process under investigation. It is perhaps worth noting at this stage that multi-objective optimisation is usually the preferred option to the single aggregated objective optimisation which 'lumps' all objectives into one and by adding weighting factors that play surrogates to the *Pareto definition* for specifying the priority of one objective on the other, in other words *Pareto-optimality* by the back-door. Irrespective of which method one uses though, it is widely recognised that the multi-objective optimization

exercise becomes meaningless when too many objectives are specified and the *Pareto* concept loses the very essence it was introduced for. Even the human brain is incapable of building a useful synthesis for effective decision-making when too many degrees of freedom are involved regardless of any candidate solutions ranking. In our case study it was possible to only include two objectives without loss of interpretability or accuracy but even if more objectives need to be incorporated in the future, such as those associated with the environment for instance then these can be taken into account within a hierarchical framework without compromising on the concept of *Pareto*-optimality.

In summary, the results achieved in this research were truly promising and showed that *right-first-time* production of the granules and tablets is achievable. By considering some aspects (*e.g*. scaling-up methods), the modelling frameworks can be implemented correctly in the pharmaceutical industry (*i.e*. on a relatively large scale). The advantages of such an implantation may include, but not limited to, developing a cost-effective product, meeting the stringent regulations imposed on the pharmaceutical industry and minimizing new product development time.

Chapter 7

Conclusions and Future Work

7.1 Conclusions

Taking a revolutionary step towards moving beyond where the pharmaceutical industry is today is indeed the main motivation behind this research work. Therefore, a *right-first-time* framework was presented in this research to (i) enhance the knowledge of the processes included in the pharmaceuticals production line, (ii) design the final product quality throughout the manufacturing unit operations, (iii) enhance the competitiveness of a company in the market, (iv) improve the supply chain management, and (v) minimize new drug development time. In this research, such a framework was developed and implemented via two phases: in the first phase various modelling paradigms that are based on data, process knowledge and laws of physics were developed to represent the key unit operations, whereas in the second phase these modelling paradigms were exploited in a *reverse-engineering* fashion via the embedding of constrained multi-objective optimization algorithms for *right-first-time* production.

Since the HSG and tabletting processes are considered to be the key unit operations of the pharmaceuticals production cycle, this research focused specifically

on these processes. Understanding such processes was followed by identifying the critical quality attributes of the granules and tablets. The design space (*i.e*. the parameters and their levels that significantly affect the critical quality attributes) was defined by conducting a set of trial experiments. The experimental data were then collected via a full factorial design of experiments.

The data hence obtained were utilized to implement some of the already exisiting data based modelling paradigms (*e.g*. an ANN and an RBF network). However, these models failed to capture the complex relationships between the inputs and the outputs of both the granulation and tabletting processes. Therefore, a new model called the integrated network was proposed in this research work. In such a model, the outputs were predicted by training the data in two consecutive phases. The first phase consists of a number of models, whereas the second phase consists of a single model. The models in both phases should be capable of capturing linear and/or nonlinear relationships. Although such a network is computationally demanding compared to the ANN and the ensample model, it predicted the properties of the granules and tablets successfully, and it also outperformed these modelling paradigms. However, such a network, similarly to the majority of the modelling paradigms do, assumes that the error is normally distributed. Such an assumption may not be valid and it may indeed lead to an unmodelled behaviour and bias. Therefore, the GMM algorithm was then incorporated in the modelling structure to refine the predictions by taking into account any of such potential bias. In this research work, the incorporated model was shown to be able to predict the properties of the granules and tablets accurately. However, such a model, which consists of RBF networks, is referred to as a black-box model, in the sense that it does not provide satisfactory explanations of

the process behaviours. Thus, there was a need to improve the interpretability of the processes involved, particularly the granulation one.

Modelling paradigms based on FLSs were introduced to model the processes under investigation, and also to linguistically describe the relationships between the process inputs and outputs in a way that one can easily understand and perhaps utilize to control the process. Although FLSs can deal with uncertainties more intrinsically, the predictive performances were worse compared to the incorporated model. Such a performance degradation may be due to the invalid assumption that the error residuals followed a normal distribution. In such a case, using the modelling approaches that can extract the hidden information by characterizing the error residuals is a common practice. However, using these approaches may change the linguistic rules extracted by the FLSs. Therefore, in this research work, the GMM algorithm was implemented in such a way that the fuzzy rules, which were used to update the predicted outputs, can be refined to compensate for any potential bias. The integration between the FLSs and the modified GMM algorithm significantly improved the predictive performance. Moreover, the process understanding was retained during the error characterization model. However, the predictive performances were not satisfactory, especially for the binder content and the porosity of the granules, and the strength of the tablets. Therefore, there was a strong need to develop a modelling framework that can not only predict the outputs but can also provide a good understanding, particularly for the granulation process.

A hybrid model based on physical and data interpretations was then proposed. Such a model consisted of three paradigms, namely, a CFD model, a PBM and an RBF network. These three models were integrated in such a way that the outputs from one

model were used as inputs to another model. The proposed hybrid model combined the strengths of the single models involved in a way that any potential limitations would be circumvented. Therefore, this model was able to (i) provide the required understanding of the granulation process and its mechanisms at the micro-level, (ii) describe the flow of the granules inside the granulation vessel, (iii) implicitly compensate for some of the assumptions that were made to simplify the physical based models, and (iv) represent the empirical parameters as a function of the granulation input variables. Furthermore, it was also able to predict the properties of the granules successfully and more accurately. However, more accurate predictions of the properties of the granules are, more often than not, required, especially in the pharmaceutical industry, where the final product should meet the stringent regulations being imposed in such an industry.

In order to improve the predictive modelling performances, a new fusion model based on fuzzy logic theory and the DS theory was proposed. The basic idea of such a model stemmed from the fact that integrating predictions from different topologies can usually lead to more accurate and robust predictions. Also, the predictive performance as a value does not usually show the user how a model performs in the design space. Thus, the fusion model combined the predicted outputs from both the hybrid and the incorporated models in a way that improved the predictive performances, particularly, in those areas where the performance of one of the models or perhaps both was not as good as desired, and also resolved any conflicts that may exist between the models included. The results obtained by the proposed fusion model proved the efficiency of such a model in improving the modelling performances and in resolving conflicts.

In general, the main aim of developing a modelling framework is either to predict process outputs or behaviours, or to control a process. The main aim of all the models that were proposed in Chapters 3, 4 and 5 was to accurately predict the properties of the granules and tablets. Since a good modelling performance was obtained by the models presented in Chapters 3 and 5, these models can be exploited further to develop a *reverse-engineering* framework that can control the processes under investigation by identifying the optimal granule properties and the optimal operating conditions of the granulation process; in order to produce granules having the optimal properties and tablets with predefined properties. This can be achieved by, for instance, embedding the multi-objective optimization paradigms to ensure the *right-first-time* production.

The *right-first-time* framework was implemented in two phases. In the first phase, the model that was developed to represent the tabletting process was inverted using a SOPSO algorithm to define the optimal granule properties to produce a tablet with predefined properties. In the second phase, the models that were developed to represent the granulation process were inverted using a new approach to identify the optimal operating conditions that should lead to the desired optimal properties. The new approach integrated a MOPSO algorithm with a FLS in order to systematically define a single optimal solution for the MOP. The proposed approach successfully identified the optimal operating conditions of the granulation process, and also it significantly minimized waste and recycling ratios.

In summary, the concept of *right-first-time* production does not need to remain a myth (Mahfouf *et al*., 2009), where it was demonstrated in this research work that achieving such a concept is real, even though it was a tricky task. Consequently, by

considering some aspects (*e.g*. scaling-up methods), developing a cost-effective product that meets the stringent regulations and minimizing new product development time can be indeed achievable targets in the pharmaceutical industry as well as in other industrial activities.

7.2 Future Work

As an extension of the research work presented in this thesis, the following research recommendations can be made:

- Improving the presented modelling frameworks: Recommendations to improve the proposed modelling frameworks were suggested in the previous chapters. These recommendations can be summarized as follows:
  - ✓ Developing an integrated network structure based on FLSs: In order to improve the interpretability of the integrated network, type-1 or type-2 FLSs can be used in the first and second phases of the network structure. In such a case, one needs to consider defining and retaining the extracted rules that can accurately represent the process under investigation.
  - ✓ Improving the hybrid model: The hybrid model can be implemented in two stages in order to take into account the three phases; the first stage should consider the binder and the particles, whereas the second stage should consider the granules and gas, followed by integrating the two stages together.

- ✓ Developing a fusion model based on a type-2 fuzzy set: Since a type-2 fuzzy set can handle uncertainties more efficiently compared to its counterpart type-1, defining the mass function using a type-2 fuzzy set can lead to a significant improvement in the predictive performance.
- ✓ Integrating a type-2 fuzzy set with the PSO algorithm to define the single optimal solution for a MOP: Once the approach can deal with uncertainties more efficiently, one can easily consider more than two objective functions.

- Scaling-up process: It is worth integrating the proposed frameworks with the scaling-up approaches presented in the related literature to facilitate the successful implementation of these frameworks on a relatively large scale.
- On-line control system: In the pharmaceutical industry, tablets production cycle has been operated in a batch mode. Recently, moving towards a continuous one has been considered, this is due to its potential advantages in time, recyclability, costs, scalability and controllability (Rogers *et al*., 2013). Therefore, in the future, the modelling and control paradigms should be adapted to model and control a continuous production line in real time.

Bibliography

Abberger, T., Seo, A., Schaefer T., 2002. The effect of droplet size and powder particle size on the mechanisms of nucleation and growth in fluid bed melt agglomeration. International Journal of Pharmaceutics. 249, 185–197.

Akkisetty, P.K., Lee, U., Reklaitis, G.V., Venkatasubramanian, V., 2010. Population balance model-based hybrid neural network for a pharmaceutical milling process. Journal of Pharmaceutical Innovation. 5, 161–168.

Aksu, B., De Beer, T., Folestad, S., Ketolainen, J., Linden, H., Lopes, J.A., De Matas, M., Oostra, W., Rantanen, J., Weimer, M., 2012. Strategic funding priorities in the pharmaceutical sciences allied to quality by design (QBD) and process analytical technology (PAT). European Journal of Pharmaceutical Sciences. 47, 402–405.

Albadarin, A.B., Lewis, T.D, Walker, G.M., 2017. Granulated polyhalite fertilizer caking propensity. Powder Technology. 308, 193–199.

Alderborn, G., 1988. Granule properties of importance to tableting. Acta Pharmaceutica Suecica. 25, 229–238.

Aulton, M.E., 2007. Aulton's pharmaceutics: The design and manufacture of medicines, Elsevier Limited, Oxford.

Badawy, S., Menning, M., Gorko, M., Gilbert, D., 2000. Effect of process parameters on compressibility of granulation manufactured in a high-shear mixer. International Journal of Pharmaceutics. 198, 51–61.

Bakalis, S., Karwe, M.V., 2002. Velocity distributions and volume flow rates in the nip and translational regions of a co-rotating, self-wiping, twin-screw extruder. Journal of Food Engineering. 51, 273–282.

Barrasso, D., El Hagrasy, A., Litster, J.D., Ramachandran, R., 2015. Multi-dimensional population balance model development and validation for a twin screw granulation process. Powder Technology. 270, 612–621.

Basu, P., Joglekar, G., Rai, S., Suresh, P., Vernon, J., 2008. Analysis of manufacturing costs in pharmaceutical companies. Journal of Pharmaceutical Innovation. 3, 30–40.

Benali, M., Gerbaud, V., Hemati, M., 2009. Effect of operating conditions and physico–chemical properties on the wet granulation kinetics in high shear mixer. Powder Technology. 190, 160–169.

Berggren, J., Alderborn, G., 2001. Effect of drying rate on porosity and tabletting behaviour of cellulose pellets. International Journal of Pharmaceutics. 227, 81–96.

Berthiaux, H., Marikh, K., Gatumel, C., 2008. Continuous mixing of powder mixtures with pharmaceutical process constraints. Chemical Engineering and Processing. 47, 2315–2322.

Biggs, C., Sanders, C., Scott, A., Willemse, A., Hoffman, A., Instone, T., Salman, A., Hounslow, M., 2003. Coupling granule properties and granulation rates in high shear granulation. Powder Technology. 130, 162–168.

Bishop, C., 2006. Pattern recognition and machine learning. Springer, New York.

Bishop, C., 1995. Neural networks for pattern recognition. Oxford: Clarendon Press, New York.

Bjorn, I., Jansson, A., Karlsson, M., Folestad, S., Rasmuson, A., 2005. Empirical to mechanistic modelling in high shear granulation. Chemical Engineering Science. 60, 3795–3803.

Bloch, I., 1996. Some aspect of Dempster-Shafer evidence theory for classification of multimodality medical images taking partial volume effect into account. Pattern Recognition Letters. 17, 905–916.

Boudraa, A., Bentabet, A., Salzenstein, F., Guillon, L., 2004. Dempster-Shafer's basic probability assignment based on fuzzy membership functions. Electronic Letters on Computer Vision and Image Analysis. 4, 1–9.

Boukouvala, F., Muzzio, F.J., Ierapetritou, M.G., 2010. Design space of pharmaceutical processes using data-driven-based methods. Journal of Pharmaceutical Innovation. 5, 119–137.

Boukouvala, F., Niotis, V., Ramachandran, R., Muzzio, F.J., Ierapetritou, M.G., 2012. An integrated approach for dynamic flowsheet modeling and sensitivity analysis of a continuous tablet manufacturing process. Computers & Chemical Engineering. 42, 30–47.

Bouwman, A.M., Henstra, M.J., Westerman, D., Chung, J.T., Zhang, Z., Ingram, A., Seville, J.P.K., Frijlink, H.W., 2005. The effect of the amount of binder liquid on the granulation mechanisms and structure of microcrystalline cellulose granules prepared by high shear granulation. International Journal of Pharmaceutics. 290, 129–136.

Bouwman, A., Visser, M., Meesters, G., Frijlink, H., 2006. The use of Stokes deformation number as a predictive tool for material exchange behaviour of granules in the

‘equilibrium phase’ in high shear granulation. International Journal of Pharmaceutics. 318, 78–85.

Buchholz, S., 2010. Future manufacturing approaches in the chemical and pharmaceutical industry. Chemical Engineering and Processing: Process Intensification. 49, 993–995.

Braumann, A., 2010. Numerical study of a stochastic particle algorithm solving a multidimensional population balance model for high shear granulation. Journal of Computational Physics. 229, 7672–7691.

Braumann, A., Goodson, M., Kraft, M., Mort, P., 2007. Modelling and validation of granulation with heterogeneous binder dispersion and chemical reaction. Chemical Engineering Science. 62, 4717–4728.

Briens, L., Logan, R., 2011. The effect of the chopper on granules from wet high-shear granulation using a PMA-1 Granulator. American Association of Pharmaceutical Scientists. 12, 1358–1365.

Capes, C., Danckwerts, P., 1965. Granule formation by the agglomeration of damp powders: Part 1. The mechanism of granule growth. Transaction Institute of Chemical Engineering. 43, 116–124.

Cavinato, M., Bresciani, M., Machin, M., Bellazzi, G., Canu, P., Santomaso, A., 2010. Formulation design for optimal high-shear wet granulation using on-line torque measurements. International Journal of Pharmaceutics. 387, 48–55.

Chan, C.W., Seville, J., Yang, Z., Baeyens, J., 2009. Particle motion in the CFB riser with special emphasis on PEPT-imaging of the bottom section. Powder Technology. 196, 318–325.

Chaturbedi, A., Bandi, C. K., Reddy, D., Pandey, P., Narang, A., Bindra, D., Tao, L., Zhao, J., Li, J., Hussain, M., Ramachandran, R., 2017. Compartment based population balance

model development of a high shear wet granulation process via dry and wet binder addition. Chemical Engineering Research and Design. 123, 187–200.

Chaudhury, A., Wu, H., Khan, M., Ramachandran, R., 2014. A mechanistic population balance model for granulation processes: Effect of process and formulation parameters. Chemical Engineering Science. 107, 76–92.

Chitu, T.M., Oulahna, D., Hemati, M., 2011. Wet granulation in laboratory scale high shear mixers: Effect of binder properties. Powder Technology. 206, 25–33.

Chitu, T.M., Oulahna, D., Hemati, M., 2011. Wet granulation in laboratory-scale high shear mixers: Effect of chopper presence, design and impeller speed. Powder Technology. 206, 34–43.

Chen, J., Mahfouf, M., Sidahmed, G., 2015. A new holistic systems approach to the design of heat treated alloy steels using a biologically inspired multi-objective optimisation algorithm. Engineering Applications of Artificial Intelligence. 37, 103–114.

Cybenko, G., 1989. Approximation by superpositions of a sigmoidal function. Mathematics of Control, Signals, and Systems. 2, 303–314.

Cybenko, G., 1988. Continuous valued neural networks with two hidden layers are sufficient. Technical Report, Department of Computer Science, Tufts University.

Danjo, K., Kojima, S., Chen, C., Sunada, H., Otsuka, A., 1997. Effect of water content on sticking during. Chemical and Pharmaceutical Bulletin. 45, 706–709.

Darelius, A., Brage, H., Rasmuson, A., Bjorn, I., Folestad, S., 2006. A volume-based multi-dimensional population balance approach for modelling high shear granulation. Chemical Engineering Science. 61, 2482–2493.

Darelius, A., Rasmuson, A., Wachem, B., Bjorn, I.N., Folestad, S., 2008. CFD simulation of the high shear mixing process using kinetic theory of granular flow and frictional stress models. Chemical Engineering Science. 63, 2188–2197.

Darelius, A., Remmelgas, J., Rasmuson, A., Wachem, B., Bjorn, I.N., 2010. Fluid dynamics simulation of the high shear mixing process. Chemical Engineering Journal. 164, 418–424.

Datta, S., Mahfouf, M., Zhang, Q., 2015. Imprecise knowledge based design and development of titanium alloys for prosthetic applications. Journal of the Mechanical Behavior of Biomedical Materials. 53, 350–365.

De Alejandro Montalvo, J., Panoutsos, G., Mahfouf, M., Catto, J.W., 2015, High dimensionality and scaling-up performance of RBF models with application to healthcare informatics. International Journal of Machine Learning and Computing. 5, 62–67.

Dempster, A.P., 1967. Upper and lower probabilities induced by a multivalued mapping. The Annals of Mathematical Statistics. 38, 325–339.

Dhanarajan, A., Bandyopadhyay, R., 2007. An energy-based population-balance approach to model granule growth in high-shear wet granulation processes. American Association of Pharmaceutical Scientists. 8, 118–125.

Ebtehaj, I., Bonakdari, H., Zaji, A., 2016. An expert system with radial basis function neural network based on decision trees for predicting sediment transport in sewers. Water Science and Technology. 74, 176–183.

Ennis, B., 2006. Theory of granulation: An engineering perspective, Handbook of pharmaceutical granulation technology. Taylor and Francis Group.

Faure, A., York, P., Rowe, R., 2001. Process control and scale-up of pharmaceutical wet granulation processes: A review. European Journal of Pharmaceutics and Biopharmaceutics. 52, 269–277.

Food and Drug Administration, 2006. Guidance for Industry, Q8 Pharmaceutical Development. Food and Drug Administration: Silver Spring, USA.

Frikha, A., Moalla, H., 2015. Analytic hierarchy process for multi-sensor data fusion based on belief function theory. European Journal of Operational Research. 241, 133–147.

Fu, J., Cheong, Y., Reynolds, G., Adams, M., Salman, A., Hounslow, M., 2004. An experimental study of the variability in the properties and quality of wet granules. Powder Technology. 140, 209–216.

Gaffour, S., Mahfouf, M., Yang, Y.Y., 2010. 'Symbiotic' data-driven modelling for the accurate prediction of mechanical properties of alloy steels. 5th IEEE International Conference Intelligent Systems. 31–36.

Gao, Y.J., Muzzio, F.J., Ierapetritou, M.G., 2012. Optimizing continuous powder mixing processes using periodic section modeling. Chemical Engineering Science. 80, 70–80.

Gernaey, K.V., Cervera-Padrell, A.E., Woodley, J.M., 2012. A perspective on PSE in pharmaceutical process development and innovation. Computers and Chemical Engineering. 42, 15–29.

Gernaey, K.V., Gani, R., 2010. A model-based systems approach to pharmaceutical product-process design and analysis. Chemical Engineering Science. 65, 5757–5769.

Gidaspow, D., 1994. Multiphase flow and fluidization: Continuum and kinetic theory descriptions. London: Academic Press.

Global pharmaceutical market forecast, 2008.

Grunenberg, A., Keil, B., Henck, J., 1995. Polymorphism in binary mixture, as exemplified by nimodipine. International Journal of Pharmaceutics. 118, 11–21.

Guo, Z., Ma, M., Wang, T., Chang, D., Jiang, T., Wang, S., 2011. A Kinetic study of the polymorphic transformation of nimodipine and indomethacin during high shear granulation. Pharmaceutical Science Technology. 12, 610–619.

Hapgood, K., Litster, J., Smith, R., 2003. Nucleation regime map for liquid bound granules. American Institution of Chemical Engineers Journal. 49, 350–361.

Hapgood, K., Tan, M., Chow, D., 2009. A method to predict nuclei size distributions for use in models of wet agglomeration. Advanced Powder Technology. 20, 293–297.

Hegedus, A., Pintye-Hodi, K., 2007. Comparison of the effects of different drying techniques on properties of granules and tablets made on a production scale. International Journal of Pharmaceutics. 330, 99–104.

Hoornaert, F., Wauters, P., Meesters, G., Pratsinis, S., Scarlett, B., 1998. Agglomeration behaviour of powders in a Lödige mixer granulator. Powder Technology. 96, 116–128.

Huang, J., Kaul, G., Utz, J., Hernandez, P., Wong, V., Bradley, D., Nagi, A., O'grady, D., 2010. A PAT approach to improve process understanding of high shear wet granulation through in-line particle measurement using FBRM C35. Journal of Pharmaceutical Sciences. 99, 3205–3212.

Immanuel, C.D., Doyle III, F.J., 2005. Mechanistic modelling of aggregation phenomena in population balances of granulation processes. IFAC Proceedings Volumes. 38, 416–421.

Immanuel, C.D., Doyle III, F.J., 2005. Solution technique for a multi-dimensional population balance model describing granulation processes. Powder Technology. 156, 213–225.

IMS, 2008. Global pharmaceutical market forecast.

Iveson, S., 2002. Limitations of one-dimensional population balance models of wet granulation processes. Powder Technology. 124, 219–229.

Iveson, S., Litster, J., 1998. Growth regime map for liquid-bound granules. American Institute of Chemical Engineering. 44, 1510–1518.

Iveson, S., Litster, J., Hapgood, K., Ennis, B., 2001. Nucleation, growth and breakage phenomena in agitated wet granulation processes: A review. Powder Technology. 117, 3–39.

Iveson, S., Wauters, P., Forrest, S., Litster, J., Meesters, G., Scarlett, B., 2001. Growth regime map for liquid-bound granules: Further development and experimental validation. Powder Technology. 117, 83–97.

Jarvinen, M.A., Paaso, J., Paavola, M., Leivisk, K., Juuti, M., Muzzio, F., Jarvinen, K., 2013. Continuous direct tablet compression: Effects of impeller rotation rate, total feed rate and drug content on the tablet properties and drug release. Drug Development and Industrial Pharmacy. 39, 1802–1808.

Katikaneni, P., Upadrashta, S., Rowlings, C., Neau, S., Hileman, G., 1995. Consolidation of ethylcellulose: Effect of particle size, press speed, and lubricants. International Journal of Pharmaceutics. 117, 13–21.

Keary, C., Sheskey, P., 2004. Preliminary report of the discovery of a new pharmaceutical granulation process using foamed aqueous binders. Drug Development and Industrial Pharmacy. 30, 831–845.

Kennedy, J.F., Eberhart, R.C., Shi, Y., 2001. Swarm intelligence. San Francisco, London.

Khayati, N., Falk, V., Monnier, N., Heussler, L., 2099. Binder liquid distribution during granulation process and its relationship to granule size distribution. Powder Technology. 195, 105–112.

Kiekens, F., Cordoba-Diaz, M., Remon, J.P., 1999. Influence of chopper and mixer speeds and microwave power level during the high-shear granulation process on the final granule characteristics. Drug development and Industrial Pharmacy. 25, 1289–1293.

Kim, H.J., Mahfouf, M., Yang, Y.Y., 2008. Modelling of hot strip rolling process using a hybrid neural network approach. Journal of Materials Processing Technology. 201, 101–105.

Knight, P.C., Instone, T., Pearson, J.M.K., Hounslow, M.J., 1998. An investigation into the kinetics of liquid distribution and growth in high shear mixer agglomeration. Powder Technology. 97, 246–257.

Knight, P., Seville, J., Wellm, A., Instone, T., 2001. Prediction of impeller torque in high shear powder mixers. Chemical Engineering Science. 56, 4457–4471.

Leader, J.J., 2004. Numerical analysis and scientific computation. Pearson, The United States of America.

Lee, K.F., Mosbach, S., Kraft, M., Wagner, W., 2015. A multi-compartment population balance model for high shear granulation. Computers and Chemical Engineering. 75, 1–13

Li, J., Tao, L., Buckley, D., Tao, J., Gao, J., Hubert, M., 2013. The effect of the physical state of binders on high-shear wet granulation and granule properties: A mechanistic approach to understand the high-shear wet granulation process. Part IV. The impact of rheological state and tip-speeds. Journal of Pharmaceutical Sciences. 102, 4384–4394.

Litster, J., 2004. The science and engineering of granulation processes. Dordrecht Springer.

Liu, L., Litster, J., Iveson, S., Ennis, B., 2000. Coalescence of deformable granules in wet granulation processes. American Institute of Chemical Engineering. 46, 529–539.

Liu, L., Smith, R., Litster, J., 2009. Wet granule breakage in a breakage only high-shear mixer: Effect of formulation properties on breakage behaviour. Powder Technology. 189, 158–164.

Liu, L., Zhou, L., Robinson, D., Addai-Mensah, J., 2013. A nuclei size distribution model including nuclei breakage. Chemical Engineering Science. 86, 19–24.

Ma, H., Andrews, G., Jones, D., Walker, G., 2010. Low shear granulation of pharmaceutical powders: Effect of formulation on granulation and tablet properties, Chemical Engineering Journal. 164, 442–448.

Mahfouf, M., Abbod, M.F., Linkens, D.A., 2003. Online elicitation of Mamdani-type fuzzy rules via TSK-based generalized predictive control. IEEE Transactions on Systems, Man, and Cybernetics Part B-Cybernetics. 33, 465–475.

Mahfouf, M., Jamei, M., Linkens, D.A., Tenner, J., 2006. Inverse modelling for optimal metal design using fuzzy specified multi-objective fitness functions. Control Engineering Procatice. 16, 179–191.

Mangwandi, C., Adams, M., Hounslow, M., Salman, A., 2011. Effect of batch size on mechanical properties of granules in high shear granulation. Powder Technology. 206, 44–52.

Mangwandi, C., JiangTao, L., Albadarin, A., Dhenge, R., Walker, G., 2015. High shear granulation of binary mixtures: Effect of powder composition on granule properties. Powder Technology. 270, 424–434.

Mansa, R., Bridson, R., Greenwood, R., Barker, H., Seville, J., 2008. Using intelligent software to predict the effects of formulation and processing parameters on roller compaction. Powder Technology. 181, 217–225.

Marshall, P., York, P., Maclaine, J., 1993. An investigation of the effect of the punch velocity on the compaction properties of ibuprofen. Powder Technology. 74, 171–177.

Maseleno, A., Hasan, M.M., Tuah, N., Tabbu, C.R., 2015. Fuzzy logic and mathematical theory of evidence to detect the risk of disease spreading of highly pathogenic avian influenza H5N1. Procedia Computer Science. 57, 348–357.

Mateljevic, M., Pavlovic, M., 1995. The best approximation and composition with inner function. Michigan Mathematical Journal. 42, 367–378.

Mauricio, J.A., 2008. Computing and using residuals in time series models. Computational Statistics & Data Analysis. 52, 1746–1763.

McKenzie, P., Kiang, S., Tom, J., Rubin, A.E., Futran, M., 2006. Can pharmaceutical process development become high tech? American Institution of Chemical Engineers Journal. 52, 3990–3994.

McLachlan, G.J., 1988. Mixture models: Inference and applications to clustering. Dekker.

McLachlan, G.J., Krishnan, T., 2008. The EM algorithm and extensions. John Wiley and Sons Inc. Hoboken, New Jersey.

Mhaskar, H.N., Micchelli, C.A., 1992. Approximation by superposition of sigmoidal and radial basis functions. Advances in Applied Mathematics. 13, 350–373.

Mendel, J.M., 2001. Uncertain rule-based fuzzy logic systems: Introduction and new directions. Prentice Hall.

Miyamoto, Y., Ogawa, S., Miyajima, M., Matsui, M., Sato, H., Takayama, K., Nagai, T., 1997. An application of the computer optimization technique to wet granulation process involving explosive growth of particles. International Journal of Pharmaceutics. 149, 25–36.

Morris, K., Griesser, U., Eckhardt, C., Stowell, J., 2001. Theoretical approaches to physical transformations of active pharmaceutical ingredients during manufacturing processes. Advanced Drug Delivery Reviews. 48, 91–114.

Mort, P., 2005. Scale up of binder agglomeration processes. Powder Technology. 150, 86–103.

Murray, T., Rough, S., Wilson, D., 2007. The Effect of drying technique on tablets formed from extrusion-spheronization granules. Chemical Engineering Research and Design. 85, 996–1004.

Murtoniemi, E., Yliruusi, J., Kinnunen, P., Merkku, P., Leiviska, K., 1994. The advantages by the use of neural networks in modelling the fluidized bed granulation process. International Journal of Pharmaceutics. 108, 155–164.

Newitt, D., Conway-Jones, J., 1958. A contribution to the theory and practice of granulation. Transaction Institute of Chemical Engineering. 36, 422–441.

Nguyen, D., Rasmuson, A., Bjorn, I.N., Thalberg, K., 2014. CFD simulation of transient particle mixing in a high shear mixer. Powder Technology. 258, 324–330.

Nunes, C.S., Mahfouf, M., Linkens, D.A., Peacock, J.E., 2005. Modelling and multivariable control in anaesthesia using neural-fuzzy paradigms Part I. Classification of depth of anaesthesia and development of a patient model. Artificial Intelligence in Medicine. 35, 195–206.

Obajemu, O., Mahfouf, M., Salomao L.A., 2014. A New interval type-2 fuzzy clustering algorithm for interval type-2 fuzzy modelling with application to heat treatment of steel. The International Federation of Automatic Control. Cape Town, South Africa.

Oliveira, J., Pedrycz, W., 2007. Advances in fuzzy clustering and its applications. Wiley-Blackwell.

Opitz, D., Maclin, R., 1999. Popular ensemble methods: An empirical study. Journal of Artificial Intelligence Research. 11, 169–198.

Osborne, J.D., Sochon, R.P.J., Cartwright, J.J., Doughty, D.G., Hounslow, M.J., Salman, A.D., 2011. Binder addition methods and binder distribution in high shear and fluidised bed granulation. Chemical Engineering Research and Design. 89, 553–559.

Parikh, D., 2010. Handbook of pharmaceutical granulation technology. Informa Healthcare, The United States of America.

Patel, D., Patel, A., Solanki, T., 2012. Formulation and evaluation of bilayer tablet by using melt granulation technique for treatment of diabetes mellitus. Journal of Pharmacy and Bioallied Science. 4, 37–39.

Patel, P., Telange, D., Sharma, N., 2011. Comparison of different granulation techniques for lactose monohydrate. International Journal of Pharmaceutical Sciences and Drug Research. 3, 222–225.

Pinto, M.A., Immanuel, C.D., Doyle III, F.J., 2007. A feasible solution technique for higher-dimensional population balance models. Computers and Chemical Engineering. 31, 1242–1256.

Plumb, K., 2005. Continuous processing in the pharmaceutical industry—changing the mind set. Chemical Engineering Research and Design. 83, 730–738.

Poon, J.M., Immanuel, C.D., Doyle III, F.J., Litster, J.D., 2008. A three-dimensional population balance model of granulation with a mechanistic representation of the nucleation and aggregation phenomena. Chemical Engineering Science. 63, 1315–1329.

Prabir, B., Girish, J., Saket, R., Suresh P., Vernon, J., 2008. Analysis of manufacturing costs in pharmaceutical companies. Journal of Pharmaceutical Innovation. 3, 30–40.

Rahmanian, N., Ghadiri, M., Jia, X., Stepanek, F., 2009. Characterisation of granule structure and strength made in a high shear granulator. Powder Technology. 192, 184–194.

Rahmanian, N., Naji, A., Ghadiri, M., 2011. Effects of process parameters on granules properties produced in a high shear granulator. Chemical Engineering Research and Design. 89, 512–518.

Ramachandran, R., Arjunan, J., Chaudhury, A., Ierapetritou, M.G., 2011. Model-based control-loop performance of a continuous direct compaction process. Journal of Pharmaceutical Innovation. 6, 249–263.

Ramachandran, R., Barton, P., 2010. Effective parameter estimation within a multi-dimensional population balance model framework. Chemical Engineering Science. 65, 4884–4893.

Ramachandran, R., Immanuel, C., Stepanek, F., Litster, J., Doyle III, F., 2009. A mechanistic model for breakage in population balances of granulation: Theoretical kernel development and experimental validation. Chemical Engineering Research and Design. 87, 598–614.

Ramaker, J., Jelgersma, M., Vonk, P., Kossen, N., 1998. Scale-down of a high-shear pelletisation process: Flow profile and growth kinetics. International Journal of Pharmaceutics. 166, 89–97.

Ramkrishna, D., 2000. Population balances: Theory and applications to particulate systems in engineering. London: San Diego Calif.

Reinhardt, U.E., 2001. Perspectives on the pharmaceutical industry. Health Affairs. 20, 136–149.

Reynolds, G.K., Biggs, C.A., Salman, A.D., Hounslow, M.J., 2004. Non-uniformity of binder distribution in high-shear granulation. Powder Technology. 140, 203–208.

Reynolds, G., Fu, J., Cheong, Y., Hounslow, M., Salman, A., 2005. Breakage in granulation: A review. Chemical Engineering Science. 60, 3969–3992.

Rogers, A., Hashemi, A., Ierapetritou, M., 2013. Modeling of particulate processes for the continuous manufacture of solid-based pharmaceutical dosage forms. Processes. 1, 67–127.

Saito, Y., Fan, X., Ingram, A., Peter, J., Seville, K., 2011. A new approach to high-shear mixer granulation using positron emission particle tracking. Chemical Engineering Science. 66, 563–569.

Saleh, M.F., Dhenge, R.M., Cartwright, J.J., Hounslow, M.J., Salman, A.D., 2015. Twin screw wet granulation: Effect of process and formulation variables on powder caking during production. International Journal of Pharmaceutics. 496, 571–582.

Salman, A., Fu, J., Gorham, D., Hounslow, M., 2003. Impact breakage of fertiliser granules. Powder Technology. 130, 359–366.

Salomao, L.A.T, Mahfouf, M., El-Samahy E., Ting C.H., 2017. Psycho-physiologically-based real time adaptive general type 2 fuzzy modelling and self-organising control of operator performance undertaking a cognitive task. IEEE Transactions on Fuzzy Systems: Special Issue on Brain Computer Interface (BCI). 25, 43–57

Sanders, C.F.W., Willemse, A.W., Salman, A.D., Hounslow, M.J., 2003. Development of a predictive agglomeration model. Powder Technology. 138, 18–24.

Sarkar, B.K., Jain, D., Pareek, R., Thacker, S., 2011. Particle size of granules and mechanical properties of Paracetamol tablets. International Journal of Pharmaceutical Sciences Review and Research. 8, 29–31.

Schaber, S.D., Gerogiorgis, D.I., Ramachandran, R., Evans, J.M.B., Barton, P.I., Trout, B.L., 2011. Economic analysis of integrated continuous and batch pharmaceutical manufacturing: A case study. Industrial and Engineering Chemistry Research. 50, 10083–10092.

Schaefer, T., Holm, P., Kristensen, H., 1990. Wet granulation in a laboratory scale high shear mixer. Pharmaceutical Technology. 52, 1147–1153.

Schaefer, T., Holm, P., Kristensen, H., 1986. Comparison between granule growth in a horizontal and a vertical high speed mixer. Archives of Pharmacal Chemistry. 14, 17–29.

Scott, A.C., Hounslow, M.J., Instone, T., 2000. Direct evidence of heterogeneity during high-shear granulation. Powder Technology. 113, 205–213.

Sen, M., Barrasso, D., Singh, R., Ramachandran, R., 2014. A multi-scale hybrid CFD-DEM-PBM description of a fluid-bed granulation process. Processes. 2, 89–111.

Shah, N., 2004. Pharmaceutical supply chains: Key issues and strategies for optimisation. Computers and Chemical Engineering. 28, 929–941.

Shanmugavadivu, P., Balasubramanian, K., 2014. Particle swarm optimized multi-objective histogram equalization for image enhancement. Optics and Laser Technology. 57, 243–251.

Simon, R., Girolami, M., 2012. A first course in machine learning. Boca Raton: CRC Press.

Singh, R., Ierapetritou, M., Ramachandran, R., 2013. System-wide hybrid MPC-PID control of a continuous pharmaceutical tablet manufacturing process via direct compaction. European Journal of Pharmaceutics and Biopharmaceutics. 85, 1164–1182.

Singh, R., Ierapetritou, M., Ramachandran, R., 2012. An engineering study on the enhanced control and operation of continuous manufacturing of pharmaceutical tablets via roller compaction. International Journal of Pharmaceutics. 438, 307–326.

Suresh, P., Basu, P.K., 2008. Improving pharmaceutical product development and manufacturing: Impact on cost of drug development and cost of goods sold of pharmaceuticals. Journal of Pharmaceutical Innovation. 3, 175–187

Troup, G.M., Georgakis, C., 2013. Process systems engineering tools in the pharmaceutical industry. Computers and Chemical Engineering. 51, 157–171.

Tu, J.Y., Fletcher, C.A.J., 1995. Numerical computation of turbulent gas–solid particle flow in a 90^{o} bend. American Institution of Chemical Engineers Journal. 41, 2187–2197.

Tu, W., Ingram, A., Seville, J., Hsiau, S., 2009. Exploring the regime map for high-shear mixer granulation. Chemical Engineering Journal. 145, 505–513.

Unler, A., Murat, A., 2010. A discrete particle swarm optimization method for feature selection in binary classification problems. European Journal of Operational Research. 206, 528–539.

Van den Dries, K., Vegt, O., Girard, V., Vromans, H., 2003. Granule breakage phenomena in a high shear mixer; influence of process and formulation variables and consequences on granule homogeneity. Powder Technology. 133, 228–236.

Van den Dries, K., Vromans, H., 2004. Qualitative proof of liquid penetration-involved granule formation in a high shear mixer. European Journal of Pharmaceutics and Biopharmaceutics. 58, 551–559.

Veen, B., Maarschalk, K., Bolhuis, G., Zuurman, K., Frijlink H., 2000. Tensile strength of tablets containing two materials with a different compaction behaviour. International Journal of Pharmaceutics. 203, 71–79.

Verkoeijen, D., Pouw, G., Meesters, G., Scarlett, B., 2002. Population balances for particulate processes-a volume approach. Chemical Engineering Science. 57, 2287–2303.

Vertyagina,Y., Mahfouf, M., 2014. A 3D cellular automata model of the abnormal grain growth in austenite. Journal of Materials Science. 50, 745–754.

Vernon, J.A., Keener, H.W., Trujillo, A.J., 2007. Pharmaceutical manufacturing efficiency, drug prices, and public health: Examining the casual links. Drug Information Journal. 41, 229–239.

Vonk, P., Guillaume, C., Ramaker, J., Vormans, H., Kossen, N., 1997. Growth mechanisms of high shear palletisation. International Journal of Pharmaceutics. 157, 93–102.

Vose, M.D., 1999. The simple genetic algorithm: Foundations and theory. Cambridge, Mass., London

Vu, T.T., Kha, H.H., Duong, T.Q., Vo, N.S., 2017. Particle swarm optimization for weighted sum rate maximization in MIMO broadcast channels. Wireless Personal Communications. 96, 1–15.

Walker, G., 2007. Future development in drum granulation modelling. In: Salman, A.D., Hounslow, M.J., Seville, J., (Eds), Granulation. Oxford: Elsevier, 249–254.

Walker, G., Holland, C., Ahmad, M., Craig, D., 2005. Influence of process parameters on fluidised hot-melt granulation and tablet pressing of pharmaceutical powders. Chemical Engineering Science. 60, 3867–3877.

Watano, S., Okamoto, T., Sato, Y., Osako, Y., 2005. Scale-up of high shear granulation based on the internal stress measurement. Chemical and Pharmaceutical Bulletin. 53, 351–354.

Watano, S., Okamoto, T., Sato, Y., Ohnishi, Y., Yasutomo, T., Osako, Y., 2005. Scale-up of wet kneading in a novel vertical high shear kneader. Chemical and pharmaceutical bulletin. 53, 18–21.

Watano, S., Sato, Y., Miyanami, K., 1997. Application of a neural network to granulation scale-up. Powder Technology. 90, 153–159.

Wauters, P., Jakobsen, R., Litster, J., Meesters, G., Scarlett, B., 2002. Liquid distribution as a means to describing the granule growth mechanism. Powder Technology. 123, 166–177.

Wen, C.Y., Yu, Y.H., 1966. Mechanics of fluidization. Chemical Engineering and Processing: Process Intensification. 62, 100–111.

Westerhuis, J., Coenegracht, P., Lerk, C., 1997. Multivariate modelling of the tablet manufacturing process with wet granulation for tablet optimization and in-process control. International Journal of Pharmaceutics. 156, 109–117.

Wu, C.Y., Hancock, B.C., Mills, A., Bentham, A.C., Best, S.M., Elliott, J.A., 2008. Numerical and experimental investigation of capping mechanisms during pharmaceutical tablet compaction. Powder Technology. 181, 121–129.

Wu, C.Y., Ruddy, O.M., Bentham, A.C., Hancock, B.C., Best, S.M., Elliott, J.A., 2005. Modelling the mechanical behaviour of pharmaceutical powders during compaction. Powder Technology. 152, 107–117.

Yang, Y.Y., Linkens, D.A., Mahfouf, M., Rose, A.J., 2003. Grain growth modelling for continuous reheating process–a neural network-based approach. ISIJ International. 43, 1040–1049.

Yang, Y.Y., Mahfouf, M., Panoutsos, G., 2012. Probabilistic characterisation of model error using Gaussian mixture model– with application to Charpy impact energy prediction for alloy steel. Control Engineering Practice. 20, 82–92.

Yang, Y.Y., Mahfouf, M., Zhang, Q., 2011. Optimal input selection for neural fuzzy modelling with application to Charpy energy prediction. IEEE International Conference on Fuzzy Systems. Taiwan, 27–30.

Yu, H., Fu, J., Dang, L., Cheong, Y., Tan, H., Wei, H., 2015. Prediction of the particle size distribution parameters in a high shear granulation process using a key parameter definition combined artificial neural network model. Industrial and Engineering Chemistry Research. 54, 10825–10834.

Yu, L.X., 2008. Pharmaceutical quality by design: Product and process development, understanding, and control. Pharmaceutical Research. 25, 781–791.

Yu. X., Hounslow, M.J., Reynolds, G.K., Rasmuson, A., Bjorn, I.N., Abrahamsson, P.J., 2017. A compartmental CFD-PBM model of high shear wet granulation. American Institution of Chemical Engineers Journal. 63, 438–458.

Zhao, Z., Zhang, Y., 2011. Design of ensemble neural network using entropy theory. Advances in Engineering Software. 42, 838–845.

Zhang, Q., Mahfouf, M., 2011. A hierarchical Mamdani-type fuzzy modelling approach with new training data selection and multi-objective optimisation mechanisms: A special application for the prediction of mechanical properties of alloy steels. Applied Soft Computing. 11, 2419–2443.

Zhang, Q., Mahfouf, M., Panoutsos, G., Beamish, K., Liu, X., 2015. Multi-objective optimal design of friction stir welding considering quality and cost issues. Science and Technology of Welding and Joining. 20, 607–615.